The Kuramoto model

Juan A. Acebrón*

Dipartimento di Ingegneria dell' Informazione, Università di Padova, Via Gradenigo, 6/B, 35131 Padova, Italy

L. L. Bonilla†

Departamento de Matemáticas, Universidad Carlos III de Madrid, Avenida de la Universidad 30, 28911 Leganés, Spain

Conrad J. Pérez Vicente‡ and Félix Ritort§

Department de Fisica Fonamental, Universitat de Barcelona, Diagonal 647, 08028 Barcelona, Spain

Renato Spigler¶

Dipartimento di Matematica, Università di Roma Tre, Largo S. Leonardo Murialdo 1, 00146 Roma, Italy

Synchronization phenomena in large populations of interacting units are the subject of intense research efforts in physical, biological, chemical and social systems. A successful approach to the problem of synchronization is to model each member of the population as a phase oscillator. Synchronization in the most representative model of coupled phase oscillators, the Kuramoto model, is extensively analyzed in this review. We present a rigorous mathematical treatment, specific numerical methods, and many variations and extensions of the original model that have appeared in the last years. Relevant applications of the model to understanding synchronization in different physical problems are also included.

Contents

*Electronic address: acebron@dei.unipd.it
†Electronic address: bonilla@ing.uc3m.es
‡Electronic address: conrad@ffn.ub.es
§Electronic address: ritort@ffn.ub.es
¶Electronic address: spigler@dmsa.unipd.it

I. INTRODUCTION

Time plays a key role for all living beings. Their activity is governed by cycles of different duration which determine their individual and social behavior. Some of these cycles are crucial for their survival. There are biological processes and specific actions that require a precise timing. Some of these actions demand a level of expertise that only can be acquired after a long period of training but others take place spontaneously. How do these actions occur? Possibly through synchronization of individual actions in a population. A few examples follow. Suppose we attend a concert. Each member of the orchestra plays a sequence of notes that, properly combined according to a musical composition, elicit a deep feeling in our senses. The effect can be astonishing or a fiasco (apart from other technical details) simply depending on the exact moment when the sound was emitted. In the meantime, our heart is beating rhythmically because thousands of cells synchronize their activity. The emotional character of the music can accelerate or decelerate the heartbeat. We are not aware of the process, but the cells themselves manage to change coherently, almost in unison. How? We see the conductor moving harmoniously her arms. Musicians know perfectly how to interpret these movements and respond with the appropriate action. Thousands of neurons in the visual cortex sensitive to specific space orientations synchronize their activity almost immediately when the baton describes a trajectory in space. This information is transmitted and processed through some outstandingly fast mechanisms. What more? Just a few seconds after the last bar, the crowds filling completely the auditorium start to applaud. At the beginning the rhythm may be incoherent, but the wish to get an encore can transform incoherent applause in a perfectly synchronized one, despite the different strength in beating or the location of individuals inside the concert hall.

These examples illustrate synchronization, one of the most captivating cooperative phenomena in nature. Synchronization is observed in biological, chemical, physical and social systems and it has attracted the interest of scientists for centuries. A paradigmatic example is the synchronous flashing of fireflies observed in some South Asia forests. At night, a myriad of fireflies lay over the trees. Suddenly, several fireflies start emitting flashes of light. Initially they flash incoherently, but after a short period of time the whole swarm is flashing in unison creating one of the most striking visual effects ever seen. The relevance of synchronization has been stressed frequently although it has not always been fully understood. In the case of the fireflies, synchronous flashing may facilitate the courtship between males and females. In other cases, the biological role of synchronization is still under discussion. Thus, perfect synchronization could lead to disaster and extinction, and therefore different species in the same trophic chain may develop different circadian rhythms to enlarge their probability of survival. Details about these and many other systems, together with many references, can be found in the recent and excellent book by Strogatz (Strogatz, 2003).

Researches on synchronization phenomena focus inevitably on ascertaining the main mechanisms responsible for collective synchronous behavior among members of a population. To attain a global coherent activity, we need interacting oscillatory units. The rhythmical activity of each element may be due to internal processes or to external sources (external stimuli or forcing). Even if the internal processes responsible for rhythmicity have different physical or biochemical origins and be very complex, one hopes to understand the essence of synchronization in terms of a few basic principles. What may these principles be?

There are different ways to tackle the problem. Suppose that the rhythmical activity of each unit is described in terms of a physical variable that evolves regularly in time. When such a variable reaches a certain threshold, the unit emits a pulse (action potential for neurons) which is transmitted to the neighborhood. Moreover, a resetting mechanism initialize the state of the unit that has fired. Then, a new cycle starts again. Essentially the behavior of each unit is similar to that of an oscillator. Assuming that the rhythm has a period T, it is convenient to introduce the concept of phase, a periodic measure of the elapsed time which can be defined in $[0, 1]$ without loss of generality. Essentially, the effect of the emitted pulse is to alter the current state of the neighbors by modifying their periods, lengthening or shortening them. This disturbance depends on the current state of the oscillator receiving the external impulse, and it can also be studied in terms of a phase-shift. The analysis of the collective behavior of the system can be carried out in this way under two conditions: (i) the phase-shift provoked by an impulse is independent of the number of impulses arriving within an interspike interval, and (ii) the arrival of one impulse affects the period of the current time interval but memory thereof is rapidly lost and the behavior in future intervals is not affected.

There is another scenario in which synchronization effects have been studied extensively. Let us consider an ensemble of nonlinear oscillators moving in a globally attracting limit cycle of constant amplitude. These are phase, or limit cycle, oscillators. We now couple them weakly to ensure that any disturbance can not take any one of them away from the global limit cycle. Then, only one degree of freedom is necessary to describe the dynamic evolution of the system. Even at this simple level

of description it is not easy to propose specific models. The first scenario of pulse-coupled oscillators is perhaps more intuitive, more direct and easier to model. However, the discrete and nonlinear nature of pulse-coupling gives rise to important mathematical complications. While the treatment of just a few pulse-coupled units can be done within the framework of dynamical systems, the description becomes much more complicated for a large number of such units. Proposing a model within the second scenario of coupled limit-cycle oscillators leaves ample room for imagination. We are forced to consider models with continuous time and specific nonlinear interactions between oscillators which are mathematically tractable. Our experience says that models with the latter property are exceptional. Nevertheless some authors have been looking for a 'solvable' model of this type for years. Winfree was the stereotype of persistent scientist (Winfree, 1967, 1980). He realized that synchronization can be understood as a threshold process. When the coupling between oscillators is strong enough, a macroscopic fraction of them synchronize to a common frequency. The model he proposed was hard to solve in its full generality, although a solvable version has been recently found (Ariaratnam and Strogatz, 2001). Thus research on synchronization proceeded along other directions.

The most successful attempt is due to Kuramoto (Kuramoto, 1975), who analyzed a model of phase oscillators rotating at disordered intrinsic frequencies and coupled through the sine of their phase differences. The Kuramoto model is simple enough to be mathematically tractable, yet sufficiently complex to be non-trivial. The model is rich enough to display a large variety of synchronization patterns and sufficiently flexible to be adapted to many different contexts. This little wonder is the object of this review. We have reviewed the progress made in the analysis of the model and its extensions during the last twenty years. We have also tried to cover the most significant areas where the model has been applied, although we realize that this is not an easy task because of its ubiquity.

The review is organized as follows. The Kuramoto model with mean field coupling is studied in Section II. In the limit of infinitely many oscillators, we discuss the characterization of incoherent, phase-locked and partially synchronized phases. The stability of the partially synchronized state, finite-size effects and open problems are also considered. Section III deals with the noisy mean-field Kuramoto model, resulting from adding external white noise sources to the original model. This section deals with the nonlinear Fokker-Planck equation describing the one-oscillator probability density in the limit of infinitely many oscillators (which is derived in Appendix A). We study synchronization by first analyzing the linear stability of the simple unsynchronized state called incoherence, at which the phase of the oscillators can have any value with the same probability. Depending on the distribution of natural frequencies, different synchronization scenarios can occur in parameter regions where incoherence is unstable. We present a complete analysis of these scenarios for a bimodal frequency distribution using bifurcation theory. Our original presentation of bifurcation calculations uses the Chapman-Enskog method to construct the bifurcating solutions, which is better than the method of multiple scales for degenerate bifurcations and simpler than center manifold calculations. Section IV describes the known results for the Kuramoto model with couplings different from mean-field. They include short-range and hierarchical couplings, models with disorder, time-delayed couplings, and models containing external fields or multiplicative noise. Extensions of the original model are discussed in Section V. Section VI discusses numerical solutions of the noisy Kuramoto model, either for the system of stochastic differential equations or for the nonlinear Fokker-Planck equation describing the one-oscillator probability density in the limit of infinitely many oscillators. Applications of the Kuramoto model are considered in Section VII. They include neural networks, Josephson junctions and laser arrays, and chemical oscillators. These applications are often directly inspired by the original model, share its philosophy and represent an additional step to develop new ideas. The last Section contains our conclusions and discusses interesting open problems and hints for future work. The Appendices are devoted to technical issues referred to in the text.

II. THE KURAMOTO MODEL

The Kuramoto model (thereafter called KM) consists of a population of N coupled phase oscillators, $\theta_i(t)$, having natural frequencies ω_i distributed with a given probability density $g(\omega)$ and whose dynamics is governed by

$$\dot{\theta}_i = \omega_i + \sum_{j=1}^{N} K_{ij} \sin(\theta_j - \theta_i), \qquad i = 1, \ldots, N. \quad (1)$$

Thus each oscillator tries to run independently at its own frequency while the coupling tends to synchronize it to all the others. By making a suitable choice of a rotating frame, $\theta_i \to \theta_i - \Omega t$, in which Ω is the first moment of $g(\omega)$, we can transform Eq. (1) to an equivalent system of phase oscillators whose natural frequencies have zero mean. When the coupling is sufficiently weak the oscillators run incoherently whereas beyond a certain threshold collective synchronization emerges spontaneously. Many different models for the coupling matrix K_{ij} have been considered such as nearest-neighbor coupling, hierarchical coupling, random long-range coupling or even state dependent interactions. All of them will be discussed throughout the review.

In this Section, we introduce the Kuramoto model with mean-field coupling among phase oscillators. For this model, synchronization is conveniently measured by an order parameter. In the limit of infinitely many oscillators, $N = \infty$, the modulus of the order parameter

vanishes if the oscillators are out of synchrony, and it is positive in synchronized states. Firstly, we present Kuramoto's calculation of oscillator partial synchronization and its bifurcation from incoherence, a state in which the oscillator phase takes on values on the interval $[-\pi, \pi]$ with equal probability. Secondly, the stability of incoherence is analyzed in the limit as $N = \infty$. For coupling constant $K < K_c$, incoherence is neutrally stable because the spectrum of the operator governing its linear stability lies on the imaginary axis. This means that disturbances from incoherence decay similarly to the Landau damping in plasmas. For $K > K_c$ and unimodal distributions of oscillator intrinsic frequencies, one eigenvalue appears and becomes positive. The partially synchronized state bifurcates from incoherence at $K = K_c$, but a rigorous proof of its stability is still missing. Lastly, finite size effects ($N < \infty$) on oscillator synchronization are discussed.

A. Stationary synchronization for mean-field coupling

The original analysis of synchronization by Kuramoto (Kuramoto, 1975, 1984) dealt with Eq. (1) in the case of mean-field coupling, $K_{ij} = K/N > 0$. Then the model (1) can be written in a more convenient form defining the (complex-valued) order-parameter

$$re^{i\psi} = \frac{1}{N}\sum_{j=1}^{N} e^{i\theta_j}. \tag{2}$$

Here $r(t)$ with $0 \le r(t) \le 1$ measures the phase coherence of the oscillators, and $\psi(t)$ measures the average phase. With this definition, Eq. (1) becomes

$$\dot{\theta}_i = \omega_i + Kr\sin(\psi - \theta_i), \quad i = 1, 2, \ldots, N, \tag{3}$$

and it is clear that each oscillator is coupled to the common average phase $\psi(t)$ with coupling strength given by Kr. The order parameter (2) can be rewritten as

$$re^{i\psi} = \int_{-\pi}^{\pi} e^{i\theta}\left(\frac{1}{N}\sum_{j=1}^{N}\delta(\theta - \theta_j)\right) d\theta. \tag{4}$$

In the limit of infinitely many oscillators, they may be expected to be distributed with a probability density $\rho(\theta, \omega, t)$ so that the mean (2) becomes an average over phase and frequency, namely,

$$re^{i\psi} = \int_{-\pi}^{\pi}\int_{-\infty}^{\infty} e^{i\theta}\,\rho(\theta, \omega, t)\,g(\omega)\,d\theta d\omega. \tag{5}$$

This equation illustrates the use of the order parameter to measure oscillator synchronization. If $K \to 0$, $\theta_i \approx \omega_i t + \theta_i(0)$, the oscillators rotate at angular frequencies given by their own natural frequencies, and $\theta \approx \omega t$ in Eq. (5). Then $r \to 0$ as $t \to \infty$ according to the Riemann-Lebesgue lemma, and the oscillators are not synchronized. In the limit of strong coupling, $K \to \infty$, the oscillators become synchronized to their mean phase, $\theta_i \approx \psi$, and Eq. (5) implies $r \to 1$. For intermediate couplings, $K_c < K < \infty$, part of the oscillators are phase-locked ($\dot{\theta}_i = 0$), and part are rotating out of synchrony with the locked oscillators. This state of *partial synchronization* yields $0 < r < 1$, and will be further explained below. Thus *synchronization in the mean-field KM (with $N = \infty$) is revealed by a non-zero value of the order parameter*. The concept of order parameter as a measure of synchronization is less useful for models with short-range coupling. In these systems, other concepts are more appropriate to study oscillator synchronization: global synchronization and clustering (Strogatz and Mirollo, 1988a,b). Global synchronization still means that all oscillators are phase-locked: $\dot{\theta}_i = 0$. *Clustering* means that there is a finite fraction of the oscillators having the same frequency (frequency synchronization) or, more generally, having the same average frequency $\tilde{\omega}_i$, defined by

$$\tilde{\omega}_i = \lim_{t\to\infty}\frac{1}{t}\int_0^t \dot{\theta}_i\,dt, \tag{6}$$

while the other oscillators may be out of synchrony. In systems with short-range coupling, more complex situations can happen. For example, the phases of a fraction of the oscillators can change at the same speed (and therefore partial synchronization occurs), while different oscillator groups have different speeds (and therefore their global order parameter is zero and incoherence results). See Section IV for details.

A continuity equation for the oscillator density can be found by noting that each oscillator in Eq. (1) moves with an angular or drift velocity $v_i = \omega_i + Kr\sin(\psi - \theta_i)$. Therefore the one-oscillator density obeys the continuity equation

$$\frac{\partial\rho}{\partial t} + \frac{\partial}{\partial\theta}\{[\omega + Kr\sin(\psi - \theta)]\,\rho\} = 0, \tag{7}$$

to be solved together with (5), with the normalization condition

$$\int_{-\pi}^{\pi}\rho(\theta, \omega, t)\,d\theta = 1, \tag{8}$$

and an appropriate initial condition. The system of equations (5) - (8) has the trivial stationary solution $\rho = 1/(2\pi)$, $r = 0$, corresponding to an angular distribution of the oscillators with equal probability in the interval $[-\pi, \pi]$. The oscillators then may run incoherently, as explained before, and therefore the trivial solution is also called the *incoherent solution*, or simply, *incoherence*. Let us now try to find a simple solution corresponding to oscillator synchronization. In the strong coupling limit, we have *global synchronization* (phase locking), so that all oscillators move with the same phase, $\theta_i = \psi$, which yields $r = 1$. For a finite coupling, we

may have a lesser degree of synchronization with a stationary amplitude $0 < r < 1$. How can we achieve this smaller value of the amplitude? A typical oscillator moving with velocity $v = \omega - Kr\sin(\theta - \psi)$ will become stably locked at an angle such that: $Kr\sin(\theta - \psi) = \omega$ and $-\pi/2 \leq (\theta - \psi) \leq \pi/2$. All such oscillators are locked in the natural laboratory frame of reference. Oscillators with frequencies satisfying $|\omega| > Kr$ cannot be locked. They rotate out of synchrony with the locked oscillators, and their stationary density obeys $v\rho = C$ (constant) according to Eq. (7). We have obtained a stationary state of *partial synchronization*, in which part of the oscillators are locked at a fixed phase while all others are rotating out of synchrony with them. The corresponding stationary density is therefore:

$$\rho = \begin{cases} \delta\left(\theta - \psi - \sin^{-1}(\frac{\omega}{Kr})\right)\, H(\cos\theta), & |\omega| < Kr, \\ \frac{C}{|\omega - Kr\sin(\theta-\psi)|} & \text{elsewhere.} \end{cases} \quad (9)$$

Here $H(x) = 1$ if $x > 0$ and $H(x) = 0$ otherwise is the Heaviside unit step function. Notice that we may equivalently write $\rho = \sqrt{K^2r^2 - \omega^2}\,\delta(\omega - Kr\sin(\theta - \psi))\,H(\cos\theta)$ for $-Kr < \omega < Kr$. The normalization condition $\int_{-\pi}^{\pi} e^{i\theta}\rho(\theta,\omega,t)\,d\theta = 1$ for each frequency yields $C = \sqrt{\omega^2 - (Kr)^2}/(2\pi)$.

We can now calculate the order parameter in the state of partial synchronization by using (5) and (9):

$$\begin{aligned} r &= \int_{-\pi/2}^{\pi/2}\int_{-\infty}^{\infty} e^{i(\theta-\psi)}\delta\left(\theta - \psi - \sin^{-1}(\frac{\omega}{Kr})\right) g(\omega)d\theta d\omega \\ &+ \int_{-\pi}^{\pi}\int_{|\omega|>Kr} e^{i(\theta-\psi)}\,\frac{C\,g(\omega)}{|\omega - Kr\sin(\theta-\psi)|}d\theta d\omega \quad (10) \end{aligned}$$

Let us assume that $g(\omega) = g(-\omega)$. Then the symmetry $\rho(\theta + \pi, -\omega) = \rho(\theta,\omega)$ implies that the second term in this equation is zero. The first term is simply

$$\begin{aligned} r &= \int_{|\omega|<Kr} \cos\left(\sin^{-1}(\frac{\omega}{Kr})\right)\, g(\omega)\,d\omega \\ &= \int_{-\pi/2}^{\pi/2} \cos\theta\, g(Kr\sin\theta)\, Kr\cos\theta\, d\theta, \end{aligned}$$

that is,

$$r = Kr\int_{-\pi/2}^{\pi/2}\cos^2\theta\, g(Kr\sin\theta)\,d\theta. \quad (11)$$

This equation has always the trivial solution $r = 0$ corresponding to incoherence, $\rho = (2\pi)^{-1}$. However, it also has a second branch of solutions, corresponding to the partially synchronized phase (9), satisfying

$$1 = K\int_{-\pi/2}^{\pi/2}\cos^2\theta\, g(Kr\sin\theta)\,d\theta. \quad (12)$$

This branch bifurcates continuously from $r = 0$ at a value $K = K_c$ obtained by setting $r = 0$ in (12), which yields $K_c = 2/[\pi g(0)]$. This formula and the argument leading to it were first found by Kuramoto (1975). The example of a Lorentzian frequency distribution,

$$g(\omega) = \frac{\gamma/\pi}{\gamma^2 + \omega^2}, \quad (13)$$

allows explicit calculations of the integrals we have been finding and was already used by Kuramoto (1975). Using Eq. (13), he found the exact result $r = \sqrt{1 - (K_c/K)}$ for all $K > K_c = 2\gamma$.

For a general frequency distribution $g(\omega)$, an expansion of the right side of Eq. (11) in powers of Kr yields the scaling law

$$r \sim \sqrt{\frac{8(K - K_c)}{-K_c^3 g''(0)}}\,, \quad (14)$$

as $K \to K_c$. Recall the definitions of the symbol $\sim$ (asymptotic) comparing two functions or one function and an asymptotic series in the limit as $\epsilon \to 0$:

$$f(\epsilon) \sim g(\epsilon) \Leftrightarrow \lim_{\epsilon\to 0}\frac{f(\epsilon)}{g(\epsilon)} = 1, \quad (15)$$

$$f(\epsilon) \sim \sum_{k=0}^{\infty}\epsilon^k f_k \Leftrightarrow [f(\epsilon) - \sum_{k=0}^{m}\epsilon^k f_k] \ll \epsilon^m, \forall m. \quad (16)$$

According to (14), the partially synchronized phase bifurcates supercritically for $K > K_c$ if $g''(0) < 0$, and subcritically for $K < K_c$ if $g''(0) > 0$, cf. Figs. 1(a) and (b). Notice that Kuramoto's calculation of the partially synchronized phase does not indicate whether this phase is stable, either globally or even locally.

B. Stability of solutions and open problems

1. Synchronization in the limit $N = \infty$

Kuramoto's original construction of incoherent and partially synchronized phases was purely stationary and did not establish their stability properties. The linear stability theory of incoherence was published by Strogatz *et al.* (1992) and interesting work on the unsolved problems of nonlinear stability theory has been carried out by Balmforth and Sassi (2000).

To ascertain the stability properties of the incoherent and partially synchronized solutions, it is better to work with the probability density $\rho(\theta,\omega,t)$. Let us explain first what is known in the limit of infinitely many oscillators described by Equations (5) - (7). The linearized stability problem for this case is obtained by inserting $\rho = 1/(2\pi) + \tilde{\mu}(\theta,t;\omega)$ with $\tilde{\mu}(\theta,t;\omega) = \exp(\lambda t)\,\mu(\theta,\omega)$ in (5) - (8), and then ignoring terms nonlinear in μ:

$$\begin{aligned} &-\omega\frac{\partial\mu}{\partial\theta} + \frac{K}{2\pi}\,\mathrm{Re}\,e^{-i\theta}\int_{-\pi}^{\pi}\int_{-\infty}^{+\infty} e^{i\theta'}\,\mu(\theta',\omega') \\ &\times g(\omega')d\theta' d\omega' = \lambda\mu, \quad (17) \\ &\int_{-\pi}^{\pi}\mu(\theta,\omega)\,d\theta = 0. \quad (18) \end{aligned}$$

If $\mathrm{Re}\lambda < 0$ for all possible λ, incoherence is linearly stable, but it is unstable if some admissible λ has positive real part. The periodicity condition implies $\mu = \sum_{n=-\infty}^{\infty} b_n(\omega) e^{in\theta}$, which inserted in Eq. (17) yields

$$(\lambda + in\omega)\, b_n = \frac{K}{2}\,(\delta_{n,1} + \delta_{n,-1})\,\langle 1, b_n\rangle. \qquad (19)$$

Here we have used that $b_{-n} = \overline{b_n}$ ($\overline{A}$ stands for the complex conjugate of A), and defined the scalar product

$$\langle \varphi, \psi\rangle = \frac{1}{2\pi}\int_{-\pi}^{\pi}\int_{-\infty}^{+\infty} \overline{\varphi(\theta,\omega)}\psi(\theta,\omega)\, g(\omega)\, d\omega\, d\theta. \quad (20)$$

Eq. (19) shows that $\lambda_n(\omega) = -in\omega$, with $n = \pm 1, \pm 2, \ldots$, belong to the continuum spectrum of the linear stability problem, provided ω is in the support of $g(\omega)$. In the case of an unimodal natural frequency distribution ($g(\omega)$ is even and non-increasing for positive ω), Strogatz *et al.* (1992) have shown that the incoherent solution is neutrally stable with the previously mentioned continuum spectrum on the imaginary axis if $K < K_c = 2/[\pi g(0)]$. For $K > K_c$, a positive eigenvalue appears (Strogatz *et al.*, 1992). Although incoherence is neutrally stable for $K < K_c$, the linearized order parameter $R(t) = \langle e^{-i\theta}, \tilde{\mu}(\theta, t; \omega)\rangle$ decays with time. This decay, due to phase mixing of integral superposition of modes in the continuum spectrum, is analogous to Landau damping in plasmas (Strogatz *et al.*, 1992). We may understand this by solving the linearized problem with initial condition $\tilde{\mu}(\theta, 0; \omega) = 2e^{i\theta}/[\pi(\omega^2+4)]$+cc for $g(\omega) = [\pi(1+\omega^2)]^{-1}$ and $K = 1$. The calculations can be carried out as indicated by Strogatz *et al.* (1992) and the result is

$$\begin{aligned}\tilde{\mu}(\theta, t; \omega) &= \left(\frac{18}{\omega^2+4} - \frac{5}{2i\omega - 1} + \frac{1}{2 - i\omega}\right)\frac{e^{i(\theta-\omega t)}}{9\pi} \\ &+ \frac{5e^{i\theta - t/2}}{9\pi(2i\omega - 1)} + \frac{e^{i\theta - 2t}}{9\pi(2 - i\omega)} + \mathrm{cc}, \qquad (21)\\ R(t) &= \frac{10}{9}e^{-t/2} - \frac{4}{9}e^{-2t}. \qquad (22)\end{aligned}$$

(Balmforth and Sassi, 2000). The function $\tilde{\mu}$ contains a term proportional to $e^{-i\omega t}$, which is non-decaying and non-separable and it does not correspond to a normal mode. As time elapses, this term becomes progressively more crenellated and, through increasing cancellations, integral averages of $\tilde{\mu}$ decay. Besides this, Eq. (21) contain two exponentially decaying terms that contribute to the order parameter (22). If $g(\omega)$ has bounded support, the order parameter may decay more slowly, algebraically with time (Strogatz *et al.*, 1992).

Numerical calculations for $K < K_c$ show that the order parameter $r(t)$ of the full KM behaves similarly to that of the linearized equation (Balmforth and Sassi, 2000). However, the probability density ρ may develop peaks in the (θ, ω) plane for intermediate times before decaying to incoherence as $t \to \infty$. See Fig. 6 of (Balmforth and Sassi, 2000). For $K > K_c$, Balmforth and Sassi (2000) show that the probability density evolves to a distribution that corresponds to Kuramoto's partially synchronized phase given by Eq. (9). Balmforth and Sassi (2000) obtained this result by numerically simulating the full KM with $K > K_c$. They also carried out different incomplete exact and perturbation calculations :

- Exact solution of the KM model for $g(\omega) = \delta(\omega)$.
- Attempted approximation of the solution for other frequency distributions near K_c assuming an unrealistic r that depends on ω.
- Regularizing the KM by adding a diffusive term to Eq. (7), and constructing the stationary probability density in the limit of vanishing diffusivity by means of boundary layer methods. This regularization corresponds to adding white noise forcing terms to the KM (1). The corresponding equation for the probability density is (7) with a diffusive term in its right hand side, which is called the nonlinear Fokker-Planck equation (NLFPE). The NLFPE will be studied in Section III.
- A mixture of multiple scales and boundary layer ideas in the same limit of vanishing diffusivity of the NLFPE but for K near values corresponding to the bifurcation of synchronized states from incoherence.

In the small diffusivity limit of the NLFPE, $D \to 0+$, the calculations by Balmforth and Sassi (2000) indicate that the probability density of the KM with unimodal frequency distribution and $K > K_c$ tends toward a stationary phase which is concentrated around the curve $\omega = Kr\sin\theta$ for $\omega^2 < K^2r^2$. The peak of the probability density is reached at $\sqrt{Kr/(2\pi D)}$. It would be useful to have consistent perturbation results for the evolution of the probability density near bifurcation points in the small noise limit $D \to 0+$ of the NLFPE and also for the KM with $D = 0$. Both cases are clearly different as shown by the fact that the synchronized phase is a distribution for the case $D = 0$ and a smooth function for $D > 0$. In particular, it is clear that Kuramoto's partial synchronization solution (9) (involving a delta function) cannot be obtained by small amplitude bifurcation calculations about incoherence, the laborious attempt by Crawford and Davies (1999) notwithstanding.

Thus understanding synchronization in the hyperbolic limit of the mean-field KM (with $N \to \infty$) requires the following. Firstly, a fully consistent asymptotic description of the synchronized phase and the synchronization transition as $D \to 0+$ should be found. As indicated by Balmforth and Sassi (2000), the necessary technical work involves boundary layers and matching. These calculations could be easier if one works directly with the equations for $\ln\rho$, as suggested in the early paper (Bonilla, 1987). Secondly and most likely harder, the same problems should be tackled for $D = 0$, where the stable synchronized phase is expected to be Kuramoto's partially

synchronized state (which is a distribution, not a smooth function). Thirdly, the problem of proving stability of the partially synchronized state remains open, and its solution could lead to interesting results in Analysis as pointed out by Strogatz (2000).

2. Finite size effects

Another way to regularize the hyperbolic problem (5) - (8) is to study a large population of finitely many phase oscillators, which are globally coupled to its mean field. The analysis of this large system may shed some light on the stability properties of the partially synchronized state. The question can be posed as follows. What is the influence of finite size effects on Kuramoto's partially synchronized state as $N \to \infty$?

One issue with kinetic equations describing populations of infinitely many elements is always that of finite size effects. This issue was already raised by Zermelo's paradox, namely that a system of finitely many particles governed by reversible classical Hamiltonian mechanics was bound to have recurrences according to Poincare's recurrence theorem. Then this system would come back arbitrarily close to its initial condition infinitely many times. Boltzmann's answer to this paradox was that the recurrence times would become infinite as the number of particles tend to infinite. Simple model calculations illustrate the following fact. A *non-recurrent* kinetic description for a system of infinitely many particles approximates the behavior of a system with a large but finite number of particles during finite time intervals, after which recurrences set in (Keller and Bonilla, 1986).

The same behavior denoting the non-commutativity of the limits $N \to \infty$ and $t \to \infty$ is also present in the KM. For instance, Hemmen and Wreszinski (1993) used a Lyapunov function argument to point out that a population of finitely many Kuramoto oscillators would reach a stationary state as $t \to \infty$. Our derivation of the NLFPE in Appendix A suggests that fluctuations scale as $N^{-\frac{1}{2}}$ as $N \to \infty$, a scaling that, for the order parameter, is confirmed by numerical simulations (Daido, 1990; Kuramoto and Nishikawa, 1987).

More precise theoretical results are given by DaiPra and den Hollander (1996) for rather general mean field models that include Kuramoto's and also spin systems. Their paper is hard to read because of the cumbersome probabilistic notation they employ. In any case, DaiPra and den Hollander (1996) obtain a central limit theorem that characterizes fluctuations about the one-oscillator probability density for $N = \infty$ as Gaussian fields having a certain covariance matrix and scaling as $N^{-\frac{1}{2}}$. Near bifurcation points, a different scaling is to be expected, by analogy with Dawson's results for related mean-field models (Dawson, 1983). Daido (1987b, 1989) explored this issue by dividing the oscillator phase and the order parameter (2) in two parts: its limit as $N = \infty$ and a fluctuating part (which was regarded as small). In the equations for the phase fluctuations, only terms linear in the fluctuation of the order parameter were retained. The result was then inserted in (2) and a self-consistent equation for the fluctuation of the order parameter was found. For unimodal frequency distributions, Daido found the scaling $[(K_c - K)N]^{-\frac{1}{2}}$ for the rms fluctuation of the order parameter as $K \to K_c-$ (from below). For coupling constants larger than K_c, he found that the fluctuation of the order parameter was consistent with the scaling $(K - K_c)^{-\frac{1}{8}} N^{-\frac{1}{2}}$ as $K \to K_c+$ (Daido, 1989). This part of Daido's analysis seems less reliable because the basic state in the limit $N = \infty$ is Kuramoto's partially synchronized state and an additional ansatz on the fluctuations about this state had to be made. Balmforth and Sassi (2000) carried out numerical explorations of finite size effects and discussed how sampling the natural frequency distribution influences the one-oscillator density. In particular, they find that sampling may give rise to unexpected effects, such as time-periodic synchronization even for populations with unimodal $g(\omega)$ (for which these effects do not appear in the limit $N = \infty$). Further work in this area would be interesting, in particular finding a formulation similar to Daido's fluctuation theory for the order parameter but for the one-oscillator probability density instead.

III. THE MEAN FIELD MODEL INCLUDING WHITE NOISE FORCES

In this Section, we analyze the mean-field KM with white noise forcing terms, which is easier to analyze than its zero noise limit, the usual KM. As a result, our understanding of the noisy model is more complete. In the limit of infinitely many oscillators, the one-oscillator probability density obeys a parabolic equation (the nonlinear Fokker-Planck equation), and not the hyperbolic equation (7) which is harder to study. The NLFPE is derived in Appendix A. The simplest solution of the NLFPE is also $\rho = (2\pi)^{-1}$, corresponding to incoherent motion of the oscillators. Firstly, we shall study its linear stability properties and show that it is *linearly stable* for sufficiently small coupling constant, unlike what happens in the KM for which incoherence is *neutrally stable* if $K < K_c$. For values of the coupling constant above a critical one, incoherence becomes linearly unstable as one or more eigenvalues in the discrete spectrum of the linearized problem acquire a positive real part. Then different bifurcation scenarios and phase diagrams occur depending on the distribution of natural frequencies $g(\omega)$. Synchronized phases can be constructed as they bifurcate from incoherence by different singular perturbation techniques. We use a particularly powerful technique, the Chapman-Enskog method, to study in detail these synchronization transitions for a bimodal frequency distribution which has a very rich phase diagram.

A. The nonlinear Fokker-Planck equation

If we add white noise forcing terms to the mean-field KM, the result is the system of stochastic differential equations:

$$\dot{\theta}_i = \omega_i + \xi_i(t) + \frac{K}{N}\sum_{j=1}^{N}\sin(\theta_j - \theta_i), \quad i = 1, \ldots, N. \quad (23)$$

Here ξ_i are independent white noise processes with expected values

$$\langle \xi_i(t) \rangle = 0, \quad \langle \xi_i(t)\xi_j(t') \rangle = 2D\delta(t-t')\,\delta_{ij}. \quad (24)$$

Introducing the order parameter (4), the model equations (23)-(24) can be written as follows:

$$\dot{\theta}_i = \omega_i + Kr\sin(\psi - \theta_i) + \xi_i(t), \quad i = 1, 2, \ldots, N. \quad (25)$$

The Fokker-Planck equation for the one-oscillator probability density $\rho(\theta, \omega, t)$ corresponding to this stochastic equation is

$$\frac{\partial \rho}{\partial t} = D\frac{\partial^2 \rho}{\partial \theta^2} - \frac{\partial}{\partial \theta}(v\rho), \quad (26)$$

$$v(\theta, \omega, t) = \omega + Kr\sin(\psi - \theta), \quad (27)$$

provided the order parameter $re^{i\psi}$ is a known function of time and we ignore the subscript i. In the limit $N \to \infty$ and provided all oscillators are initially independent, we can derive Eq. (5):

$$re^{i\psi} = \int_{-\pi}^{\pi}\int_{-\infty}^{+\infty} e^{i\theta}\rho(\theta, \omega, t)g(\omega)\, d\theta\, d\omega, \quad (28)$$

which together with (26) constitute the NLFPE (see Appendix A for details). Notice that Equation (26) becomes (7) if $D = 0$. The system (26) - (28) is to be solved with the normalization condition

$$\int_{-\pi}^{\pi} \rho(\theta, \omega, t) d\theta = 1, \quad (29)$$

the periodicity condition, $\rho(\theta + 2\pi, \omega, t) = \rho(\theta, \omega, t)$, and an appropriate initial condition for $\rho(\theta, \omega, 0)$. The natural frequency distribution $g(\omega)$ is a non-negative even function to be considered later.

B. Linear stability analysis of incoherence

The simplest solution of the NLFPE is $\rho_0 = 1/(2\pi)$, with order parameter $r = 0$, which represents incoherent or non-synchronized motion of all oscillators. A natural method to study how synchronized phases with $r > 0$ may issue from incoherence is to analyze its linear stability as a function of the parameters of the model, and then construct the possible solutions bifurcating from it. As explained in the previous Section, this program was already started by Kuramoto in the hyperbolic case $D = 0$. In the parabolic case $D > 0$, the first results were obtained by Strogatz and Mirollo (1991). The linearized stability problem for this case may be obtained by inserting $\rho = 1/(2\pi) + \tilde{\mu}(\theta, t; \omega)$ with $\tilde{\mu}(\theta, t; \omega) = \exp(\lambda t)\,\mu(\theta, \omega)$ in (26) and (28), and then ignoring terms nonlinear in μ:

$$D\frac{\partial^2 \mu}{\partial \theta^2} - \omega\frac{\partial \mu}{\partial \theta} + K\,\mathrm{Re}\left(e^{-i\theta}\langle e^{-i\theta'}, \mu\rangle\right) = \lambda\mu, \quad (30)$$

$$\int_{-\pi}^{\pi} \mu(\theta, \omega)\, d\theta = 0. \quad (31)$$

Incoherence is linearly stable if it is always $\mathrm{Re}\lambda < 0$, and it is unstable if some admissible λ has positive real part. The periodicity condition implies $\mu = \sum_{n=-\infty}^{\infty} b_n(\omega)e^{in\theta}$, which inserted in Eq. (30) yields

$$(\lambda + in\omega + n^2 D)\, b_n = \frac{K}{2}\,(\delta_{n,1} + \delta_{n,-1})\,\langle 1, b_n\rangle. \quad (32)$$

Here we have used that $b_{-n} = \overline{b_n}$, and the scalar product (20). Similarly to the KM, the numbers

$$\lambda_n(\omega) = -D\,n^2 - in\omega, \quad n = \pm 1, \pm 2, \ldots, \quad (33)$$

with ω belonging to the support of $g(\omega)$, constitute the continuous spectrum of the linear stability problem. In fact, a nonhomogeneous linear problem with a homogeneous part given by (32) cannot be solved for an arbitrary source term if $\lambda = \lambda_n$. Notice that the continuous spectrum lies to the left side of the imaginary axis if $D > 0$ ($b_0 = 0$ because of the normalization condition (31)). Then the "eigenvalues" (33) have negative real parts (and therefore correspond to stable modes).

The case $n = \pm 1$ is special for two reasons. Firstly, the right hand side of Eq. (32) is no longer zero and we obtain $b_1 = (K/2)\langle 1, b_1\rangle/(\lambda + i\omega + D)$. Then, provided $\langle 1, b_1\rangle \neq 0$, we find the following equation (Strogatz and Mirollo, 1991):

$$\frac{K}{2}\int_{-\infty}^{+\infty} \frac{g(\nu)}{\lambda + D + i\nu}\, d\nu = 1. \quad (34)$$

The solutions of this equation are the eigenvalues of the linear stability problem (30) (independent of ω). Since the continuous spectrum lies on the left half plane, the discrete spectrum determines the linear stability of the incoherence solution. Secondly, the NLFPE and therefore the linear stability equation (30) are invariant under the reflection symmetry, $\theta \to -\theta$, $\omega \to -\omega$ because $g(\omega)$ is even. This implies that there are two independent eigenfunctions corresponding to each simple solution λ of (34):

$$\mu_1(\theta, \omega) = \frac{\frac{K}{2}\,e^{i\theta}}{D + \lambda + i\omega}, \quad \mu_2(\theta, \omega) = \frac{\frac{K}{2}\,e^{-i\theta}}{D + \lambda - i\omega}. \quad (35)$$

Notice that these two linearly independent eigenfunctions are related by the reflection symmetry. When λ is real, these eigenfunctions are complex conjugate of each other. When λ is a multiple solution of Eq. (34), the eigenvalue λ is no longer semisimple (Crawford, 1994).

C. The role of $g(\omega)$: Phase diagram of the Kuramoto model

The mean-field KM for infinitely many oscillators may have different stable solutions (also called *phases*) depending on the natural frequency distribution $g(\omega)$, the values of the coupling constant K, and the diffusivity D. Many phases appear as stable solutions bifurcating from known particular solution that loses its stability at a critical value of a parameter. The simplest solution of the NLFPE is incoherence, and therefore much effort has been devoted to studying its stability properties depending on K, D and parameters characterizing $g(\omega)$. As explained in Section II, we can always consider that the first moment of $g(\omega)$ is zero, shifting the oscillator phases if necessary. Most of the work reported in the literature refers to even $g(\omega)$, with $g(-\omega) = g(\omega)$. In addition, if $g(\omega)$ has a single maximum at $\omega = 0$, we call it a *unimodal frequency distribution*. For general even unimodal frequency distributions, Strogatz and Mirollo (1991) proved that the eigenvalue equation (34) has *at most one* solution, which is necessarily real and it satisfies $\lambda + D > 0$. Explicit calculations can be carried out for discrete ($g(\omega) = \delta(\omega)$) and Lorentzian ($g(\omega) = (\gamma/\pi)/(\omega^2 + \gamma^2)$) frequency distributions. We find $\lambda = -D - \gamma + K/2$, with $\gamma = 0$ for the discrete distribution. Clearly, incoherence is linearly stable for points (K, D) above the critical line $D = -\gamma + K/2$, and unstable for points below this line, cf. Fig. 1(c). In terms of the coupling constant, incoherence is linearly stable if $K < K_c \equiv 2D + 2\gamma$, and unstable otherwise. This conclusion also holds for $D = 0$ in the general unimodal case, for which Strogatz and Mirollo (1991) proved Kuramoto's result $K_c = 2/[\pi g(0)]$ ($K_c = 2\gamma$ in the Lorentzian example). In the case $D = 0$, the stability analysis is complicated by the fact that the continuous spectrum lies on the imaginary axis.

For even or asymmetric multimodal frequency distributions, the eigenvalues may be complex (Bonilla *et al.*, 1992). The simple discrete bimodal distribution $g(\omega) = [\delta(\omega - \omega_0) + \delta(\omega + \omega_0)]/2$ has been studied extensively (Acebrón and Bonilla, 1998; Bonilla *et al.*, 1992, 1998b; Crawford, 1994). In this case, Eq. (34) has two solutions $\lambda^{\pm} = -D + [K \pm \sqrt{K^2 - 16\omega_0^2}]/4$. The stability boundaries for the incoherent solution can be calculated by equating to zero the greatest of $\mathrm{Re}\lambda^+$ and $\mathrm{Re}\lambda^-$. The resulting *phase diagram* (K, D) is depicted in Fig. 2 (Bonilla *et al.*, 1992). If the coupling is small enough ($K < 2D$), incoherence is linearly stable for all ω_0, whereas it is always unstable if the coupling is strong enough, $K > 4D$. For intermediate couplings, $2D < K < 4D$, incoherence may become unstable in two different ways. For $\omega_0 < D$, $\lambda^{\pm}$ are real and incoherence is linearly stable provided $K < K_c = 2D\,[1 + (\omega_0/D)^2]$, and unstable if $K > K_c$. For $\omega_0 > D$, $\lambda^{\pm}$ are complex conjugate and they have zero real parts at $K_c = 4D$.

What happens in regions of the phase diagram where incoherence is unstable? Typically there appear stable solutions with $r > 0$, which correspond to synchronized phases. As discussed below, their study has been made by means of bifurcation theory for parameter values close to critical lines of the phase diagram where incoherence is neutrally stable. These analytical results are supplemented by numerical solution of the NLFPE far from critical lines or by numerical continuation of synchronized solutions bifurcating from incoherence (Acebrón *et al.*, 2001a). Besides this, Acebrón and Bonilla (1998) found a singular perturbation method that describes synchronization for multimodal $g(\omega)$ arbitrarily far from critical lines. The idea is to consider a $g(\omega)$ that has m maxima located at $\omega_0\Omega_l$, where $\omega_0 \to \infty$: $g(\omega)d\omega \sim \sum_{l=1}^{m} \alpha_l \delta(\Omega - \Omega_l)d\Omega$, and then use a method of multiple scales. The main result is that the solution of the NLFPE splits (at lowest order) in l phases, each obeying a NLFPE with a discrete unimodal frequency distribution centered at Ω_l and a coupling constant $\alpha_l K$. Depending on the value of $\alpha_l K$, the lth phase is either synchronized or incoherent. The order parameter is sum of the order parameters of the corresponding phases, each with weight α_l. If first order terms are also included, the results of the multiple scales method describe rather well incoherence and oscillator synchronization for multimodal frequency distributions (both with or without reflection symmetry), even for relatively low values of ω_0 (Acebrón and Bonilla, 1998). Related work on multimodal frequency distributions include (Acebrón *et al.*, 1998, 2001a). An interesting open problem is to generalize the method of Acebrón and Bonilla (1998) so that both the location and the width of the peaks in $g(\omega)$ are taken into account.

D. Synchronized phases as bifurcations from incoherence, $D \neq 0$

At the parameter values for which incoherence ceases to be linearly stable, synchronized phases (stable solutions of the NLFPE $\rho(\theta, \omega, t)$ with $r > 0$) may bifurcate from it. In this rather technical subsection, we shall construct these bifurcating solution branches in the vicinity of the bifurcation point by means of the Chapman-Enskog method, as explained by Bonilla (2000). We shall study the KM model with the discrete bimodal natural frequency distribution, whose phase diagram is depicted in Fig. 2. The stability boundaries in this rich phase diagram separate regions where incoherence is unstable to either stationary modes if $\omega_0 < D$, and $K > K_c = 2D\,[1 + (\omega_0/D)^2]$, or to oscillatory modes if $\omega_0 > D$, and $K > K_c = 4D$. The bifurcating solutions are as follows:

1. If $\omega_0 < D/\sqrt{2}$, the synchronized phases bifurcating from incoherence are stationary and stable. The bifurcation is supercritical: the synchronized phases exist for $K > K_c$.

2. If $D/\sqrt{2} < \omega_0 < D$, the bifurcation is subcritical:

an unstable branch of synchronized stationary solutions bifurcates for $K < K_c$, reaches a limit point at a smaller coupling constant, and there it coalesces with a branch of stable stationary stationary solutions having larger r.

3. If $\omega_0 > D$, the synchronized phases bifurcating from incoherence are oscillatory and have a time-periodic order parameter. Two branches of solutions bifurcate supercritically at $K_c = 4D$: a branch of unstable rotating waves and a branch of stable standing waves.

4. At the special point $\omega_0 = D/\sqrt{2}$ and $K_c = 3D$, the bifurcation to stationary solutions changes from super to subcritical. Near this point, we can extend our bifurcation analysis to describe analytically how the subcritical branch of stationary solutions turns into a branch of stable solutions at a limit point.

5. At the special point $\omega_0 = D$ and $K_c = 4D$, which we call *the tricritical point*, a line of Hopf bifurcations coalesces with a line of stationary bifurcations and a line of homoclinic orbits. The study of the corresponding $O(2)$-symmetric Takens-Bogdanov bifurcation indicates how the oscillatory branches die at a homoclinic orbit of an unstable stationary solution.

The Chapman-Enskog method is flexible enough to analyze all these bifurcations and, at the same time, simpler than alternatives such as constructing the center manifold (Crawford, 1994). Except at the two special bifurcation points, the simpler method of multiple scales explained in Appendix B yields the same results (Bonilla *et al.*, 1992, 1998b). The Chapman-Enskog method (Chapman and Cowling, 1970) was originally employed by Enskog (1917) in the study of the hydrodynamic limit of the Boltzmann equation. It becomes the averaging method for nonlinear oscillations (Bogoliubov and Mitropolsky, 1961), and it is equivalent to assuming a center manifold in bifurcation calculations (Crawford, 1994).

1. Bifurcation of a synchronized stationary phase

Let $\omega_0 < D$ and consider K close to its critical value $K_c = 2D\,[1 + (\omega_0/D)^2]$. The largest eigenvalue satisfies $\lambda \sim (K - K_c)/[2(1 - \omega^2/D^2)]$ as $K \to K_c$. As indicated in Eq. (35), there are two eigenfunctions associated to this eigenvalue, $e^{i\theta}/(D + i\omega)$ and its complex conjugate. Except for terms decaying exponentially fast in time, the solution of the linearized stability problem at $K = K_c$ is therefore $A\,e^{i\theta}/(D + i\omega)$+cc, where A is a constant and cc means complex conjugate of the preceding term. Let us now suppose that $K = K_c + \varepsilon^2 K_2$, where ε is a positive small parameter and this scaling for K will be explained later. The probability density corresponding to initial conditions close to incoherence will have the form $\rho \sim (2\pi)^{-1} + \varepsilon\, A(\tau)\, e^{i\theta}/(D + i\omega)$+cc. The correction to incoherence will be close to the solution of the linearized stability problem, but now we can assume that the complex constant A varies slowly with time. How slowly? The linearized solution depends on time through the factor $e^{\lambda t}$, and $\lambda = O(K - K_c) = O(\varepsilon^2)$, so that we can assume $\tau = \varepsilon^2 t$. Then the probability density can be written as

$$\begin{aligned}\rho(\theta,\omega,t;\varepsilon) &\sim \frac{1}{2\pi}\left\{1 + \varepsilon\,\frac{A(\tau;\varepsilon)e^{i\theta}}{D+i\omega} + \text{cc}\right.\\ &\left. + \sum_{n=2}^{\infty}\varepsilon^n\,\rho_n(\theta,t,\omega;A,\overline{A})\right\}\\ &\sim \frac{1}{2\pi}\,\exp\left\{\varepsilon\,\frac{A(t;\varepsilon)e^{i\theta}}{D+i\omega} + \text{cc}\right.\\ &\left. + \sum_{n=2}^{\infty}\varepsilon^n\,\sigma_n(\theta,t,\omega;A,\overline{A})\right\}. \end{aligned} \tag{36}$$

The corrections to $1/(2\pi)$ can be telescoped in an exponential with small argument, which ensures that the probability density is always positive. Typically, the exponential ansatz increases the parameter region in which the asymptotic expansion is a good approximation to the probability density. The functions σ_n and ρ_n are related by the equations

$$\begin{aligned}&\sigma_1 = \rho_1 = \frac{A(t;\varepsilon)e^{i\theta}}{D+i\omega} + \text{cc}, \quad \rho_2 = \sigma_2 + \frac{\sigma_1^2}{2},\\ &\rho_3 = \sigma_3 + \sigma_1\sigma_2 + \frac{\sigma_1^3}{3!},\\ &\rho_4 = \sigma_4 + \sigma_1\sigma_3 + \frac{\sigma_2^2}{2} + \frac{\sigma_1^2\sigma_2}{2} + \frac{\sigma_1^4}{4!},\end{aligned} \tag{37}$$

and so on. They depend on a fast scale t corresponding to stable exponentially decaying modes, and *on a slow time scale through their dependence on A*. All terms in (36) which decrease exponentially in time will be omitted. In (36), the slowly varying amplitude A obeys the equation

$$\frac{dA}{d\tau} = \sum_{n=0}^{\infty}\varepsilon^n\,F^{(n)}(A,\overline{A}). \tag{38}$$

The functions $F^{(n)}(A,\overline{A})$ are determined from the conditions that ρ_n or σ_n be bounded as $t \to \infty$ (on the fast time scale), for fixed A, and periodic in θ. Moreover, they cannot contain terms proportional to the solution of the linearized homogeneous problem, $e^{\pm i\theta}/(D \pm i\omega)$, because all such terms can be absorbed in the amplitudes A or $\overline{A}$ (Bonilla, 2000). These two conditions imply that

$$\langle e^{-i\theta}, \rho_n\rangle = 0, \qquad n > 1. \tag{39}$$

The normalization condition (29) together with (36) imply

$$\int_{-\pi}^{\pi}\rho_n(\theta,t,\omega;A,\overline{A})\,d\theta = 0, \qquad n \geq 2. \tag{40}$$

To find ρ_n, we substitute (36) and (38) in (26) and (28) and use (39) to simplify the result. This yields the following hierarchy of linear nonhomogeneous equations:

$$\mathcal{L}\rho_2 \equiv (\partial_t - D\partial_\theta^2 + \omega\partial_\theta)\rho_2 + K_c\partial_\theta\left\{\mathrm{Im}e^{-i\theta}\langle e^{-i\theta'},\rho_2\rangle\right\}$$
$$= -K_c\partial_\theta\left\{\rho_1\mathrm{Im}\; e^{-i\theta}\langle e^{-i\theta'},\rho_1\rangle\right\} + \mathrm{cc}, \tag{41}$$

$$\begin{aligned}\mathcal{L}\rho_3 = &- K_c\,\partial_\theta\left\{\rho_2\mathrm{Im}\; e^{-i\theta}\langle e^{i\theta'},\rho_1\rangle\right\}\\ &- K_2\partial_\theta\mathrm{Im}\; e^{-i\theta}\langle e^{-i\theta'},\rho_1\rangle\\ &- F^{(0)}\,\partial_A\rho_1 + \mathrm{cc},\end{aligned} \tag{42}$$

and so on. Clearly, $\rho_1 = A(t)\,e^{i\theta}/(D+i\omega)$+cc obeys the linearized stability problem (30) with $\lambda = 0$, $\mathcal{L}\rho_1 = 0$ up to terms of order ε. Thus it is not obvious that each linear nonhomogeneous equation of the hierarchy has a bounded periodic solution. What is the necessary solvability condition to ensure that the linear nonhomogeneous equation,

$$\mathcal{L}\rho_n = h(\theta;\rho_1,\ldots,\rho_{n-1}) = Qe^{i\theta} + \ldots \tag{43}$$

has a solution of the required features?

To answer this question, we assume that in fact (43) has a bounded periodic solution of the form $\rho_n = Pe^{i\theta} + \ldots$. Then P is given by

$$P = \frac{K_c\langle 1,P\rangle}{2(D+i\omega)} + \frac{Q}{D+i\omega}, \tag{44}$$

wherefrom we obtain the *nonresonance condition*

$$\langle 1, \frac{Q}{D+i\omega}\rangle = 0, \tag{45}$$

first found by Bonilla *et al.* (1992). Notice that we obtain (45) even if $\langle 1,P\rangle \neq 0$. $e^{i\theta}$ times the term proportional to $\langle 1,P\rangle$ in (44) is a solution of $\mathcal{L}\rho = 0$ and should therefore be absorbed in the definitions of A and $\overline{A}$. This implies (39).

Inserting ρ_1 in the right side of (41), we find

$$\mathcal{L}\rho_2 = \frac{2A^2}{D+i\omega}e^{2i\theta} + \mathrm{cc}, \tag{46}$$

whose solution is

$$\rho_2 = \frac{A^2}{(D+i\omega)(2D+i\omega)}e^{2i\theta} + \mathrm{cc}. \tag{47}$$

We see that ρ_1 contains odd harmonics and ρ_2 contains even harmonics (a possible θ independent term is omitted in ρ_2 because of the normalization condition). A moment of reflection shows that this is true in general: ρ_{2n} contains harmonics $e^{i2j\theta}$, $j = 0,\pm1,\ldots,\pm n$, and ρ_{2n+1} contains harmonics $e^{i(2j+1)\theta}$, $j = -(n+1),\ldots,n$. The nonlinearity of the NLFPE causes resonant terms to appear in the equations for ρ_{2n+1}, and they have to be eliminated by the terms containing $F^{(2n)}$. Then we can set $F^{(2n+1)} = 0$ and we only need the scaling $K - K_c = O(\varepsilon^2)$. The ultimate reason for these cancellations is of course the $O(2)$ symmetry of our problem: the reflection symmetry and invariance under constant rotations, $\theta \to \theta + \alpha$ (Crawford, 1994).

Similarly, the nonresonance condition for (42) yields

$$\begin{aligned}F^{(0)} &= \langle 1, \frac{1}{(D+i\omega)^2}\rangle^{-1}\left[\frac{2K_2\,A}{K_c^2}\right.\\ &\left.-\langle 1, \frac{1}{(D+i\omega)^2(2D+i\omega)}\rangle\,A\,|A|^2\right]\\ &= \frac{K_2\,A}{2\left(1-\frac{\omega_0^2}{D^2}\right)} - \frac{2\left(1-\frac{2\omega_0^2}{D^2}\right)A\,|A|^2}{\left(1-\frac{\omega_0^2}{D^2}\right)\left(4+\frac{\omega_0^2}{D^2}\right)D}.\end{aligned} \tag{48}$$

Keeping this term in (38), we obtain $dA/d\tau \sim F^{(0)}$. This reduced equation has the stationary solution $|A| = \sqrt{(K_2D/4)[4+(\omega_0/D)^2]/[1-2(\omega_0/D)^2]}$. The order parameter corresponding to this solution is

$$r \sim \sqrt{\frac{(K-K_c)\,D\left(4+\frac{\omega_0^2}{D^2}\right)}{K_c^2\left(1-\frac{2\omega_0^2}{D^2}\right)}}, \tag{49}$$

which was obtained by Bonilla *et al.* (1992) using a different procedure. The solution (49) exists for $K > K_c$ (supercritical bifurcation) if $\omega_0 < D/\sqrt{2}$, whereas it exists for $K < K_c$ (subcritical bifurcation) if $\omega_0 > D/\sqrt{2}$. The amplitude equation (38) implies that the supercritical bifurcating solution is stable and that the subcritical solution is unstable.

We can describe the transition from super to subcritical bifurcation at $\omega_0 = D/\sqrt{2}$, $K_c = 3D$, by calculating $F^{(4)}$ and adding it to the right hand side of (38). As explained in Appendix C, the result is

$$\begin{aligned}\frac{dA}{d\tau} &= K_2\left(1-\varepsilon^2\frac{K_2-2\sqrt{2}\omega_2}{D}\right)A\\ &-\frac{4(7K_2-4\sqrt{2}\omega_2)\varepsilon^2}{9D^2}\,A\,|A|^2 - \frac{272\varepsilon^2}{171D^3}\,A\,|A|^4.\end{aligned} \tag{50}$$

The stationary solutions of this equation are the possible stationary synchronized phases. We see that stable phases bifurcate supercritically for $K_2 > 0$ if $K_2 > 2\sqrt{2}\omega_2$, whereas a branch of unstable stationary solutions bifurcates subcritically for $K_2 < 0$ if $K_2 < 2\sqrt{2}\omega_2$. This branch of unstable solutions coalesce with a branch of stable stationary synchronized phases at the limit point $K_2 \sim -19\varepsilon^2(7K_2 - 4\sqrt{2}\omega_2)^2/612$.

2. Bifurcation of synchronized oscillatory phases

The bifurcation at complex eigenvalues can be easily described by the same method. The main difference is

that now the different solution of the linearized problem:

$$\rho_1 = \frac{A_+(t)}{D+i(\Omega+\omega)}e^{i(\Omega t+\theta)} + \text{cc} + \frac{A_-(t)}{D+i(\Omega-\omega)}e^{i(\Omega t-\theta)} + \text{cc}, \quad (51)$$

where $\Omega^2 = \omega_0^2 - D^2$, $K_c = 4D$ and the eigenvalues with zero real part are $\lambda(K_c) = \pm i\Omega$. For the two slowly varying amplitudes we postulate equations of the form

$$\frac{dA_\pm}{d\tau} \sim \sum_{n=0}^{\infty} \varepsilon^{2n} F_\pm^{(2n)}(A_+, A_-, \overline{A_+}, \overline{A_-}). \quad (52)$$

Following the method already explained, the nonresonance conditions for Eq. (42), with σ_1 given by Eq. (51), yield $F_+^{(0)}$ and $F_-^{(0)}$. The corresponding amplitude equations are (Bonilla *et al.*, 1998b)

$$\dot{A}_+ = \alpha A_+ - (\beta|A_-|^2 + \gamma|A_+|^2)\, A_+,$$
$$\dot{A}_- = \alpha A_- - (\beta|A_+|^2 + \gamma|A_-|^2)\, A_-, \quad (53)$$

where $\dot{} = d/d\tau$, and

$$\alpha = \frac{1}{4} - \frac{iD}{4\Omega}, \quad \beta = \frac{D + i\frac{D^2+\omega_0^2}{\Omega}}{K_2\,(4D^2+\omega_0^2)},$$
$$\gamma = \frac{2(3D^2+4\omega_0^2) + iD\,\frac{3D^2+2\omega_0^2}{\Omega}}{DK_2\,(9D^2+16\omega_0^2)}. \quad (54)$$

To analyze the vector amplitude equations (53), we shall define the new variables

$$u = |A_+|^2 + |A_-|^2, \quad v = |A_+|^2 - |A_-|^2. \quad (55)$$

By using (53), we obtain the following system for u and v:

$$\dot{u} = 2\,\text{Re}\,\alpha\, u - \text{Re}(\gamma+\beta)\, u^2 - \text{Re}(\gamma-\beta)\, v^2,$$
$$\dot{v} = 2\,\text{Re}\,\alpha\, v - 2\,\text{Re}\,\gamma\, uv. \quad (56)$$

Clearly, $u = v$ or $u = -v$ correspond to *travelling wave* (TW) solutions with only one of the amplitudes $A_\pm$ being different from zero. $v \equiv 0$ corresponds to *standing wave* (SW) solutions: a combination of rotating and counter-rotating travelling waves with the same amplitude. We can easily find the phase portrait of Eqs. (56) corresponding to α, β and γ given by Eqs. (54) (see Fig. 3). Up to, possibly, a constant phase shift, we have the following explicit solutions

$$A_+(\tau) = \sqrt{\frac{\text{Re}\,\alpha}{\text{Re}\,\gamma}}\; e^{i\mu\tau}, \quad A_-(\tau) \equiv 0,$$
$$\mu = \text{Im}\,\alpha - \frac{\text{Im}\,\gamma}{\text{Re}\,\gamma}\,\text{Re}\,\alpha \quad (57)$$

(or $A_+(\tau) \equiv 0$ and $A_-(\tau)$ as $A_+(\tau)$ above) in the case of TW solutions, and

$$A_+(\tau) = A_-(\tau) = \sqrt{\frac{2\text{Re}\,\alpha}{\text{Re}\,(\gamma+\beta)}}\; e^{i\nu\tau},$$
$$\nu = \text{Im}\,\alpha - \frac{\text{Im}\,(\gamma+\beta)}{\text{Re}\,(\gamma+\beta)}\,\text{Re}\,\alpha \quad (58)$$

in the case of SW solutions. Notice that both SW and TW bifurcate supercritically with $\|r_{SW}\|/r_{TW} > 1$. $\text{Re}(\beta+\gamma)$ and $\text{Re}\gamma$ are both positive when $K_2 = 1$; whereas the square roots in (57) and (58) become pure imaginary if $K_2 = -1$. This indicates that the bifurcating branches cannot be subcritical. An analysis of the phase portrait corresponding to (56) shows that the SWs are always *globally stable*, while the TWs are *unstable*. Such result was first pointed out by Crawford (1994).

3. Bifurcation at the tricritical point

At the tricritical point, $K = 4D$, $\omega_0 = D$, a branch of oscillatory bifurcating phases coalesces with a branch of stationary bifurcating phases and a branch of homoclinic orbits, in a $O(2)$-symmetric Takens-Bogdanov bifurcation point. Studying the bifurcations in a vicinity of this point tells us how the stable and unstable branches of oscillatory phases, SW and TW respectively, end as the coupling is changed. Analyzing transitions at the tricritical point is a little more complicated because it requires changing the assumptions on the amplitude equation (Bonilla, 2000; Bonilla *et al.*, 1998b). First of all, at the tricritical point, $\langle 1, (D+i\omega)^{-2}\rangle = \text{Re}(D+iD)^{-2} = 0$. This innocent looking fact implies that the term $-F^{(0)}\partial_A\rho_1$ on the right side of (42) does not appear in the nonresonance condition and therefore using the same ansatz as in Eqs. (36) and (38) will not deliver an amplitude equation. Secondly, the oscillatory ansatz (51) breaks down too because $\Omega = 0$ at the tricritical point, and the factor multiplying A_- is simply the complex conjugate of the factor multiplying A_+. Thus there is only one independent complex amplitude and we are back to Eq. (36) How do we extricate ourselves from this predicament?

To succeed, we must recognize that there is a basic slow time scale in this region different from τ. The eigenvalues with largest real part are

$$\lambda = -D + \frac{K}{4} + i\sqrt{\omega_0^2 - \left(\frac{K}{4}\right)^2}$$
$$= i\varepsilon\sqrt{2D\left(\omega_2 - \frac{K_2}{4}\right)} + \frac{K_2\varepsilon^2}{4} + O(\varepsilon^3)$$

and its complex conjugate, provided $K - 4D = K_2\varepsilon^2$, $\omega_0 - D = \omega_2\varepsilon^2$ with $\omega_2 > K_2/4$. Therefore the time dependent factors $e^{\lambda t}$ appearing in the solution of the

linearized problem indicate that disturbances about incoherence vary on a slow time scale $T = \varepsilon t$ near the tricritical point. This leads to the following Chapman-Enskog ansatz:

$$\rho(\theta,\omega,t;\varepsilon) = \frac{1}{2\pi}\left\{1+\varepsilon\frac{A(T;\varepsilon)}{D+i\Omega}e^{i\theta}+\text{cc} + \sum_{j=2}^{4}\varepsilon^j\rho_j(\theta,t,T;A,\overline{A})+O(\varepsilon^5)\right\}, \quad (59)$$

$$\frac{d^2A}{dT^2} = F^{(0)}(A,\overline{A})+\varepsilon F^{(1)}(A,\overline{A})+O(\varepsilon^2), \quad (60)$$

The equation for A is second order [not first order as (38)] because resonant terms appear at $O(\varepsilon^3)$ for the first time, and they are proportional to $A_{TT} = d^2A/dT^2$. $F^{(0)}$ and $F^{(1)}$ are calculated in Appendix D. The resulting amplitude equation is

$$A_{TT}-\frac{D}{2}(K_2-4\Omega_2)A-\frac{2}{5}|A|^2A = \varepsilon\left(\frac{K_2}{2}A_T-\frac{23}{25D}|A|^2A_T-\frac{1}{5D}(|A|^2A)_T\right)+O(\varepsilon^2), \quad (61)$$

Equation (61) has the *scaled normal form* studied by Dangelmayr and Knobloch (1987) [cf. their equations (3.3), p. 2480]. Following these authors, we make the substitution

$$A(T;\varepsilon) = R(T;\varepsilon)e^{i\phi(T;\varepsilon)} \quad (62)$$

in Eq. (61), separate real and imaginary parts, and obtain the perturbed Hamiltonian system

$$R_{TT}+\frac{\partial V}{\partial R} = \varepsilon\left(\frac{K_2}{2}-\frac{38}{25D}R^2\right)R_T,$$
$$L_T = \varepsilon\left(\frac{K_2}{2}-\frac{28}{25D}R^2\right)L. \quad (63)$$

Here $L = R^2\phi_T$ is the angular momentum, and

$$V \equiv V(R) = \frac{L^2}{2R^2}-\frac{D}{4}\left(K_2-4\omega_2\right)R^2-\frac{R^4}{10} \quad (64)$$

is the potential. This system has the following special solutions:

(*i*) The *trivial solution*, $L = 0$, $R = 0$, which corresponds to the incoherent probability density, $\rho = 1/2\pi$. Such solution is stable for $K_2 < 0$ if $\omega_2 > 0$ and for $(K_2 - 4\omega_2) < 0$ if $\omega_2 < 0$.

(*ii*) The *steady-states* (SS), $L = 0$, $R = R_0 = \sqrt{5D\left(\omega_2-\frac{K_2}{4}\right)} > 0$, which exists provided that $\omega_2 > K_2/4$. This solution is always unstable.

(*iii*) The *travelling waves* (TW), $L = L_0 = R_0^2\sqrt{2D\left(\omega_2-\frac{19}{56}K_2\right)} > 0$, $R = R_0 = \frac{5}{2}\sqrt{\frac{DK_2}{14}} > 0$, which exist provided that $K_2 > 0$ and $\omega_2 > 19K_2/56$; these solutions bifurcate from the trivial solution at $K_2 = \omega_2 = 0$. When $\omega_2 = 19K_2/56$, the branch of TWs merges with the steady-state solution branch. This solution is always unstable.

(*iv*) The *standing waves* (SW), $L = 0$, $R = R(T)$ periodic. Such solutions have been found explicitly in Section 5.1 of (Dangelmayr and Knobloch, 1987). The SWs branch off the trivial solution at $K_2 = \omega_2 = 0$, exist for $\omega_2 > 11K_2/19 > 0$, and terminate by merging with a homoclinic orbit of the steady-state (*ii*) on the line $\omega_2 = 11K_2/19$ [see equation (5.8) of (Dangelmayr and Knobloch, 1987)]. This solution is always stable.

All these results are depicted in Fig. 4 below, which corresponds to Fig. 4, IV-, in the general classification (stability diagrams) reported in (Dangelmayr and Knobloch, 1987), p.267. The bifurcation diagram near the tricritical point for $\omega_0 > D$ fixed is depicted in Fig. 5. Notice that it agrees with the information specified above.

Note that equation (59) yields, to leading order,

$$\rho(\theta,\omega,t;\varepsilon) \sim \frac{1}{2\pi}\left[1+\varepsilon\frac{Re^{i(\phi+\theta)}}{D+i\omega}+cc\right], \quad (65)$$

and hence, from (28), $re^{i\psi} \sim \varepsilon Re^{-i\phi}/(2D)$. It follows that $r \sim R/(2D)$ and $\psi \sim -\phi$, which shows that, essentially, the solution $A(T;\varepsilon)$ to equation (61) coincides with the conjugate of the complex order parameter [defined by (28)]. For this reason, in Fig. 5 the ordinate can be either R or r. In Fig. 6, we have depicted the global bifurcation diagram which completes that shown in Fig. 5 of (Bonilla *et al.*, 1992).

In closing, the Chapman-Enskog method can be used to calculate any bifurcations appearing for other frequency distributions and related NLFPEs. As discussed in Section II.B, nontrivial extensions are needed in the case of the hyperbolic limit, $D \to 0+$.

IV. VARIATIONS OF THE KURAMOTO MODEL

We have seen during the preceding section how the long-range character of the coupling interaction in the KM allows to obtain many analytical results. Yet, one might ask how far the results there obtained do extend beyond the mean-field limit in finite dimensions. Also one might wonder how synchronization effects in the KM are modified by keeping long-range interactions but including additional sources of quenched disorder, multiplicative noise or time-delayed couplings. Unfortunately, many of the analytical techniques developed in the preceding section hardly cover many of these new topics. In particular, the treatment of short-range couplings (oscillators embedded in lattice with nearest-neighbor interactions) presents formidable difficulties both at the analytical and numerical level that challenges our current

understanding of the mechanisms behind the emergence of synchronization. The next sections are devoted to discuss several of these new cases. It is not exaggerated to say that our knowledge is still quite poor in many of these cases and that major work remains to be done.

A. Short-range models

A natural extension of the KM discussed in Sec. III includes short-range interaction effects (Daido, 1988; Sakaguchi *et al.*, 1987; Strogatz and Mirollo, 1988a,b). Kuramoto and coworkers (Sakaguchi *et al.*, 1987) have considered the case where oscillators occupy the sites of a d-dimensional cubic lattice and interactions occur between nearest neighbors,

$$\dot{\theta}_i = \omega_i + K \sum_{(i,j)} \sin(\theta_j - \theta_i) \tag{66}$$

where the pair (i, j) stands for nearest-neighbor oscillators and the ω_i are independent random variables chosen according to the distribution $g(\omega)$. Compared to the KM (23) the coupling parameter K has not to be scaled by the total number of oscillators. However, convergence of the model (66) in the large d limit requires K to scale like $1/d$. Although the model can be extended to include stochastic noise (i.e. at finite temperature) most of the work on this type of models has been done at $T = 0$. Solving the short-range version of the KM is a hopeless task (except for special cases such as one dimensional models -see below- or Cayley-tree structures) due to the difficulty to incorporate the randomness in any sort of renormalization-group analysis. In short-range systems one usually distinguishes between different synchronization regimes. Global synchronization, which implies that all the oscillators are in phase, is rarely seen except for $K \propto N \to \infty$. Phase locking or partial synchronization is observed more frequently. It denotes the situation where a local ensemble of oscillators verify $\dot{\theta}_i = const$, $\forall i$. A weaker situation concerns clustering or entrainment. Usually this term refers (although sometimes it has been used in the sense of phase locking) to the case where a finite fraction of the oscillators have the same average frequency $\tilde{\omega}_i$ defined by,

$$\tilde{\omega}_i = \lim_{t\to\infty} \frac{\theta_i(t)}{t} \tag{67}$$

There is no proof that such a limit exists. However, if it does not exist, synchronization is not possible whatsoever. The condition of clustering is less stringent than phase locking, therefore it is expected that its absence precludes the existence of phase locking. Note, that the previous definitions do not exhaust all possible types of synchronized stationary solutions, such as for instance, the existence of moving traveling wave structures. The concept of synchronization (global or partial) is different form the concept of phase coherence introduced in the context of the KM in Section 2, see equation (2). Phase coherence is a stronger condition than synchronization as it assumes that all phases θ_i are clustered around a given unique value and so are their velocities $\dot{\theta}_i$. The contrary is not necessarily true, as phases can change at the same speed (synchronization takes place) while having completely different values (incoherence). Coherence seems less general than synchronization as the former bears connection to the type of ferromagnetic ordering present in the KM. Although this type of ordering is expected to prevail in finite dimensions synchronization seems more appropriate to discuss oscillator models with structural disorder built in.

For short-range systems one would like to understand several questions such as,

- The existence of a lower critical dimension above which any kind of entrainment is possible. In particular, it is relevant to prove the existence of phase locking and clustering for large enough dimensionality and the differences between both types of synchronization.
- The topological properties of the entrained clusters and the possibility to define a dynamical correlation length describing the typical length scale of these clusters.
- The existence of an upper critical dimension above which the synchronization transition is of the mean-field type.
- The resulting phase diagram in the presence of thermal noise.

In (Sakaguchi *et al.*, 1987) the authors have proposed some heuristic arguments showing that any type of entrainment (global or local) can occur only for $d \geq 2$. This conjecture is supported by the absence of entrainment in one dimension. Strogatz and Mirollo (1988a,b) however, have shown that no phase locking can occur at any finite dimension. As phase locking occurs in mean-field theory this result suggests that the upper critical dimension in the model is infinite. Particularly interesting results are obtained in one dimension (a chain of oscillators). In this case, and for the case of a normal distribution of natural frequencies ω_i, it can be proven that the probability of phase locking vanishes for $N \to \infty$ and is only finite if $K \sim \sqrt{N}$. The same result can be obtained for any distribution (not necessarily Gaussian) of independently distributed natural frequencies, the proof consists of showing that the probability of phase locking is related to the probability that the height of a Brownian bridge [1]

[1] A Brownian bridge is defined as a Brownian motion described by n moves of length x_i extracted from a given probability distribution and where the end-to-end distance $l(n) = \sum_{i=1}^{n} x_i$ is constrained to have a fixed value for a given number n of steps.

is not larger than a maximal amount which depends on the parameter K and the mean value of the frequency distribution. However, one of the most interesting results in these studies is the use of block renormalization group arguments to show whether clustering can occur in finite dimensions. Nearly at the same time, Strogatz and Mirollo (1988a,b) and Daido (1988) have presented a similar argument but leading to slightly different yet compatible conclusions. In (Strogatz and Mirollo, 1988a,b) the goal is to calculate the probability $P(N,K)$ that a cubic region S containing a finite fraction αN ($\alpha < 1$) of the oscillators can be entrained into a single common frequency. Following to (Strogatz and Mirollo, 1988a,b) let us assume the macroscopic cluster S to be divided into cubic subclusters S_k of side l, the total number of subclusters being $N_s = \alpha N/l^d$ which is of order N. For each subcluster k the average frequency Ω_k and phase Θ_k are defined as follows,

$$\Omega_k = \frac{1}{l^d}\sum_{i\in S_k}\omega_i \quad ; \quad \Theta_k = \frac{1}{l^d}\sum_{i\in S_k}\theta_i \tag{68}$$

Summing (66) over all oscillators contained in each subcluster S_k we get,

$$\dot{\Theta}_k = \Omega_k + \frac{K}{l^d}\sum_{(i,j)\in\partial S_k}\sin(\theta_j-\theta_i) \tag{69}$$

where the sum in the r.h.s runs over all links (i,j) crossing the surface ∂S_k delimiting the region S_k. Because the sine function is bounded and there are $2dl^{d-1}$ terms in the surface this implies,

$$|\dot{\Theta}_k - \Omega_k| \leq \frac{2dK}{l} \tag{70}$$

If S is a region of clustered oscillators around the frequency $\tilde{\omega}$ then, after time averaging, the limit (67) gives $|\tilde{\omega}-\Omega_k| \leq \frac{2dK}{l}$ for all $1 \leq k \leq N_s$. Because the Ω_k are uncorrelated random variables, the probability that such a condition is simultaneously satisfied for all N_s oscillators is p^{N_s} (p being the typical probability that $|\tilde{\omega}-\Omega_k| \leq \frac{2dK}{l}$ is satisfied for a given oscillator). This probability is therefore exponentially small with the number of subclusters $N_s \sim O(N)$,

$$P(N,K) \sim N\exp(-cN) \tag{71}$$

where c is a constant and the multiplicative factor N in front of the exponential arises from the number of all possible ways the cluster S can be embedded into the lattice. Therefore, the probability vanishes in any dimension in the large population limit. This proof assumes that entrained clusters have a compact structure (such as a cubical shape). However, this must not be necessarily true. Had the clusters a non-compact shape (such as space filling sponges or lattice animal -tree like- structures) then the proof would not hold anymore (since the number of subclusters N_s must not necessarily scale like $1/l^d$). Therefore this result does not preclude the existence of macroscopic entrainment in non-compact clusters.

This result does not seem to be necessarily in contradiction with a very similar argument reported by Daido (1988) who has shown the existence of a lower critical dimension d_l depending upon the tails of a category of frequency distributions $g(\omega)$. For

$$g(\omega) \sim |\omega|^{-\alpha-1} \qquad |\omega| \gg 1 \tag{72}$$

then normalization requires $\alpha > 0$. Moreover, Daido considers that $\alpha \leq 2$ for distributions with an infinite variance, the limiting case $\alpha = 2$ corresponding to the case of a distribution with finite variance (such as the Gaussian distribution). The argument by Daido uses a similar block decimation procedure as outlined in eqs. (68,69), however he concludes differently than Strogatz and Mirollo (1988a,b). Having defined the subcluster or block frequencies Ω_k and phases Θ_k in (68), Daido shows that only for $d < \alpha/(\alpha-1)$, and in the $l \to \infty$ limit, (70) converges to the fixed point dynamical equation,

$$\dot{\Theta}_k = \Omega_k \qquad \forall k \tag{73}$$

showing that no clustering can occur for $0 < \alpha \leq 1$ in any dimension, however for $1 < \alpha \leq 2$ macroscopic entrainment should be observed for dimensions above $d_l = \frac{\alpha}{\alpha-1}$. For the Gaussian case, $\alpha = 2$ and entrainment occurs above $d_l = 2$ as suggested also in (Sakaguchi *et al.*, 1987). Numerical evidence in favor of a synchronization transition in $d = 3$ (Daido, 1988) does not appear much compelling. Overall the issue about the correct value of the upper critical dimension remains yet open.

The KM in an ultrametric tree has been also considered (Lumer and Huberman, 1991, 1992). The authors consider a general version of the model (66) where N oscillators sit in the leaves of a hierarchical tree of branching ratio b and L levels, see Figure 7. The coupling between oscillators K_{ij} is not uniform but depends on their ultrametric distance l_{ij}, i.e. the number of levels in the tree separating the leaves from its common ancestor,

$$K_{ij} = Kd(l_{ij}) \tag{74}$$

where $d(x)$ is a monotonically decreasing function of the distance. The existence of a proper thermodynamic limit requires, for $d(x)$ in the large L, N limits,

$$\sum_{i=1}^{N} K_{ij} = K \quad , \quad \forall j \tag{75}$$

For a given value of K, as the ultrametric distance l_{ij} increases, entrainment fades away, however as K increases more and more levels tend to synchronize. Therefore, this model introduces in a simple way the clusterization of synchronization, thought to be relevant in the perception problem at the neural level (see Sec. VII.A). The simplest function $d(x)$ that incorporates such effects is

an exponential decay $d(x) \sim 1/a^x$, where the coupling strength decreases by a factor a at consecutive levels. It can be shown (Lumer and Huberman, 1992) that a cascade of synchronization events occurs whenever $b \geq a^{\frac{\alpha}{\alpha-1}}$ where α is defined by (72). In that regime the model displays a nice devil staircase behavior when plotting the synchronization parameter as a function of K, characteristic of the emergent differentiation in the response of the system to an external perturbation. Other topologies of connections beyond the simple cubic lattice structure have been also considered. In (Niebur *et al.*, 1991b) the authors analyze spatial correlation functions in a square lattice of oscillators with nearest-neighbor, Gaussian (i.e. the intensity of the interaction between two sites decays with their distance according to a Gaussian law) and sparse connections (each oscillator is coupled to a small and randomly selected subset of neighbors). Overall, they find that entrainment is greatly enhanced with sparse connections. Whether this result is linked to the supposed non-compact nature of the clusters is yet to be seen.

An intermediate case between the long range KM and its short-range version (66) is when the couplings among oscillators decay as a power law $1/r^\alpha$ of their mutual distance r. The intensity of the coupling is then properly normalized in such a way that the interaction term in (66) remains finite in the large population limit. For the normalized case and in one dimension it has been shown (Rogers and Wille, 1996) that a synchronization transition occurs if $\alpha < \alpha_c(K)$ with $\alpha_c(K_c) = 2/[\pi g(\omega = 0)]$) corresponding to the KM (see paragraph just after formula (11)). It is found that $\alpha < 2$ is required for a synchronizing transition to occur at finite K, the same condition is found for one-dimensional (1D) Ising and XY models to have a finite-temperature transition. For the non-normalized case results are more interesting (Marodi *et al.*, 2002) as they show a transition in the population size (rather than in the coupling constant K) for $\alpha < d$. In that case, if the population is allowed to grow above a critical value $N_c(K, \alpha < d)$, synchronization occurs. The relevance of this result stems from the fact that large enough three dimensional populations of oscillators, interacting through a signal whose intensity decays like $1/r^2$ (e.g. sound or light), can synchronize whatever the value of the coupling K.

Before finishing this overview of short-range models let us mention that the complexity of the phenomenon of synchronization in two-dimensions has been emphasized in another study by Kuramoto and coworkers (Sakaguchi *et al.*, 1988) where they study a model where the coupling function has been slightly modified to account for an enhancement of the oscillator frequencies upon their interaction,

$$\dot{\theta}_i = \omega_i + K \sum_{(i,j)} \Big(\sin(\theta_j - \theta_i - \alpha) + \sin(\alpha) \Big) \qquad (76)$$

with $-\frac{\pi}{2} \leq \alpha \leq \frac{\pi}{2}$. Note that this is a non-variational model, i.e. the interaction term does not correspond to the gradient of a two-body potential. The effect of the parameter α is to decrease the entrainment between oscillators that have different natural frequencies, giving rise to a higher value of the critical coupling. Notably this model has been found to describe synchronization of Josephson junctions arrays (see (153) and ensuing discussion). The parameter α has an interesting effect already in the non-disordered model $\omega_i = 0$ (for $\alpha = 0$ this is the XY model) where neighboring phases inside a vortex can differ a lot, thereby inducing an increase in the local frequency. The vortex acts as a pacemaker enhancing entrainment in the surrounding medium.

B. Models with disorder

The standard Kuramoto model has already disorder built in. However one can include additional disorder in the coupling among the oscillators. Daido has considered the general mean-field model (Daido, 1992b),

$$\dot{\theta}_i = \omega_i + \sum_{(i,j)} K_{ij} \sin(\theta_j - \theta_i + A_{ij}) + \xi_i(t) \qquad (77)$$

where the couplings K_{ij} are Gaussian distributed,

$$P(K_{ij}) = \frac{N}{\sqrt{2\pi K^2}} \exp\Big(-\frac{N K_{ij}^2}{2K^2} \Big) \qquad (78)$$

the frequencies are distributed according to a distribution $g(\omega)$ and ξ is a Gaussian noise. The A_{ij} are real valued numbers that lie in the range $[-\pi, \pi]$ and stand for potential vector differences between sites which amount to random phase shifts [2]. The interest of this model lies in the fact that frustration, a new ingredient beyond disorder, is introduced. Frustration implies that the reference oscillator configuration that makes vanish the coupling term in (77) (i.e. the second term in the r.h.s of (77)) is incoherent, i.e. $\theta_i - \theta_j \neq 0$. This is due to the competing nature of the different terms involved in that sum that contribute with either a positive or a negative sign. This makes the reference configuration extremely hard to find using available optimization algorithms. Compared to the non disordered models, few studies have been devoted to the disordered case, however they are very interesting as they seem to display synchronization to a glassy phase rather than a ferromagnetic-like one. Moreover, as structural disorder tends to be widespread in many physical systems, disordered models do not seem

[2] Indeed the potential vector terms A_{ij} appearing in (79) can be thought as the difference of quenched potential vector values $A_{ij} = A_i - A_j$. As $\vec{H} = \nabla \times \vec{A}$ the circulation of the potential vector along an elementary plaquette or loop must be proportional to the value external field $\sum_{(i,j)\in\square} A_{ij} \propto |\vec{H}|$. In mean-field models there are loops of all possible lengths, the constraint cannot be satisfied for all plaquettes, so the A_{ij} are quenched variables usually taken from a random distribution.

to be less relevant to real oscillator systems than their ordered counterparts.

1. Disorder in the coupling: the oscillator glass model

The model (77) with disorder in the couplings K_{ij} and $A_{ij} = 0$ has been the subject of some recent works (Daido, 1987a, 1992b, 2000; Stiller and Radons, 1998, 2000). It is given by the expression,

$$\dot{\theta}_i = \omega_i + \sum_{(i,j)} K_{ij} \sin(\theta_j - \theta_i) + \xi_i(t) \qquad (79)$$

where the K_{ij} are given by (78). For $\omega_i = 0$ this is the XY spin-glass model (Kirkpatrick and Sherrington, 1978; Sherrington and Kirkpatrick, 1975) introduced to mimic the behavior of frustrated magnets. It is well known that XY spin-glass model has a transition at a critical noise intensity $D_c = 1$ from a paramagnetic ($D > D_c$) to a spin-glass phase ($D < D_c$). In the presence of frequencies a synchronization transition is expected to occur from an incoherent to a synchronized glassy phase. The most complete study (yet with contradictory results, see below) has been done without noise and for a normal frequency distribution $g(\omega)$ in two different works, one by Daido (1992b), the other by Stiller and Radons (1998). Daido (1992b) has performed a detailed numerical analysis of the distribution $p(h)$ of the local field h_j acting on each oscillator defined by,

$$p(h) = \frac{1}{N} \sum_{j=1}^{N} \delta(h - h_j) \qquad (80)$$

$$h_j = \frac{1}{K} \sum_{l=1}^{N} K_{jl} \exp(i\theta_l) \qquad (81)$$

Daido shows how $p(h)$ crosses, as the value of K is increased, from a pure Gaussian distribution (with its maximum located at $h^* = 0$) over a non-Gaussian function whose value h^* (where the maximum is located) becomes positive. This establishes the value of the critical coupling as $K_c \simeq 8$.

Glassy systems are known for their characteristic slow relaxational dynamics leading to phenomena such as aging in correlations and response functions and violations of the fluctuation-dissipation theorem (Crisanti and Ritort, 2003). Synchronization models are expected to show similar non-equilibrium relaxation phenomena (albeit aging is not expected to occur in the stationary state). In particular, Daido also considered the order parameter,

$$Z(t) = \frac{1}{N} \sum_{j=1}^{N} \exp(i\theta_j(t)) \qquad (82)$$

showing that $Z(t)$ decays exponentially with time in the incoherent phase ($K < K_c$) and as a power law of time in the synchronized phase. These results have been contested in a subsequent work by Stiller and Radons (1998) who have considered the analytical solution of the dynamics of the same model but using the path integral formalism of Martin-Siggia-Rose to reduce the N-oscillator problem to a single oscillator problem with some correlated noise. The resulting dynamical equations can be self-consistently solved by using the approach developed by Eisfeller and Opper for the Sherrington-Kirkpatrick model (Eissfeller and Opper, 1978). The advantage of this method is that one directly gets dynamical results in the infinite-size limit. The disadvantage is that the time required to solved the dynamics up to M time steps grow as M^2, therefore less than $M = 1000$ time steps can be typically solved. Stiller and Radons (1998) have suggested that a power law for $Z(t)$ is not observed above $K_c \sim 8$, however the results they report in favor of their claim are questionable. In particular Stiller and Radons dynamic calculations reach only time scales much smaller than those reached by Daido using Brownian simulations (see Sec. VI.A) who reaches times of order of 100 Monte Carlo steps. It is difficult to sustain a discussion on the asymptotic behavior of $Z(t)$ with the short timescales considered in both works. This issue has raised some controversy (Daido, 2000; Stiller and Radons, 2000) which has not been yet settled. Although Stiller and Radons conclude that theirs and Daido results might be compatible after all, the discrepancies turn out to be serious enough to question the validity of the results of one of the two works. Indeed, there is a discrepancy between the critical value K_c derived in both works from measurements in the stationary regime. Stiller and Radons have introduced the equivalent of the Edwards-Anderson parameter $\tilde{q}$ for the XY case,

$$\tilde{q} = \lim_{t\to\infty} \lim_{N\to\infty} \lim_{t_0\to\infty} ReC(t_0, t_0 + t) \quad , \qquad (83)$$

where $C(t, s)$ is the two-times complex-valued correlation function

$$C(t, s) = \frac{1}{N} \sum_{j=1}^{N} \exp(i(\theta(t) - \theta(s))) \quad . \qquad (84)$$

The order of the limits in (83) is important: the $t_0 \to \infty$ limit assures that the stationary regime is reached first, the $N \to \infty$ limit ensures ergodicity breaking and the $t \to \infty$ limit measures the equilibrium order within one ergodic component. Measurements of $\tilde{q}$ reveal a neat transition around $K_c = 24$ (Fig.3 in (Stiller and Radons, 1998)), nearly three times larger than the value reported by Daido (Fig. 2 in (Daido, 1992b)). The origin of this discrepancy is unknown to us. Further work is needed to resolve this question.

Before finishing this section let us mention that the study of the model (79) with site disordered couplings has been considered by Bonilla *et al.* (1993) for the KM with interactions of the Van Hemmen type $K_{ij} = \frac{K_0}{N} + \frac{K_1}{N}(\xi_i\eta_j + \eta_i\xi_j)$ where ξ_i, η_i are random independent

identically distributed quenched variables that may take values ± 1 with probability 1/2. The model is exactly solvable so the resulting phase diagram can be analytically computed. These authors find, depending on the ratio between K_0 and K_1, several phases: incoherence, synchronization, spin-glass phase and mixed phase where oscillators are partially coherently synchronized and partially in phase opposition.

2. The oscillator gauge glass model

The oscillator gauge glass model has been seldom studied. We quote it here for completeness. It corresponds to the model (77) where $K_{ij} = K/N$ and frustration arises solely from the random phase shifts $A_{ij} \in [-\pi, \pi]$ (see footnote 2). Note that this term by itself is enough to induce frustration. For instance, if $A_{ij} = 0$ or π with probability 1/2 then this model coincides with the previous oscillator glass model where $K_{ij} = \pm 1$ with identical probability. In general, for non-disordered models (in the absence of natural frequencies), and in the absence of an external magnetic field, the vector potential components around a plaquette add to zero. In the presence of a field this term is an integer number times the value of the quantized flux, therefore the present oscillator gauge glass model in two-dimensions can be seen as a simplified version of overdamped Josephson junctions arrays. We limit ourselves to mention a study (Park *et al.*, 1998) of the phase diagram of the oscillator gauge glass model by mapping it to an equilibrium gauge glass model where the stationary states are taken as the equilibrium states of the corresponding Boltzmann system. However, as has been already explained in Sec. VI.C, this approach does not guarantee a full characterization of the stationary solutions.

C. Time-delayed couplings

One of the most natural and well motivated extensions of the KM concerns the analysis of time-delayed coupling between oscillators. In biological networks, electric signals propagate along neural axons at a finite velocity. Thus delays due to transmission are natural elements in any theoretical approach to information processing. Time delays can change substantially the dynamical properties of coupled systems. In general, the dynamic behavior becomes much richer and in occasions even surprising. One might think that time delays tend to break or difficult coherence in populations of interacting units, but this is not always the rule of thumb. An important example has been the focus of intense research in the last years: synchronization in chaotic systems. It has been proved that a delayed coupling is the key element to anticipate and control the time evolution of coupled chaotic oscillators by synchronizing their dynamics (Pikovski *et al.*, 2001; Voss, 2001). In excitable systems the situation is quite similar. It has been reported that delayed couplings can favor the existence of rapid phase-locked behavior in networks of integrate and fire oscillators (Gerstner, 1996).

How important are time delays for a population of coupled phase oscillators? This depends on the ratio of the time delay to the natural period of a typical oscillator. In general, the delay should be kept if the transmission time lag is much longer than the oscillation period of a given unit, (Izhikevich, 1998). On the other hand, the delay can be neglected if it is comparable to the period of the oscillators.

Let us start by discussing the dynamic properties of short-range coupled Kuramoto models with time delayed couplings (Nakamura *et al.*, 1994; Niebur *et al.*, 1991a; Schuster and Wagner, 1989):

$$\dot{\theta}_i(t) = \omega_i + \xi_i(t) + \frac{K}{N} \sum_j \sin(\theta_j(t-\tau) - \theta_i(t)). \quad (85)$$

Here the sum is restricted to nearest neighbors and τ is a constant time delay. In this model, each oscillator interacts with its neighbors in terms of the phase that they had at the time they sent a synchronizing signal.

In a simple system of two oscillators, Schuster and Wagner (1989) found the typical fingerprint of delays in several relevant differences between this model and the standard KM. In the case $\tau = 0$, one synchronization state is stable. However, for non-zero delays and given values of τ and K, there are multiple stable solutions of Eq. (85) with more than one synchronization frequency and different basins of attraction. In a remarkable application, this model has been used recently to explain the experimentally observed oscillatory behavior of a unicellular organism (Takamatsu *et al.*, 2000).

Keeping in mind these results, it is not difficult to imagine what will happen for large ensembles of oscillators. In a 1D system, Nakamura *et al.* (1994) have shown that complex structures emerge spontaneously for $N \to \infty$. They are characterized by many stable coexisting clusters, each formed of a large number of entrained units, oscillating with different frequencies. These structures have also been observed for a distribution of time-delays (Zanette, 2000). Another peculiarity of the model has been observed for large coupling intensity and large delays. In this regime, the system exhibits frequency suppression resulting from the existence of a large number of metastable states. In two dimensions, Niebur *et al.* (1991a) have shown that the system evolves towards a state with the lowest possible frequency, selected from all the possible solutions of (85) for given values of K and τ . More recently, Jeong *et al.* (2002) have shown that distance-dependent time delays induce various spatial structures such as spirals, traveling rolls or more complex patterns. They also analyze their stability and the relevance of initial conditions to select these structures.

The mean-field model has been studied theoretically by analyzing the corresponding NLFPE (Choi *et al.*, 2000;

Luzyanina, 1995; Yeung and Strogatz, 1999). Similarly to the case of short-range coupling, the delay gives rise to multistability even for identical oscillators and without external white noise. The phase diagram (K, τ) contains regions where synchronization is a stable solution of the dynamic equations, other regions where coherence is strictly forbidden, and still others where coherent and incoherent states coexist. The existence of all these regimes has been corroborated by simulations (Kim *et al.*, 1997b; Yeung and Strogatz, 1999). The same qualitative behavior has been found for non trivial distributions of frequencies. As in the standard KM, in noisy systems there is a critical value of the coupling K_c, above which the incoherent solution is unstable. K_c depends on the distribution of frequencies, the noise strength and the delay. Choi *et al.* (2000); Yeung and Strogatz (1999) have carried out a detailed analysis of the bifurcation at K_c for the NLFPE corresponding to Eq. (85). Kori and Kuramoto (2001) have studied the same problem for more general phase oscillator models.

D. External fields

A natural extension of the original KM is to add external fields, which gives rise to a much richer dynamic behavior. External fields can model the external current applied to a neuron so as to describe the collective properties of excitable systems with planar symmetry. For other physical devices, such as Josephson junctions, a periodic external force can model an oscillating current at the junctions.

The Langevin equation governing the dynamics of the extended model is

$$\dot{\theta}_i = \omega_i + \xi_i(t) + \frac{K}{N}\sum_{j=1}^{N}\sin(\theta_j - \theta_i) + h_i \sin\theta_i \qquad (86)$$

Shinomoto and Kuramoto (1986) studied the case $h_i = h \quad \forall i$. They analyzed the NLFPE associated to (86) and found two different regions of the phase diagram: a region of time-periodic physical observables, and a region of stable stationary synchronized states.

Sakaguchi (1988) replaced the last term in Eq. (86) by $h\sin(\theta_i - \omega_f t)$, where ω_f is the frequency of the external force. Notice that by defining $\psi_i = \theta_i - \omega_f t$, we again obtain Eq. (86) for ψ_i, but with natural frequencies $\omega_i - \omega_f$. Therefore the time-periodic external force is equivalent to modifying the statistical properties of the distribution $g(\omega)$. In general, there will be a competition between forced entrainment and mutual entrainment. If the strength of h is large, the oscillators tend to be entrained with the external force. On the other hand if h is small there will be a macroscopic fraction of the population mutually entrained displaying a synchronous collective motion whose frequency is the mean natural frequency of the population.

Arenas and Pérez-Vicente (1994a) studied the phase diagram of a KM with a distribution of random fields $f(h)$. They solved the NLFPE through a generating functional of the order parameters, and found analytical expressions thereof, which fully agreed with numerical simulations. Provided $f(h)$ is centered at $h = 0$, they found a phase transition between an incoherent state with $r = 0$ and a synchronized state, which is similar to the transition in the static model or in the model of identical oscillators (Arenas and Pérez-Vicente, 1993)). The only difference is that the critical K_c is larger. This is reasonable because larger values of the coupling constant are necessary to counteract the effect of rotation caused by the distribution of frequencies. When the distribution of fields is not centered in the origin there is an effective force which makes $r \neq 0$ ($r \propto \langle h\rangle$ for small K/D and for $\langle h\rangle \ll 1$) for any value of the ratio K/D, thereby precluding phase transitions, just as in the static case.

Provided $\int h f(h) dh \neq 0$, densities having time-dependent solutions with nonzero order parameters (Arenas and Pérez-Vicente, 1994a; Sakaguchi, 1988; Shinomoto and Kuramoto, 1986). Acebrón and Bonilla (1998) studied these solutions using the two-timescale asymptotic method mentioned in Section III.C. The probability density splits into independent components corresponding to different peaks in the multimodal distribution of frequencies. Each density component evolves towards a stationary distribution in a comoving frame rotating with the frequency corresponding to the appropriate peak in $g(\omega)$. Thus the overall synchronous behavior can be determined by studying synchronization of each density component (Acebrón and Bonilla, 1998).

Inspired by biological applications, Frank *et al.* (2000) analyze the behavior of phase oscillators in presence of forces which derive from a potential with various Fourier modes. They study in detail the transition from incoherence to phase locking. Finally, Coolen and Pérez-Vicente (2003) have studied the case of identical oscillators with disordered couplings and subject to random pinning fields. This system is extremely frustrated and several spin-glass phases can be found. The equilibrium properties of the model depend on the symmetries of the pinning field distribution and on the level of frustration due to the random interactions between oscillators.

E. Multiplicative noise

To end this section, we shall discuss the effect of multiplicative noise on the collective properties of phase oscillators. As far as we know, there have been two different approaches to this problem.

Park and Kim (1996) have studied the following rather complex version of the KM:

$$\dot{\theta}_i = \omega_i + \frac{K + \sigma\eta_i(t)}{N}\sum_{j=1}^{N}\sin(\theta_j - \theta_i) + h\sin(\nu\theta_i). \quad (87)$$

Here η_i is a zero-mean delta-correlated Gaussian noise with unit variance, σ measures the intensity of the noise and ν is an integer. The phase oscillators in this model are subject to an external pinning force and therefore they represent excitable units. Thus Eq. (87) describes the effect of multiplicative noise on a population of excitable units. Through analytical and numerical studies of the NLFPE, Park and Kim (1996) have found the phase diagram of the model (h, σ) for different values of ν. For identical oscillators, there are new phases in which two o more stable clusters of synchronized oscillators can coexist. This phenomenology is strictly induced by the multiplicative noise, without having to include time delays or high Fourier modes in the coupling.

Kim *et al.* (1997a, 1996) have supplemented Eq. (87) with additive noise. Surprisingly, the additive noise tends to suppress the effects triggered by the multiplicative noise, such as the bifurcation from one-cluster phase to the two-cluster state. The new phase diagram exhibits very rich behavior with interesting nonequilibrium phenomena such as reentrant transitions between different phases. The interesting physics induced by the combination of both types of noise inspired Kim *et al.* (1997c) to propose a new mechanism for noise-induced current in systems under symmetric periodic potentials.

Reimann *et al.* (1999) tackled the problem from a different standpoint. They considered the standard mean-field equation (23) with a non-equilibrium Gaussian noise characterized by

$$< \xi_i(t) >= 0, \quad < \xi_i(t)\xi_j(t') >= 2D(\theta_i)\delta_{ij}\delta(t-t'), \quad (88)$$

where $D(\theta) = D_0 + D_1\cos(\theta)$ and $D_0 \geq D_1 \geq 0$. The authors consider only one Fourier mode to make their analysis simpler, and study the particular choice $D_0 = D_1 = Q/2$. Under these conditions, for identical oscillators and for arbitrarily weak coupling, time-dependent oscillatory synchronization appears for a certain value of the ratio K/Q, via spontaneous symmetry breaking. By means of numerical simulations, the authors also study the effect of multiplicative noise in systems with short-range coupling. In this case, even more complex behaviors including hysteretic phenomena and negative mobility are found.

Recently and only for identical oscillators, Kostur *et al.* (2002) have studied Eq. (86) for $h_i = -1\ \forall i$ with both additive and symmetric dichotomic noise. For the latter noise, they found a complex phase diagram with five different regions: incoherence, bistability, phase locking, hysteretic phenomena and an oscillatory regime.

V. BEYOND THE KURAMOTO MODEL

Many generalizations of the KM have been proposed to analyze synchronization phenomena in more complex situations. Firstly, periodic coupling functions that contain more harmonics than the simple sine function considered by Kuramoto have been proposed. Secondly, there are oscillator models described by two angles (tops models) or by a phase and an amplitude (amplitude oscillators). Lastly, the dynamics of the KM is changed if phase oscillators have inertia, making synchronization harder but facilitating spontaneous phase oscillations.

A. More general periodic coupling functions

An immediate generalization of the mean-field KM is

$$\dot{\theta}_i = \omega_i + \frac{K}{N}\sum_{j=1}^{N} h(\theta_j - \theta_i), \quad (89)$$

where $h(\theta)$ is a general coupling function of period 2π, and the intrinsic oscillator frequencies ω_i are distributed with probability density $g(\omega)$ as usual. By shifting all phases, $\theta \to \theta + \Omega t$, and selecting Ω appropriately, we can set $\int_{-\infty}^{\infty}\omega g(\omega)d\omega = \int_{-\pi}^{\pi} h(\theta)d\theta = 0$, without loss of generality. What can we say about oscillator synchronization in this more general context?

A particularly successful theoretical approach is due to Daido (1992a, 1993a,b, 1994, 1995, 1996a,b), who generalized Kuramoto's ideas on the order parameter and the partially synchronized state. Let us assume that the oscillators are phase-locked with a common frequency $\omega_e(t) = \dot{\psi}$. Let us suppose that there exist the following order parameters

$$Z_j \equiv X_j + \imath Y_j = \lim_{t\to\infty}\frac{1}{N}\sum_k \exp\{\imath j[\theta_k(t) - \psi_e(t)]\}. \quad (90)$$

If the coupling function is expanded in Fourier series as

$$\begin{aligned} h(\theta) &= \sum_{j=1}^{\infty}\left(h_j^s\sin(j\theta) + h_j^c\cos(j\theta)\right) \quad (91)\\ &= \sum_{j=-\infty}^{\infty} h_j e^{\imath j\theta}, \end{aligned}$$

then a simple calculation shows that we can write Eq. (89) in the following form:

$$\dot{\theta}_i = \omega_i - K\, H(\theta_i - \psi_e(t)), \quad (92)$$

provided we define the *order function* H as

$$\begin{aligned} H(\psi) &\equiv -\sum_{j=-\infty}^{\infty} h_j Z_j e^{-\imath j\theta}\\ &= \sum_{j=1}^{\infty}\left\{(h_j^s X_j - h_j^c Y_j)\sin(j\psi)\right.\\ &\quad \left.-(h_j^c X_j + h_j^s Y_j)\cos(j\psi)\right\}. \quad (93) \end{aligned}$$

Note the similarity of Eq. (92) to Kuramoto's expression (3). Assuming that $H(\psi)$ has only one maximum

and one minimum in the interval $-\pi \leq \psi \leq \pi$, Daido derives a self-consistent functional equation for H (Daido, 1992a) [3]. This equation always has the trivial solution $H(\psi) = 0$, which corresponds to incoherent behavior of the oscillators. Nontrivial solutions describe synchronized states of the oscillator population. Furthermore, one expects that, for sufficiently large K, the onset of mutual entrainment is a bifurcation of a non trivial order function from incoherence. Keeping in mind this framework Daido has considered several particular cases (Daido, 1992a, 1993a,b). If the Fourier series of the coupling function contains only odd harmonics, there is spontaneous synchrony above the following critical K_c

$$K_c = \frac{2}{\pi g(\omega_e) h_1^s}. \tag{94}$$

This shows that K_c depends on the first harmonic but does not depend on the higher modes. Notice that the KM belongs to this family of models (in fact $h(\theta) = \sin\theta$) and (94) is consistent with the results given in Section II. The bifurcation to the synchronized state is supercritical provided $g''(\omega_e) < 0$ and $h_1^s > 0$. These results are confirmed by numerical simulations.

Daido (1994) has elaborated a bifurcation theory of the order function, whose L^2 norm, $\|H\| \equiv \sqrt{\int_{-\pi}^{\pi} H(\psi)^2 d\psi}$, as a function of the coupling constant K can be represented in a bifurcation diagram. Near the critical coupling, $\|H\| \propto (K - K_c)^\beta$, which defines the critical exponent β. It turns out that the KM describes the scaling behavior of a reduced family of phase oscillators for which $\beta = 1/2$, whereas $\beta = 1$ for the vast majority of coupling functions (Daido, 1994, 1996b). This fact suggests the existence of different classes of universality. Crawford (1995) confirmed most of these findings by means of standard bifurcation theory, while Balmforth and Sassi (2000) have given a simple mode-coupling explanation of the different scalings in an example with $h_1^s = 1, h_2^s = \sigma$, as the only non-zero harmonics.

The previous theory can be generalized to order functions having several peaks in the interval $(-\pi, \pi)$ (Daido, 1995, 1996a). In this case, the oscillators may choose among different coexisting phase-locking states, and their resulting dynamical behavior is more complex than in the standard situation, in which only one type of entrainment is possible (Daido, 1996a). If the order function has more than one local maximum and a local minimum, then there is an overlap region with at least two branches for which $H'(\psi) > 0$. Oscillators whose frequency lies in the overlap region may synchronize to the phase of one stable branch depending on their initial condition. The number of possible such states is exponentially large and the entropy per oscillator is an appropriate order parameter characterizing the corresponding macroscopic state (Daido, 1996a).

Works by other authors confirm the predictions of the order function formalism. For instance, Hansel *et al.* (1993b) considered coupling functions with two Fourier modes and a free parameter that controls the attractive/repulsive character of the interaction between oscillators. Besides the usual states typical of the KM, the incoherent state and the synchronized state, they found more complex dynamical situations for appropriate values of the control parameter. For instance, there were switching two-cluster states connected by heteroclinic orbits. Each cluster contained a group of phase-locked oscillators running at a common frequency. Other studies discussing a large variety of clustering behavior for coupling functions having a large number of Fourier modes are (Golomb *et al.*, 1992; Okuda, 1993; Tass, 1997).

Bonilla *et al.* (1998a) have studied singular coupling functions such as $h(\theta) = \delta'(\theta)$, $\delta(\theta)$, $\mathrm{sign}(\theta)$, etc. that have infinitely many nonvanishing Fourier modes. They show that the dynamics of these models can be exactly solved using the moment approach discussed in Section VI.C. Consider the generating function for the moments,

$$\hat{\rho}(x, y, t) = \frac{1}{2\pi} \sum_{k=-\infty}^{\infty} \sum_{m=0}^{\infty} \exp(-ikx) \frac{y^m}{m!} H_k^m(t), \tag{95}$$

$$H_k^m(t) = \frac{1}{N} \sum_{j=1}^{N} \exp[ik\theta_j(t)] \omega_j^m.$$

Its time evolution satisfies

$$\frac{\partial \hat{\rho}}{\partial t} = -\frac{\partial}{\partial x}\Big[v(x,t)\,\hat{\rho}\Big] + T\frac{\partial^2 \hat{\rho}}{\partial x^2} - \frac{\partial^2 \hat{\rho}}{\partial x \partial y}, \tag{96}$$

where the drift velocity $v(x,t)$ is defined as

$$v(x,t) = -K \sum_{n=-\infty}^{\infty} h_n H_{-n}^0 \exp(inx). \tag{97}$$

The moment-generating function and the one-oscillator probability density are related by

$$\hat{\rho}(x, y, t) = \int_{-\infty}^{\infty} e^{y\omega} \rho(x, \omega, t) g(\omega)\, d\omega \tag{98}$$

Interestingly Bonilla *et al.* (1998a) noticed that, for particular couplings and for $g(\omega) = \delta(\omega)$ [then $\hat{\rho} = \rho(x,t)$], it is possible to map synchronization into other physical problems. For instance for $h(\theta) = \delta'(\theta)$, (96) becomes

$$\frac{\partial \rho}{\partial t} \;=\; K\frac{\partial}{\partial x}\left(\rho \frac{\partial \rho}{\partial x}\right) \;+\; T\frac{\partial^2 \rho}{\partial x^2} \tag{99}$$

which is used to describe porous media. It can be shown that in this case the incoherent solution is stable and

[3] Actually, Daido assumes that $h(\theta)$ has period 1, and therefore his formulas refer to the interval $(0, 1)$ instead of the interval $(-\pi, \pi)$ used in this paper.

therefore entrainment between oscillators is not allowed. For $h(\theta) = \delta(\theta)$, (96) becomes the Burgers equation

$$\frac{\partial \rho}{\partial t} \;=\; 2K\rho\frac{\partial \rho}{\partial x} \;+\; T\frac{\partial^2 \rho}{\partial x^2} \qquad (100)$$

and synchronization is possible only at zero temperature. Finally for $h(\theta) = \mathrm{sign}(\theta)$, it is possible to reduce the equation for ρ to a pair of coupled nonlinear partial differential equations. Their stationary solutions can be calculated explicitly in terms of elliptic functions, and therefore the bifurcation diagram can be constructed analytically for all K. In this case, multiple solutions bifurcate from incoherence for different values of the coupling constant. Let us also mention that these authors establish a link between their approach and Daido's order function.

One-dimensional chains of phase oscillators with nearest neighbor interactions (and also beyond nearest neighbors) and arbitrary coupling function have been also studied recently (Ren and Ermentrout, 2000). Given the complexity of the problem these authors have studied general properties of the model such as the conditions required to ensure the existence of phase locking solutions. Numerical examples are provided to confirm the theoretical predictions.

B. Tops models

The KM deals with interacting units that behave as oscillators that are described by a unique variable, their phase. However, it is not difficult to imagine other situations where the variables that mutually interact are not oscillators but classical spins described by the azimuthal and polar angles. In Ritort (1998) the tops model (TM) has been introduced and its phase diagram solved in the mean-field case.

Although the name "top" is a misnomer (tops are described by three Euler angles, rather than only two) it maybe more appropriate than the more correct "spin" term in order to avoid confusion with the overwhelming variety of spin models already existing in the literature. The TM could have experimental relevance whenever precession motion is induced by an external perturbation acting upon the orientational degrees of freedom of a system. It can describe synchronized responses of living units (such as bacteria) endowed with orientational magnetic properties or complex resonance effects in random magnets or NMR.

The model consists of a population of N spins $\{\vec{\sigma_i}, 1 \leq i \leq N$ (of unit length) that precess around a given orientation $\hat{n}_i$ at a given angular velocity ω_i. Larmor precession of spin i is therefore described by a vector $\vec{\omega}_i = \omega_i \hat{n}_i$. Moreover the spins in the population mutually interact trying to align in the same direction. The TM equations of motion are

$$\dot{\vec{\sigma_i}} = \vec{\omega}_i \times \vec{\sigma_i} - \frac{K}{N}\sum_{j=1}^{N}\frac{\partial \mathcal{E}(\vec{\sigma_i}, \vec{\sigma_j})}{\partial \sigma_i} + \vec{\eta_i}(t) \qquad (101)$$

where K is the coupling constant and $\mathcal{E}(\vec{\sigma_i}, \vec{\sigma_j})$ is the two-body energy term that rotational invariance symmetry requires to be a function of the scalar product $\vec{\sigma_i}\vec{\sigma_j}$, the simplest case corresponding to the linear form $\mathcal{E}(\vec{\sigma_i}, \vec{\sigma_j}) = \vec{\sigma_i}\vec{\sigma_j}$. Natural frequencies $\vec{\omega_i}$ are chosen from a distribution $P(\vec{\omega_i})$. The term $\vec{\eta_i}(t)$ is a Gaussian noise of zero mean and variance equal to $6T$, the factor 6 arising from the three degrees of freedom. As it stands (101) is not yet well defined as the unit length of the vector $\vec{\sigma_i}$ is not constant, as can be seen by multiplying both sides of the equation by $\vec{\sigma_i}$. To avoid this problem it is convenient to project the spins onto the surface of a sphere of unit radius. This requires the introduction of the azymuthal $\theta_i \in [0, \pi]$ and polar angles $\phi_i \in [0, 2\pi)$, $\vec{\sigma_i} = (\cos(\phi_i)\sin(\theta_i), \sin(\phi_i)\sin(\theta_i), \cos(\theta_i))$. The main difficulty in this procedure arises from the noise term that has to describe Brownian motion over a spherical surface (see for instance (Coffey *et al.*, 1996)). Working in spherical coordinates requires also that the natural frequency vectors $\vec{\omega_i}$ have to be specified in terms of their modulus ω_i, their azymuthal and polar angles (μ_i, λ_i). Note at this point that three variables enter into the description of the disordered units, rather than only one variable (i.e. the natural frequency ω_i) in the KM. This complexity of the TM over the KM is compensated by the richness of the orientational synchronization effects captured in the former. The resulting equations of motion are,

$$\dot{\theta}_i = -KF_\theta(\theta_i, \phi_i, \vec{m}) + \omega_i G_\theta(\theta_i, \phi_i, \lambda_i, \mu_i) + \xi_i^\theta \qquad (102)$$

$$\dot{\phi}_i \sin\theta_i = -KF_\phi(\theta_i, \phi_i, \vec{m}) + \omega_i G_\phi(\theta_i, \phi_i, \lambda_i, \mu_i) + \xi_i^\phi, \qquad (103)$$

where $F_\theta, F_\phi, G_\theta, G_\phi$ are functions easily inferred by transforming the first two-terms in the r.h.s. of (101) to spherical coordinates and $\vec{m} = \frac{1}{N}\sum_{i=1}^{N}\vec{\sigma_i}$ is the average magnetization that plays the role of the order parameter in the TM just like the parameter r in the KM (see equation (2) in Sec. II). The noises ξ_i^θ, ξ_i^ϕ are Gaussian correlated with variance $2T$ and average $T\cot(\theta_i)$ and 0 respectively.

The solution of the TM poses additional mathematical difficulties compared to the KM, however most of the calculations can be done working in the appropriate framework and for the simplest disordered case. In (Ritort, 1998) calculations have been presented in the sole presence of orientational disorder where $\omega_i = \omega \quad \forall i$, the natural frequency distribution is then given by a function $p(\mu, \lambda)$. Maybe the easiest approach to solve the model is to use the moment representation (see Sec. VI.C) by introducing the following set of moments,

$$M_{lm}^{pq} = \frac{1}{N}\sum_{i=1}^{N} Y_{lm}(\theta_i, \phi_i) Y_{pq}(\mu_i, \lambda_i). \qquad (104)$$

This formulation allows for a simple analysis of both the stationary solutions and their stability in the $(\tilde{K} = K/T, \tilde{\omega} = \omega/T)$ plane, as well as providing with an efficient method to numerically investigate the dynamics

in the $N \to \infty$ limit. Several axially symmetric disorder distributions where $p(\mu, \lambda) \equiv p(\mu)$ have been investigated in (Ritort, 1998): a) Antiferromagnetically oriented precessing frequencies with $p(\mu) = \frac{1}{4\pi}\delta(\mu - 0) + \frac{1}{4\pi}\delta(\mu - \pi)$, b) precessing orientations lying in the XY plane, $p(\mu) = \frac{1}{2\pi}\delta(\mu - \frac{\pi}{2})$ and c) isotropic disorder $p(\mu) = \frac{1}{4\pi}$. While case a) corresponds to a purely relaxational model (the mean-field antiferromagnet) displaying a single synchronization transition at $\tilde{K} = 3$, models b) and c) show more complex dynamical behavior. For instance, in case c) it is found that the incoherent solution is stable for $\tilde{K} < 3$, unstable for $\tilde{K} > 9$ and stable in the region $3 < \tilde{K} < 9$ if $\tilde{\omega}^2 > (12\tilde{K} - 36)/(9 - \tilde{K})$ yielding a rich pattern of dynamical behaviors.

More work needs yet to be done on the TM, specially interesting would be an experimental verification of orientational entrainment in magnetic systems or magnetized living cells where non-linear effects are introduced by the inertial effects induced by the Larmor precession of magnetic moments in a field.

C. Synchronization of amplitude oscillators

A population of weakly coupled limit-cycle oscillators is well-described by the KM because each oscillator reaches its limit cycle in a time which is small in comparison with the time the oscillators take to interact with one another. On the other hand, as the inter-oscillator coupling increases, both time scales become of the same order. Then the oscillator *amplitudes*, and not only their phases, are affected by their interaction. In this case, we need a more complete model.

Similarly to the KM, one can consider different classes of coupling between the oscillators: nearest neighbors [also called diffusive] coupling (Bar-Eli, 1985), random coupling between each oscillator and an arbitrary number of neighbors (Satoh, 1989) , and "all-to-all" [global] coupling (Ermentrout, 1990; Matthews *et al.*, 1991; Matthews and Strogatz, 1990). Incidentally, it should be observed that in several papers the term "diffusive coupling" is used to refer to "all-to-all" coupling instead of to nearest neighbor interaction. In fact, only the latter coupling corresponds to the discretized Laplace operator.

In this section, we shall discuss amplitude models subject to a global interaction only. So far, many more results are known for these simpler models. A widely studied case is the following system of linearly coupled oscillators, each being near a supercritical Hopf bifurcation:

$$\dot{z}_j = (1 - |z_j|^2 + i\,\omega_j)\, z_j + \frac{K}{N}\sum_{i=1}^{N}(z_i - z_j), \qquad (105)$$

for $j = 1, \ldots, N$. Here z_j is the position of the jth oscillator in the complex plane, ω_j is its natural frequency selected from a given distribution, $g(\omega)$, and K is the coupling strength. In the general case, the Hopf normal form also contains a term proportional to $i|z_j|^2 z_j$ (Crawford, 1991), which has been omitted in Eq. (105) for the sake of simplicity.

The oscillators in Eq. (105) are characterized by two degrees of freedom (e.g., the amplitude and phase). Thus, the behavior is richer than that of phase oscillators governed by the KM. In particular, *amplitude death* and *chaos* may appear in some range of parameters characterizing the oscillator populations, such as coupling strength and natural frequency spread (Matthews and Strogatz, 1990). When both amplitudes and phases vary in time, all the oscillator amplitudes may die out: $|z_j| = 0$ for every j. This behavior is called "amplitude death" or "oscillator death", which occurs when: (i) the coupling strength is of the same order as the attraction to the limit cycle, and (ii) the frequency spread is sufficiently large (Ermentrout, 1990). In biological systems, this may be responsible for the loss of rhythmicity.

Apparently, Yamaguchi and Shimizu (1984) were the first to derive the model equation (105). They considered a system of weakly globally coupled Van der Pol oscillators, that included white noise sources. Bonilla *et al.* (1987) also analyzed Eq. (105) (with noise) for a population of identical oscillators. They studied the nonlinear Fokker-Planck equation for the one-oscillator probability density, and found a transition from incoherence to a time-periodic state via a supercritical Hopf bifurcation (Bonilla *et al.*, 1988).

A comprehensive analysis for Eq. (105) can be found in (Matthews *et al.*, 1991; Matthews and Strogatz, 1990; Mirollo and Strogatz, 1990). The phenomenon of amplitude death and its stability regions have been analyzed in (Mirollo and Strogatz, 1990), in terms of the coupling strength and the spread of natural frequencies. In the same paper it was also shown that an infinite system gives a good description of large finite systems. In (Matthews *et al.*, 1991; Matthews and Strogatz, 1990), a detailed study of all possible bifurcations occurring in Eq. (105) has been presented, discussing locking, amplitude death, incoherence, and unsteady behavior (Hopf oscillations, large oscillations, quasiperiodicity, and chaos). In (Matthews *et al.*, 1991), the earlier contributions by Shiino and Francowicz (1989) and by Ermentrout (1990) were surveyed. By means of a self-consistent equation, Shiino and Francowicz (1989) established the existence of partially locked solutions and of amplitude death states, but they did not study analytically their stability. On the other hand, Ermentrout (1990) was probably the first to point out the phenomenon of amplitude death, and to study analytically its stability for certain frequency distributions and values of the coupling.

Recently, Monte and D'ovidio (2002) have revisited the dynamical behavior of this model, considering particularly the time evolution of the order parameter. They use an expansion, valid in the limit of strong coupling and narrow frequency spread, whatever the size of the population may be. Their study is based on an arbitrary assumption that truncates the hierarchy yielding the or-

der parameter, but it recovers qualitatively several known features of amplitude oscillators. However, this analysis does not reveal amplitude death, due to the limitation on the frequency spread.

D. Kuramoto model with inertia

The dynamics of the oscillators in the KM is *overdamped*, and therefore it may miss important features present in a population of coupled mechanical oscillators. By including the effects of inertia, Eqs. (25) are transformed in the following system of second order stochastic differential equations:

$$m\,\ddot{\theta}_i + \dot{\theta}_i \;=\; \Omega_i + K\,r\sin(\psi-\theta_i) + \xi_i(t), \quad (106)$$

for $i = 1,\ldots,N$. Now Ω_i represents the natural frequency of the ith oscillator, while $\dot{\theta}_i = \omega_i$ is the instantaneous frequency. Adding inertia to the noisy KM makes it possible to achieve both phase and frequency synchronization, something that it is not possible in the original overdamped KM (Acebrón *et al.*, 2000; Acebrón and Spigler, 1998). The physical motivation for adding inertia to the KM comes from the work by Ermentrout (1991) on the synchronous flashing of southeast Asia fireflies, and on alterations of circadian cycles in mammalians. Ermentrout (1991) introduces an adaptive effect of the firing frequency in the KM, as the simplest model for synchronous firing with small phase lags, in the following way:

$$\dot{\theta}_i = \omega_i, \quad \dot{\omega}_i = \frac{\Omega_i-\omega_i}{m} + \frac{K}{m}\sum_{j=1}^{N} H_{ij}(\theta_j-\theta_i), \quad (107)$$

for $i = 1,\ldots,N$. Tanaka *et al.* (1997a,b) have considered the case of a mean-field, sinusoidal coupling, $H_{ij}(\theta_j-\theta_i) = N^{-1}\sin(\theta_j-\theta_i)$, which yields Eq. (106) without white noise sources. In this noiseless case, an extension of the analysis of Section II shows that inertia may cause bistability between incoherence and a partially synchronized state, which appears via a subcritical bifurcation from incoherence (Tanaka *et al.*, 1997a,b).

The analysis of the noisy model (106) proceeds as in Section III. Firstly, in the limit of infinitely many oscillators, the corresponding NLFPE for the one-oscillator probability density is (Acebrón and Spigler, 1998):

$$\frac{\partial\rho}{\partial t} = \frac{D}{m^2}\frac{\partial^2\rho}{\partial\omega^2} - \frac{1}{m}\frac{\partial}{\partial\omega}[\big(-\omega+\Omega+Kr\sin(\psi-\theta)\big)\rho] - \omega\frac{\partial\rho}{\partial\theta} \quad (108)$$

(cf. Appendix A for a formal derivation in the case of the KM). Here the order parameter is given by,

$$re^{i\psi} = \int_{-\infty}^{+\infty}\int_{-\pi}^{\pi}\int_{-\infty}^{+\infty} e^{i\theta}\rho(\theta,\omega,\Omega,t)\,g(\Omega)d\Omega d\theta d\omega, \quad (109)$$

where $g(\Omega)$ is the natural-frequency distribution. As in the NLFPE for the KM, initial value and 2π-periodic boundary conditions with respect to θ should be prescribed. Moreover, a suitable decay of $\rho(\theta,\omega,\Omega,t)$ as $\omega\to\pm\infty$ is required. The initial profile $\rho(\theta,\omega,\Omega,0)$ should be normalized, $\int_{-\infty}^{+\infty}\int_0^{2\pi}\rho(\theta,\omega,\Omega,0)d\theta\,d\omega = 1$.

Secondly, we find the stationary angle-independent incoherent solution:

$$\rho_0(\omega,\Omega) = \frac{1}{2\pi}\sqrt{\frac{m}{2\pi D}}e^{-\frac{m}{2D}(\omega-\Omega)^2}. \quad (110)$$

The linear stability of this solution can be analyzed by following the same procedure as for the KM in Section III. We set $\rho = \rho_0 + e^{\lambda t}\mu(\theta,\omega,\Omega)$ and find an eigenvalue equation for μ. Then μ is written as a Fourier series in the phase θ, and we obtain a hierarchy of integrodifferential equations for the Fourier coefficients. ¿From this hierarchy, Acebrón *et al.* (2000) obtained the following eigenvalue problem:

$$1 = \frac{K\,e^{mD}}{2}\sum_{p=0}^{\infty}\frac{(-mD)^p\,\left(1+\frac{p}{mD}\right)}{p!} \times\int_{-\infty}^{+\infty}\frac{g(\Omega)\,d\Omega}{\lambda+D+i\Omega+\frac{p}{m}}. \quad (111)$$

Note that this equation reduces to the eigenvalue equation for the KM in the limit of vanishing inertia $m\to 0$. The critical coupling, $K = K_c$, can be found setting $\mathrm{Re}\lambda = 0$, and the solution branches bifurcating from incoherence depend on the natural frequency distribution $g(\Omega)$, and the parameters D and m.

For the unimodal frequency distribution, $g(\Omega) = \delta(\Omega)$, all stationary probability densities have the form

$$\rho_s(\theta,\omega) = \sqrt{\frac{m}{2\pi D}}e^{-\frac{m}{2D}\omega^2}\frac{e^{\frac{K}{D}r\cos(\psi-\theta)}}{\int_{-\pi}^{\pi}e^{\frac{K}{D}r\cos(\psi-\theta)}d\theta}, \quad (112)$$

where

$$r\,e^{i\,\psi} = \int_{-\pi}^{\pi}\int_{-\infty}^{+\infty} e^{i\,\theta}\,\rho_s(\theta,\omega)\,d\omega\,d\theta. \quad (113)$$

Clearly, the integral over ω in (113) can be calculated immediately, and the resulting equation for the order parameter is exactly the same one as in the case of the KM. Hence the order parameter of all the stationary states and the critical value of the coupling constant are the same ones as in the KM. In other cases, inertia changes the KM results. For a Lorentzian frequency distribution $g(\Omega) = (\varepsilon/\pi)/(\varepsilon^2+\Omega^2)$, the critical coupling is

$$K_c = 2\varepsilon(m\,\varepsilon+1) + \frac{2(2+3m\,\varepsilon)}{2+m\,\varepsilon}\,D + O\left(D^2\right), \quad (114)$$

in the limit as $D\to 0+$. Kuramoto's value, $K_c = 2(D+\varepsilon)$, is recovered if $m = 0$. Since the critical coupling increases with m, inertia makes synchronization

harder to achieve. For the bimodal frequency distribution, $g(\Omega) = [\delta(\Omega - \Omega_0) + \delta(\Omega + \Omega_0)]/2$, the stability diagram is depicted in Fig. 8. Again, increasing inertia, the noise strength D or the frequency spread ε stabilizes incoherence, thereby making it more difficult to achieve a stationary synchronized state.

For a general frequency distribution, and inspired by the linear stability analysis of incoherence, we can expand the probability density in an orthonormal basis formed by normalized parabolic cylinder functions $\psi_n(\omega)$:

$$\rho(\theta,\omega,\Omega,t) = \left(\frac{2\pi D}{m}\right)^{-\frac{1}{4}} e^{-\frac{m\omega^2}{4D}} \sum_{n=0}^{\infty} c_n(\theta,\Omega,t)\psi_n(\omega) \quad (115)$$

The coefficients c_n are 2π-periodic functions of the angle and obey a hierarchy of coupled partial differential equations (Acebrón *et al.*, 2000). Retaining a suitable number of such coefficients, a number that decreases as the mass decreases, we can close the hierarchy and analyze the solutions branching off incoherence.

Both supercritical and subcritical bifurcations may occur, depending on the value of m. This contrasts with the noisy KM, in which bifurcations from incoherence are always supercritical if the frequency distribution is unimodal. For a Lorentzian frequency distribution, Fig. 9 shows that a crossover from supercritical to subcritical bifurcation always occurs if the inertia is sufficiently large. For a bimodal natural frequency distribution, bifurcations to stable time-periodic (standing wave) synchronized solutions occur, just as in the KM of Section III (Acebrón *et al.*, 2000). Thus, inertia seems to stabilize incoherence, making synchronization more difficult to achieve, and it may also 'harden' the synchronization transition from a supercritical to subcritical bifurcation.

An interesting point of the previous discussion is that the closure assumption to few terms works better for small inertia. This observation can be made precise by analyzing Eq. (106) in the limit of small inertia. Provided the diffusive term is of the same order as the term multiplying m^{-1} (the hyperbolic limit), a Chapman-Enskog method yields the NLFPE for the KM plus its first-order corrections due to inertia (Bonilla, 2000). Similar results were obtained earlier by Hong *et al.* (1999b) who used an arbitrary closure assumption, thereby omitting relevant terms that the systematic Chapman-Enskog procedure provides (Bonilla, 2000).

Other investigators of the KM with inertia, add time-periodic forcing or time-delayed terms. Hong *et al.* (1999a) considered the equations without white noise terms:

$$m\,\ddot{\theta}_i + \dot{\theta}_i \;=\; \Omega_i + K\,r\sin(\psi - \theta_i) + A_i\cos(\Omega t), \quad (116)$$

for $i = 1,\ldots,N$. Here Ω is the frequency of external driving, and A_i is its amplitude, which may be random. They found that inertia suppresses synchronization and stabilizes incoherence, similarly to the model with $A_i = 0$ studied by Tanaka *et al.* (1997a,b). Moreover, only oscillators locked to the external driving contribute to the collective synchronization in the KM (Choi *et al.*, 1994). If inertia is added, both unlocked oscillators and those locked to the external driving force contribute to the collective synchronization.

The main effect of adding inertia and time-delays to the KM is the emergence of spontaneous phase oscillations without an external driving force (Hong *et al.*, 2002). These oscillations tend to suppress synchronization, and their frequency decreases if time-delay and inertia decrease. Hong *et al.* (2002) describe the phase diagram of the time-delayed KM with inertia, and the effects of inertia, time delay and coupling constant on the instability boundaries separating incoherence and synchronized states. For any finite values of inertia and time delay, the synchronized state changes from stationary to oscillatory as the coupling becomes sufficiently large. However, we know that the amplitude of the oscillators becomes relevant for strong couplings, which calls for additional research of this limit.

Another promising research venue concerns the *stochastic resonance* phenomena (Bulsara and Gammaitoni, 1996; Gammaitoni *et al.*, 1998). Hong and Choi (2000) have studied noise-induced resonance and synchronization in systems of globally coupled oscillators with finite inertia.

VI. NUMERICAL METHODS

A. Simulating finite size oscillator populations

1. Numerical treatment of stochastic differential equations

In this Section, we review general ideas about the numerical treatment of stochastic differential equations. More details can be found in the review papers by Platen (1999) and Higham (2001), and in the book by Kloeden and Platen (1999).

An autonomous stochastic differential equation (SDE) has the form

$$\begin{aligned} d\mathbf{X}(t) &= \mathbf{f}(\mathbf{X}(t))dt + \mathbf{g}(\mathbf{X}(t))d\mathbf{W}(t), \quad (117)\\ \mathbf{X}(0) &= \mathbf{X}_0, \quad 0 < t \le T, \end{aligned}$$

which should be considered as an abbreviation of the integral equation

$$\mathbf{X}(t) = \mathbf{X}_0 + \int_0^t \mathbf{f}(\mathbf{X}(s))ds + \int_0^t \mathbf{g}(\mathbf{X}(s))d\mathbf{W}(s), \quad (118)$$

for $0 < t \le T$. Here $\mathbf{f}$ is a given $n-$dimensional vector function, $\mathbf{g}$ is a given $n \times n$ matrix valued function, and $\mathbf{X}_0$ represents the initial condition. $\mathbf{W}(t)$ denotes an $m-$dimensional vector whose entries are independent standard scalar Brownian motion (Wiener process), and the second integral on the right-hand side of Eq. (118) should be intended as a stochastic integral in the sense of Itô. Recall that the formal derivative, $d\mathbf{W}/dt$, of the Brownian motion is the so-called white noise. The solution $\mathbf{X}(t)$ to Eq. (117) or (118) is an $n-$dimensional

stochastic process, that is an $n-$dimensional random variable vector for each t. When $\mathbf{g} = \mathbf{0}$ the problem becomes deterministic and then Eq. (117) is an ordinary differential equation.

The simplest numerical scheme to compute the solution to Eq. (117) is the natural generalization of the Euler method, that here takes on the form

$$\mathbf{X}_j = \mathbf{X}_{j-1} + \mathbf{f}(\mathbf{X}_{j-1})\Delta t + \mathbf{g}(\mathbf{X}_{j-1})\Delta \mathbf{W}_j, \qquad (119)$$

for $j = 1, \ldots, M$. Here $\Delta \mathbf{W}_j = (\mathbf{W}_j - \mathbf{W}_{j-1})$ and $\mathbf{X}_j$ represents an approximation of $\mathbf{X}(t_j)$, $t_j = j\Delta t$, and $\Delta t = T/M$. As it is well known, the Brownian increments $\mathbf{W}_j - \mathbf{W}_{j-1}$ are random variables distributed according to a Gaussian distribution with zero mean and variance Δt. Therefore, Eq. (117) can be solved generating suitable sequences of random numbers. As for the error one encounters in approximating solutions to Eq. (117), there are two different types, depending on whether one is interested in obtaining either the paths or the moments. In the literature, these are referred to as *strong* and *weak* approximations, respectively. In the strong schemes, one should estimate the error

$$\varepsilon_s = E(|\mathbf{X}(T) - \mathbf{X}_M|), \qquad (120)$$

which provides a measure of the closeness of the paths at the end of the interval. In the weak scheme, instead, one is interested only in computing moments or other functionals of the process $\mathbf{X}(t)$. For instance, the error in the first moment is given by

$$\varepsilon_w = E(\mathbf{X}(T)) - E(\mathbf{X}_M). \qquad (121)$$

Note that estimating the latter is less demanding. It can be shown that the Euler scheme is of order 1/2, that is $\varepsilon_s = \mathcal{O}(\Delta t^{1/2})$ as a strong method, but of order 1, ($\varepsilon_w = \mathcal{O}(\Delta t)$) as a weak method. Higher order methods, however, do exist, for instance the stochastic generalization of the Heun method,

$$\begin{aligned}
\overline{\mathbf{X}}_j &= \mathbf{X}_{j-1} + \mathbf{f}(\mathbf{X}_{j-1})\Delta t + \mathbf{g}(\mathbf{X}_{j-1})\Delta \mathbf{W}_j, \qquad (122)\\
\mathbf{X}_j &= \mathbf{X}_{j-1} + \frac{1}{2}\left[\mathbf{f}(\mathbf{X}_{j-1}) + \mathbf{f}(\overline{\mathbf{X}}_j)\right]\Delta t \\
&+ \frac{1}{2}\left[\mathbf{g}(\mathbf{X}_{j-1}) + \mathbf{g}(\overline{\mathbf{X}}_j)\right]\Delta \mathbf{W}_j,\ j = 1, \ldots, M, \qquad (123)
\end{aligned}$$

and others based on the stochastic Taylor formula, e.g. the Taylor formula of order 3/2, which for the scalar case, reads (Kloeden and Platen, 1999),

$$\begin{aligned}
X_j &= X_{j-1} + f(X_{j-1})\Delta t + g(X_{j-1})\Delta W_j \\
&+ \frac{1}{2} g(X_{j-1}) g'(X_{j-1})\left[(\Delta W_j)^2 - \Delta t\right] \\
&+ \frac{(\Delta t)^2}{2}\left[f(X_{j-1})f'(X_{j-1}) + \frac{1}{2}(g(X_{j-1}))^2 f''(X_{j-1})\right] \\
&+ f'(X_{j-1})g(X_{j-1})\Delta Z_j + [f(X_{j-1})g'(X_{j-1}) \\
&+ \frac{1}{2}(g(X_{j-1}))^2 g''(X_{j-1})\Big][\Delta t \Delta W_j - \Delta Z_j] \\
&+ \frac{1}{2}\left[g(X_{j-1})(g'(X_{j-1}))^2 + (g(X_{j-1}))^2 g''(X_{j-1})\right] \\
&\times \left[\frac{1}{3}(\Delta W_j)^2 - \Delta t\right]\Delta W_j, \qquad (124)
\end{aligned}$$

where ΔZ_j are random variables distributed according to a Gaussian distribution with zero mean, variance $(\Delta t)^3/3$, and correlation $E(\Delta W_j \Delta Z_j) = (\Delta t)^2/2$. Using the Heun method to compute paths (strong scheme), the error can be shown to be $\varepsilon_s = \mathcal{O}(\Delta t)$, while the corresponding weak scheme is $\mathcal{O}(\Delta t^2)$. If can be proved that the path computation based on such a formula is $\varepsilon_s = \mathcal{O}(\Delta t^{3/2})$, and $\mathcal{O}(\Delta t^3)$ as a weak scheme.

2. The Kuramoto model

The KM for N globally coupled nonlinear oscillators with white noise sources is governed by the system of stochastic differential equations (23) and (24). This system can be solved numerically by the methods described in the previous subsection (Acebrón and Spigler, 2000; Sartoretto *et al.*, 1998). In Fig. 10, plots of the amplitude of the order parameter as a function of time, obtained using Euler, Heun, and Taylor of order 3/2, are compared. The reference solution is provided solving the nonlinear Fokker-Planck equation (26) - (27) with a spectral (thus extremely accurate) method (Acebrón *et al.*, 2001b). Experiments were conducted for increasing values of N, showing that results stabilize already for $N = 500$.

In the thermodynamic limit ($N \to \infty$), the average over the distribution function of the entire oscillator population is the same as the average of $\theta_i(t)$ over all the realizations of the noise. To obtain the latter, we consider a sufficiently large number of oscillators, N. Numerical simulations show that a few hundred oscillators are enough, cf. Fig. 11. In Fig. 12, the amplitude of the order parameter for N oscillators, $r_N(t)$, is compared with its limiting value as $N \to \infty$. This figure shows that $\Delta r_N = |r_N - r| \propto N^{-1/2}$, as N increases.

B. Simulating infinitely many oscillators

In this subsection, we discuss finite differences and spectral numerical methods to solve the NLFPE (26) - (27), which we shall rewrite as

$$\frac{\partial \rho}{\partial t} = D\frac{\partial^2}{\partial \theta^2} - \omega\frac{\partial \rho}{\partial \theta} - I[\rho]\,\frac{\partial \rho}{\partial \theta} + J[\rho]\,\rho, \qquad (125)$$

where

$$\begin{aligned}
I[\rho] &= \int_{-\infty}^{+\infty}\int_{-\pi}^{\pi} g(\omega)\sin(\phi - \theta)\rho(\phi, \omega, t)\, d\phi d\omega, \\
J[\rho] &= \int_{-\infty}^{+\infty}\int_{-\pi}^{\pi} g(\omega)\cos(\phi - \theta)\rho(\phi, \omega, t)\, d\phi d\omega. \qquad (126)
\end{aligned}$$

1. Finite differences

If we use forward differences in time and centered differences in the angle, we obtain the following explicit finite-difference scheme for the NLFPE:

$$\rho_i^{n+1} = \rho_i^n + D\frac{\Delta t}{\Delta\theta^2}\left(\rho_{i+1}^n - 2\rho_i^n + \rho_{i-1}^n\right) - \omega\frac{\Delta t}{2\Delta\theta}\left(\rho_{i+1}^n - \rho_{i-1}^n\right) - \frac{\Delta t}{2\Delta\theta}I[\rho_i^n]\left(\rho_{i+1}^n - \rho_{i-1}^n\right) + J[\rho_i^n]\,\rho_i^n, \quad (127)$$

with $i = 1, \ldots, i_{max}$, $n = 0, 1, \ldots, n_{max}$. Here ρ_i^n is an approximation to $\rho(i\Delta\theta, n\Delta t, \omega)$, and initial and boundary data are prescribed. The parameter ω in (127) should be selected in the support of the natural frequency distribution, $g(\omega)$. Except for discrete distributions, the integral terms $I[\rho_i^n]$ and $J[\rho_i^n]$ involve integration over the frequencies, and a quadrature formula should be chosen according to the specific form of $g(\omega)$. For instance, Acebrón *et al.* (2000) have used successfully the Gauss-Laguerre quadrature in the case of a Lorentzian frequency distribution.

If we use an explicit scheme, the size of the time step has to be kept sufficiently small due to stability reasons. Using an implicit finite-difference scheme, such as Crank-Nicholson's (Acebrón and Bonilla, 1998; Bonilla *et al.*, 1998b), we can in principle increase the time step (for a given $\Delta\theta$). The trouble is that our problem is nonlinear, and therefore we need to implement an additional iterative procedure at each time step to find ρ_i^{n+1}. This reduces in practice the time step to rather small values, as illustrated by numerical experiments. In Fig. 13, the analytical solution corresponding to the case $g(\omega) = \delta(\omega)$,

$$\rho_0(\theta) = \frac{e^{K\,r_0\cos(\psi_0-\theta)}}{\int_{-\pi}^{\pi} d\theta\, e^{K\,r_0\cos(\psi_0-\theta)}}, \quad (128)$$

where

$$r_0\, e^{i\,\psi_0} = \int_{-\pi}^{\pi} d\theta\, e^{i\theta}\rho_0, \quad (129)$$

is compared with the results of the numerical solution computed by either implicit finite differences or by a spectral method. Note that insertion of Eq. (128) into (129) yields a nonlinear equation for r_0 and ψ_0, whose solution can be computed to very high accuracy by the Brent method (Press *et al.*, 1992).

2. Spectral method

Since the one-oscillator probability density ρ is 2π-periodic in θ, a suitable spectral numerical method to solve the NLFPE is to write ρ as a Fourier series and integrate the resulting differential equations for the Fourier coefficients (Sartoretto *et al.*, 1998; Shinomoto and Kuramoto, 1986). This spectral method is very efficient, and the Fourier series converges exponentially fast as the number of harmonics increases (Fornberg, 1996).

Inserting

$$\rho = \sum_{n=-\infty}^{\infty} \rho_n(t,\omega)\, e^{i\,n\,\theta},$$
$$\rho_n(t,\omega) = \frac{1}{2\pi}\int_{-\pi}^{\pi} \rho\, e^{-i\,n\,\theta}\, d\theta, \quad (130)$$

in the NLFPE leads to the following system of infinitely many ordinary differential equations

$$\dot\rho_n = -n^2 D\ \rho_n - i\,n\,\omega\ \rho_n - n\frac{K}{2}\left[\rho_{n+1}\int_{-\infty}^{\infty}\rho_{-1}g(\omega)d\omega - \rho_{n-1}\int_{-\infty}^{\infty}\rho_1 g(\omega)\,d\omega\right], \quad n = 0, \pm1, \pm\ldots. \quad (131)$$

For each frequency ω in the support of $g(\omega)$, Eqs. (131) are truncated after a suitable number of harmonics ρ_n. The resulting system is then solved accurately by using a high-precision scheme, such as a variable-step Runge-Kutta-Felhberg routine (Press *et al.*, 1992), as done by Acebrón *et al.* (2001a).

If we want to obtain the order parameter but not the density, it is better to use a different Fourier series expansion for ρ (Acebrón and Bonilla, 1998):

$$\rho(\theta,t,\omega) = \frac{1}{2\pi}\sum_{j=1}^{N}\left[R_j\cos(j(\psi-\theta)) + \Psi_j\sin(j(\psi-\theta))\right], \quad (132)$$

where

$$R_n(\omega,t) = \int_{-\pi}^{\pi}\cos(n(\psi-\theta))\,\rho\,d\theta,$$
$$\Psi_n(\omega,t) = \int_{-\pi}^{\pi}\sin(n(\psi-\theta))\,\rho\,d\theta. \quad (133)$$

To obtain differential equations for R_n and Ψ_n, we take their time derivatives, use the NLFPE, and simplify the result using integration by parts. We obtain

$$\dot R_n = -n^2 D R_n + n\omega\Psi_n + \frac{nKr}{2}(R_{n-1} - R_{n+1}) - n\frac{d\psi}{dt}\Psi_n,$$
$$\dot\Psi_n = -n^2 D\Psi_n - n\omega R_n + \frac{nKr}{2}\left(\Psi_{n-1} - \Psi_{n+1}\right) + n\frac{d\psi}{dt}R_n,$$
$$r\frac{d\psi}{dt} = \int_{-\infty}^{+\infty}\omega R_1(\omega,t)g(\omega)\,d\omega, \quad (134)$$

where

$$r(t) = \int_{-\infty}^{+\infty} R_1(\omega,t)\,g(\omega)\,d\omega,$$
$$0 = \int_{-\infty}^{+\infty}\Psi_1(\omega,t)\,g(\omega)\,d\omega. \quad (135)$$

Further simplification results if $g(\omega)$ is an even function. Then R_1 is also even in ω, and therefore the last equation in (134) yields $d\psi/dt = 0$. Comparison of Eqs. (130) and (132) shows that

$$\rho_n = \frac{1}{2\pi}\,(R_n + i\Psi_n)\,e^{-in\psi}. \tag{136}$$

The hierarchy of equations for the real and imaginary parts of ρ_n is somewhat more involved than (134) because it contains the real and imaginary parts of the integrals $\int_{-\infty}^{+\infty} \rho_1(t,\omega)\,g(\omega)\,d\omega$. The numerical integration of (134) is faster than that of (131).

The spectral method (131) has been analyzed by Acebrón *et al.* (2001b), who obtained explicit bounds for the space derivatives. These bounds play a role in estimating the error term in the Fourier expansion, whose L^2 norm satisfies:

$$\|\varepsilon_N(\theta,t,\omega)\| \leq \frac{\sqrt{C_p}}{(N+1)^p}. \tag{137}$$

Here C_p is an estimate for the pth-derivative of ρ with respect to θ and N is the number of harmonics kept in the Fourier series for the oscillator density. In practice, C_p depends on the initial data and it increases rapidly with the parameter $(K/D)\int_{-\infty}^{+\infty} g(\omega)\,d\omega$. Then large values of the coupling constant K and small noise strength D require a large number of harmonics, as illustrated in Fig. 13. In Fig. 14, $|\rho_n|$ is plotted as a function of n for several values of K.

In Fig. 15, we depict the global L^2-error as a function of N, with $N = 1/\Delta\theta$. This Figure shows that the spectral method outperforms the finite difference method. The CPU time needed to implement the spectral method with $N = 12$ harmonics was approximately 25 times smaller than using finite differences with $\Delta\theta = 0.04$, $\Delta t = 10^{-4}$.

3. Tracking bifurcating solutions

Beyond bifurcation points, stationary or oscillatory solution branches can be constructed by means of numerical continuation algorithms. These algorithms track both stable and unstable solutions, but it is trivial to asign stability to bifurcating branches by means of the bifurcation calculations presented in Section III.D or to carry out a direct simulation of the NLFPE to decide the issue. We have used the numerical continuation code *AUTO* (Doedel, 1997) to follow bifurcating branches in the system of nonlinear deterministic ordinary differential equations provided by the previously discussed spectral method. As a sample, Fig. 16 shows a bifurcation diagram for the NLFPE with unimodal frequency distribution. More elaborate pictures corresponding to multimodal frequency distributions are shown in (Acebrón *et al.*, 2001a).

C. The moments approach

Pérez-Vicente and Ritort (1997) have proposed an alternative derivation of the NLFPE for the mean-field KM to that in Appendix A. The advantage of this approach is three-fold: 1) it provides an efficient way to numerically solve the mean-field equations in the large N limit free of finite-size effects, 2) it provides a simple proof that the stationary solutions of the dynamics are not Gibbsian and therefore they cannot be derived within a Hamiltonian formalism (Park and Choi, 1995), and 3) it can be used as a ground basis to include fluctuations beyond mean-field in the framework of certain approximate closure schemes. The idea of the approach relies in the rotational symmetry of the KM, $\theta_i \to \theta_i + 2\pi$. The most general set of observables invariant under these local transformations are,

$$H_k^m(t) = \frac{1}{N}\sum_{j=1}^{N} \exp(ik\theta_j(t))\omega_j^m \tag{138}$$

where k, m are integers with $m \geq 0$. Note that $H_k^m(t) = (H_{-k}^m(t))^*$. Under the dynamics (23), these observables do not fluctuate in the large N limit, i.e. are both reproducible (i.e. independent of the realization of noise) and self-averaging (independent of the realization of the random set of ω_i [4]). The set of observables (138) closes the dynamics in the limit $N \to \infty$ after averaging over the noise,

$$\frac{\partial H_k^m}{\partial t} = -\frac{kK}{2}(H_{k+1}^m\,H_{-1}^0 - H_{k-1}^m\,H_1^0) - k^2 D H_k^m + ikH_k^{m+1}. \tag{139}$$

The order parameter of Eq. (4) has been introduced in (139) through the relation $H_1^0 = r\exp(i\psi)$. Equation (139) leads immediately to the NLFPE (26) - (27) in terms of the one-oscillator probability density,

$$\begin{aligned}\rho(\theta,\omega,t)\,g(\omega) &= \frac{1}{N}\sum_{j=1}^{N}\delta(\theta_j(t)-\theta)\delta(\omega_j-\omega) \\ &= \frac{1}{2\pi}\int_{-\infty}^{\infty}\hat{\rho}(\theta,is,t)\,e^{-is\omega}ds, \end{aligned}\tag{140}$$

with the definition,

$$\hat{\rho}(\theta,s,t) = \frac{1}{2\pi}\sum_{k=-\infty}^{\infty}\sum_{m=0}^{\infty}\exp(-ik\theta)\frac{s^m}{m!}H_k^m(t). \tag{141}$$

The solution of the hierarchy (139) requires the specification of the initial conditions $H_k^m(t=0)$ where the values of $H_0^m = \overline{\omega^m} = \int \omega^m g(\omega)d\omega$ are solely determined by the frequency distribution $g(\omega)$. The equations can be solved

[4] Of course the specific set of natural frequencies must be considered as typical (the non-disordered choice $\omega_i = \omega$ is excluded).

using standard numerical integration schemes. For many purposes a Heun scheme suffices (see Sec. VI.A). A maximum number of moments needs to be considered, usually several tens of moments are enough. The method is particularly adapted to models where m takes a finite number of values. For instance, in the bimodal case (section III.C) the set of moments H_k^m splits into two subsets H_k^+ and H_k^- corresponding to the case where m is even or odd respectively. In this case the number of moments that have to be integrated is considerably reduced. Moreover, to reduce *boundary* effects, periodic boundary conditions within the set of moments are implemented. If k runs from $-L$ up to L then there are $2L+1$ possible values for the integer k. For periodic conditions we have $H_{L+1}^m = (H_{-L}^m)^*$ and $H_{-L-1}^m = (H_L^m)^*$. At any time $H_1^0 = r\exp(i\psi)$ sets the time evolution of the synchronization parameter r. In Figures 17, 18 and 19 we show some results obtained for the simple discrete bimodal distribution with $L = 100$ and only two values of m: H_k^+ and H_k^-. The initial condition corresponds to $\theta_i = 0$ in all cases. Figures 17 and 18 illustrate the evolution of the real and imaginary parts of the order parameter $H_1^0 = r\exp(i\psi)$ for parameter values in the incoherent and synchronized regimes respectively. After the transients have died down, Fig. 19 shows the parameter $r(t)$ in the oscillatory synchronized phase. The results obtained with the method of moments are compared with those given by a Brownian simulation.

The moment formalism allows us to prove that the stationary distribution is not Gibbsian. It has been shown (Hemmen and Wreszinski, 1993) that the following Hamiltonian

$$\mathcal{H} = -\frac{K}{N}\sum_{1\le i<j\le N}[\cos(\theta_i-\theta_j)-\omega_i\theta_i] \qquad (142)$$

is a Lyapunov function for finite N, whose minima describe completely phase-locked states at $T = 0$. Later, by the usual arguments of equilibrium statistical mechanics, this Lyapunov function has been employed to characterize stationary states of the KM in the thermodynamic limit, either at zero or finite temperature (Park and Choi, 1995). Pérez-Vicente and Ritort (1997) have objected that this last result applies to Gibbsian states, but not to general stationary states. In (142) we have to assume that $-\pi < \theta_i < \pi$ for $\mathcal{H}$ to be a univalued function. As the Langevin equation

$$\dot\theta_i = -\frac{\partial\mathcal{H}}{\partial\theta_i} + \xi_i \qquad (143)$$

leads to the NLFPE (cf. AppendixA), this may suggest that indeed (142) has all the properties of an energy function. In fact, it is well known that the stationary distribution of (143) is Gibbsian only if the probability currents across the boundaries $\theta_i = -\pi, \pi$ vanish. Only in this case, the stationary one-oscillator probability density is described by the equilibrium distribution obtained from (142). In the general case, Appendix E shows that the moments of the Gibbsian equilibrium distribution function are not stationary (Pérez-Vicente and Ritort, 1997). Moreover, the Hamiltonian (142) is not a Lyapunov function because it is not bounded from below although it decays in time. Only at $T = 0$ and finite N, the local minima of (142) correspond to globally synchronized solutions.

The moment approach has been extended to other models such as random tops (Sec. V.B) and synchronization models without disorder (Sec. V.A). It provides an alternative and equivalent way of clarifying some dynamical aspects of synchronization models (Aonishi and Okada, 2002).

VII. APPLICATIONS

The outstanding adaptability and remarkable applicability of the KM makes it suitable to be studied in many different contexts ranging from physics to chemistry. Here, we present some of the most relevant examples discussed in the literature along the last years but certainly its potential use is still growing and new applications will be considered in the future.

A. Neural networks

Perception: an old fascinating and unsolved neurophysiological problem that has attracted the attention of many neuroscientists for decades. The basic and fundamental task of sensory processing is to integrate stimuli across multiple and separate receptive fields. Such a binding process is necessary to create a complete representation of a given object. Perhaps, the most illustrative example is the visual cortex. Neurons that detect features are distributed over different areas of the visual cortex. These neurons process information from a restricted region of the visual field, and integrate it through a complex dynamical process that allow us to detect objects, separate them from the background, identify their characteristics, etc. All these tasks give rise to cognition as their combined result.

What kind of mechanisms might be responsible for the integration of distributed neuronal activity? There is a certain controversy around this point. It is difficult to find a good explanation using exclusively models which encode information only from the levels of activity of individual neurons (Softky and Koch, 1993). There are theories which suggest that the exact timing in a sequence of firing events is crucial for certain perception tasks (Abeles, 1991). On the other hand it has been argued (Tovee and Rolls, 1992) that long time oscillations are irrelevant for object recognition. Notice that oscillations and synchrony need to be distinguished. Cells can synchronize their responses without experimenting oscillatory discharges and conversely responses can be oscillatory without being synchronized. The important

point is the correlation between the firing pattern of simultaneously recorded neurons. In this context, the idea that global properties of stimuli are identified through correlations in the temporal firing of different neurons has gained support from experiments in the cat primary visual cortex showing oscillatory responses coherent over large distances and sensitive to global properties of stimuli (Eckhorn *et al.*, 1988; Gray *et al.*, 1989). Oscillatory response patterns reflect organized temporal structured activity that is often associated with synchronous firing.

These experimental evidences have motivated an intense theoretical research looking for models able to display stimulus dependent synchronization in neuronal assemblies. It would be a formidable task to enumerate and discuss all of them because mainly concern populations of integrate-and-fire neurons which are beyond the scope of this review. Here we will focus exclusively on studies where the processing units are modeled as phase oscillators. At this point, let us mention that there are two different theoretical approaches. The first line of reasoning is very biologically oriented trying as a main goal to reproduce, at least qualitatively, experimental results. The second is more formal and is connected with associative memory models of attractor neural networks which have been matter of extensive study in the last years.

1. Biologically oriented models

Phase oscillators can be used as elementary units in models of neural information processing. We can accept this fact as a natural consequence of the previous discussion but it is desirable to look for solid arguments supporting this choice. In order to describe the emergence of oscillations in a single column of the visual cortex, Schuster and Wagner (1990a,b) have proposed a model of excitatory and inhibitory neurons. The main ingredients of the model are: (i) a non-homogeneous spatial distribution of connections. Neurons are densely connected at a local scale but sparsely on a larger scale. This combination of short and long range couplings gives rise to the existence of local clusters of activity. (ii) the activity of the neurons is measured in terms of their mean-firing rate. For sufficiently weak coupling, it is possible to describe the dynamics of the whole population in terms of a single mean-field equation. Except for a more complex form of the effective coupling between units, this equation is analogous to that governing the evolution of the phase for a limit-cycle oscillator. In the case of the model by Schuster and Wagner (1990a,b), the coupling strength depends on the activity of the two coupled clusters, and this remarkable feature is the key to reproduce stimulus-dependent coherent oscillations.

Sompolinsky and coworkers refined and extended the previous idea in a series of papers (Grannan *et al.*, 1993; Sompolinsky *et al.*, 1990, 1991). They proposed a similar model with more elaborated inter-neuron coupling (synapses), in which many calculations can performed analytically. They consider a KM with effective coupling between oscillators given by $K_{ij}(r,r') = V(r)\ W(r,r')\ V(r')$, where V denotes the average level of activity of the pre and postsynaptic cell and $W(r,r')$ the specific architecture of the connections. To be more precise, $W(r,r')$ has two terms, one describing strong interactions between neurons in the same cluster (with large overlapping receptive fields) and another describing the weak coupling between neurons in different clusters (without common receptive fields). In addition, neurons respond to a preferred orientation as they do in certain regions of the visual cortex. With all these ingredients, the model displays a extremely rich range of behaviors. Their results agree remarkably well with experiments, even to small dynamic details, which has established this research as a reference for similar studies. It provides a mechanism to link and segment stimuli that span multiple receptive fields through coherent activity of neurons.

The idea of reducing the complexity of neuron dynamics to simplified phase-oscillator equations has been very fruitful in different contexts. For instance, in order to model the interaction of the septo-hippocampal region and cortical columns, Kazanovich and Borisyuk (1994) analyzed a system of peripheral oscillators coupled to a central oscillator. Their goal was to understand the problem of attention focusing. Depending on the parameters of the model, they found different patterns of entrainment between groups of oscillators. Hansel *et al.* (1993a) studied phase-locking in populations of Hodgkin-Huxley neurons interacting through weak excitatory couplings. They used the phase reduction technique to show that in order to understand synchronization phenomena one must analyze the effective interaction between oscillators. They found that, under certain conditions, weak excitatory coupling leads to an effective inhibition between neurons due to a decrease in their firing rates. A little earlier, Abbott (1990) had carried out a similar program using a piece-wise linear FitzHugh-Nagumo dynamics (Fitzhugh, 1961) instead of the Hodgkin-Huxley equations. As in previous models, a convenient reduction of the original dynamical evolution led to a simplified model where neurons can be treated as phase oscillators.

More recently, Seliger *et al.* (2002) have discussed mechanisms of learning and plasticity in networks of phase oscillators. They studied the long time properties of the system by assuming a Hebbian-like principle. Neurons with coherent mutual activity strengthen their synaptic connections (long-term potentiation) while they weaken their connections (long-term depression) in the opposite situation. The slow dynamics associated to the synaptic evolution gives rise to multistability, i.e, coexistence of multiple clusters of different sizes and frequencies. The work by Seliger *et al.* (2002) is essentially numerical. More elaborate theoretical work can be carried out provided neurons and couplings evolve on widely separated times scales, fast for neurons and slow for couplings. An example is the formalism developed by Jongen *et al.* (2001) for a XY spin-glass model. Further work in

this direction is desirable.

2. Associative memory models

The field of neural networks has experienced a remarkable advance during the last 15 years of the last century. One of the main contributions is the seminal paper published by Hopfield (1982), which is the precursor of the current studies in computational neuroscience. He discovered that a spin system endowed with suitable couplings can exhibit an appealing collective behavior which mimicks some basic functions of the brain. To be more precise, Hopfield considered a system of formal neurons modelled as two-state units, representing the active and passive states of real neurons. The interactions between units (synaptic efficacies) followed Hebbian learning (Hebb, 1949). The resulting model exhibits an interesting phase diagram with paramagnetic, spin-glass and ferromagnetic phases, the latter having effective associative-memory properties. The dynamics of the Hopfield model is a heat-bath Montecarlo process governed by the Hamiltonian

$$H = -\sum_{i<j} J_{ij} S_i S_j \tag{144}$$

where S represents the two states of the neuron (± 1) and the couplings J_{ij} represent the synaptic strength between pairs of neurons. The latter is given by a Hebbian prescription

$$J_{ij} = \frac{1}{N} \sum_{\mu=1}^{p} \xi_i^\mu \xi_j^\mu, \tag{145}$$

where each set ξ_i^μ represents a pattern to be learnt. Hopfield showed that the configurations ξ_i^μ are attractors of the dynamics: if the initial state is in the basin of attraction of a given pattern (partial information about a given memory), the system evolves toward a final state having a large overlap with this learnt configuration. This evolution mimics a typical associative memory process.

Typical questions concern the number of patterns that can be stored into the system (in other words, the amount of information that can be processed by the model), the size of the basin of attraction of the memories, the robustness of the patterns in front of noise as well as other minor aspects. Usually, all these issues are tackled analytically by means of a standard method in the theory of spin glasses: the replica approach (Mezard *et al.*, 1987). It is not the goal of this review to discuss the technique, simply to give the main results. The number of patterns p that can be stored scales with the size of the system (number of neurons N) as $p \approx 0.138N$. Therefore the storage capacity defined as the ratio $\alpha = \frac{p}{N}$ is 0.138. A detailed analysis of the whole phase diagram $\alpha - T$ can be found in many textbooks (Amit, 1989; Hertz *et al.*, 1991; Peretto, 1992).

The conventional models of attractor neural networks (ANN) characterize the activity of the neurons through binary values, corresponding to the active and non-active state of each neuron. However in order to reproduce synchronization between members of a population, it is convenient to introduce new variables which provide information about the degree of coherence in the time response of active neurons. This can be done by associating a phase to each element of the system, thereby modelling neurons as phase oscillators. A natural question is whether large populations of coupled oscillators can store information after a proper choice of the matrix J_{ij}, as in conventional ANN. Cook (1989) considered a static approach (no frequencies) where each unit of the system is modelled as a q-state clock and the Hebbian learning rule (145) is used as a coupling. Since the J_{ij} are symmetric, it is possible to define a Lyapunov function whose minima coincide with the stationary states of (144). Cook solved the model by deriving mean-field equations in the replica-symmetric approximation. In the limit $q \to \infty$ and zero temperature, she found that the stationary storage capacity of the network is $\alpha_c = 0.038$, much smaller than the storage capacity of the Hopfield model (q=2), $\alpha_c = 0.138$, or the model with q=3 where $\alpha_c = 0.22$. Instead of fixing the couplings J_{ij}, Gerl *et al.* (1992) posed the question of estimating the volume occupied in the space of couplings J_{ij} by those obeying the stability condition $\xi_i^\mu \sum_j J_{ij} \xi_j^\mu > \kappa \geq 0$. By using a standard formalism due to Gardner (1988), they found that, in the optimal case and for a fixed stability κ, the storage capacity decreases as q increases, and that the information content per synapse grows if κ scales as q^{-1}. Although this final result seems promising, it has serious limitations given by the size of the network (since $N > q$) and also because the time required to reach the stationary state is proportional to q, as corroborated by Kohring (1993). Other models with similar features display the same type of behavior (Noest, 1988).

In the same context, the first model of phase oscillators having an intrinsic frequency distribution was studied by Arenas and Pérez-Vicente (1994b). These authors considered the standard KM dynamics discussed in previous sections with coupling constants given by

$$J_{ij} = \frac{K}{N} \sum_{\mu=1}^{p} \cos(\xi_i^\mu - \xi_j^\mu) \tag{146}$$

where K is the intensity of the coupling. This form preserves the basic idea of Hebb's rule adapted to the symmetry of the problem. Now the state of the system, described by a N-dimensional vector whose i-th component is the phase of i-th oscillator, is changing continuously in time. However, this is not a problem. If there is phase-locking, the differences between the phases of different oscillators remain constant in time. Then it is possible to

store information as a difference of phases between pairs of oscillators, which justifies the choice of the learning rule given in (146). Thus if the initial state is phase-locked with one of the embedded patterns, the final state will also have a macroscopic correlation with the same pattern at least for small p.

In the limit of $\alpha \to 0$, Arenas and Pérez-Vicente (1994b) showed that the degree of coherence between the stationary state and the best retrieved pattern is

$$m = \langle \frac{\sum_{-\infty}^{\infty} \frac{(-1)^n}{\omega^2 + D^2 n^2} I_n(\beta m) I_{n-1}(\beta m)}{\sum_{-\infty}^{\infty} \frac{(-1)^n}{\omega^2 + D^2 n^2} I_n^2(\beta m)} \rangle_\omega. \qquad (147)$$

Here m is analogous to the order parameter r defined in previous sections, I_n is the modified Bessel functions of the first kind and of order n, $\beta = \frac{J}{2D}$ and $<>_\omega$ means an average over the frequency distribution. In contrast with conventional models of ANN which, in the limit $\alpha \to 0$, have a positive overlap below the critical temperature, in this model phase locking can be destroyed if the distribution of frequencies is sufficiently broad. From a linear analysis of (147) it is straightforward to show that there is no synchronization if

$$\int_{-\infty}^{\infty} \frac{g(\omega)}{(\frac{\omega^2}{D^2} + 1)} d\omega < \beta^{-1}. \qquad (148)$$

Similarly, Hong *et al.* (2001) found that, for zero temperature and for a Gaussian distribution of frequencies of width σ, a retrieval state can only exist above a critical coupling K_c/σ. The quality of the retrieval depends on the amount of stored patterns. Their numerical simulations show a rather complex time evolution towards the stationary state. An analysis of the short-time dynamics of this network was performed in (Pérez-Vicente *et al.*, 1996) .

The situation is more complex for networks which store an infinite number of patterns (finite α). There have been some attempts to solve the retrieval problem through a standard replica-symmetry formalism (Park and Choi, 1995). However, as it has been already discussed in Section VI.C, there is no Lyapunov function in such a limit. Therefore, other theoretical formalisms are required to elucidate the long-time collective properties of associative memory models of phase oscillators.

The long-time properties of networks of phase oscillators without a Lyapunov function have been successfully determined by the so-called self-consistent signal-to-noise analysis (SCSNA) (Shiino and Fukai, 1992, 1993). To apply this formalism it is necessary to have information about the fixed-point equations describing the equilibrium states of the system. To be more precise, the method relies on the existence of TAP-like equations (Thouless *et al.*, 1977) which, derived in the context of spin-glasses, have been very fruitful in more general scenarios. These equations relate the equilibrium time-average of spins (phase oscillators) to the effective local field acting on them. In general, the effective and the time-averaged local fields are different, and their difference is the Onsager reaction term. This reaction term can be computed by analyzing the free energy of the network. Once the TAP equations are available, the local field is split in 'signal' and 'noise' parts. Then the SCSNA yields expressions for the order parameters of the problem and the (extensive) number of stored patters is determined as a result. This method has been applied by different authors. For the standard Hebbian coupling given in (145), Aonishi (1998); Aonishi *et al.* (2002); Uchiyama and Fujisaka (1999); Yamana *et al.* (1999); Yoshioka and Shiino (2000) found special associative memory properties for some particular frequency distributions. For instance, in absence of noise and for a discrete three-mode frequency distribution Yoshioka and Shiino (2000) observed the existence of two different retrieval regions separated by a window where retrieval is not possible. In the $\omega - \alpha$ phase diagram, for sufficiently low temperature, one finds a non-monotonic functional relationship. This remarkable behavior, direct consequence of having non-identical oscillators, is not observed in standard models of ANN. In the right limit, one recovers the results given by Arenas and Pérez-Vicente (1994b); Cook (1989).

There are complementary aspects of phase-oscillator networks that are worth studying. For instance, how many patterns can be stored in networks with diluted synapses (Aoyagi and Kitano, 1997; Kitano and Aoyagi, 1998) or with sparsely coded patterns (Aoyagi, 1995; Aoyagi and Nomura, 1999)? So far, these analysis have been carried out for systems with identical oscillators, so that a static approach can be used. The main result is that a network of phase oscillators is more robust against dilution than the Hopfield model. On the other hand, for low levels of activity (sparse coded patterns) the storage capacity diverges as $\frac{1}{a \log a}$ for $a \to 0$(a is the level of activity) as in conventional models of ANN. It is an open problem to analyze the effect of an intrinsic frequency distribution on the retrieval properties of these networks.

B. Josephson junctions and laser arrays

Besides the extensive development that synchronization models, in particular the KM, has undergone, another track has been followed over the recent years. In fact, several applications to Physics and Technology have been explored in detail, most important the case of superconducting Josephson junctions arrays and that of laser arrays. Even though a few other physical applications have been found, such as that to isotropic gas of oscillating neutrinos (Pantaleone, 1998), beam steering in phased arrays (Heath *et al.*, 2000), and nonlinear antenna technology (Meadows *et al.*, 2002), below we discuss at some length the first two subjects mentioned above. The main purpose in these applications is, in fact, synchronizing a large number of single elements, in order to in-

crease the effective output power. As is well known, the KM provides perhaps the simplest way to describe such a collective behavior, and it has been shown that the dynamics of Josephson junctions arrays (Wiesenfeld, 1996) as well as that of laser arrays (Kozireff *et al.*, 2000, 2001; Vladimirov *et al.*, 2003) can be conveniently mapped into it.

1. Josephson junctions arrays

Josephson junctions are superconductive devices capable of generating high frequency voltage oscillations, typically in the range 10^{10}-10^{12} Hz (Duzer and Turner, 1999; Josephson, 1964). They are natural voltage-to-frequency transducers. Applications to both analog and digital electronics have been made, to realize amplifiers and mixers for submillimetric waves, to detect infrared signals from distant galaxies, and within SQUIDs (Superconducting Quantum Interference Devices) as very sensitive magnetometers.

A large number N of interconnected Josephson junctions may let cooperate in such a way to achieve a large output power, because the power is proportional to V^2, which turns out to be proportional to N^2, provided that all members oscillate in synchrony. Moreover, the frequency bandwidth decrease as N^{-2} (Duzer and Turner, 1999). Networks of Josephson junction arrays coupled in parallel lead to nearest neighbors (that is diffusive) coupling, and more precisely to sine-Gordon discrete equations with soliton solutions. On the other hand, Josephson junction arrays connected in series through a load exhibit "all-to-all" (that is global) coupling (Wiesenfeld *et al.*, 1996). Moreover, the latter configuration can be transformed into a KM.

The model equations are

$$\frac{\hbar C_j}{2e}\ddot{\phi}_j + \frac{\hbar}{2e\,r_j}\dot{\phi}_j + I_j \sin\phi_j + \dot{Q} = I_B, \quad j = 1, \ldots, N \tag{149}$$

for the junctions, and

$$L\ddot{Q} + R\dot{Q} + \frac{1}{C}Q = \frac{\hbar}{2e}\sum_{k=1}^{N}\dot{\phi}_k \tag{150}$$

for the load circuit (see Fig. 20). Here ϕ is the difference between the phases of the wave functions associated with the two superconductors, Q is the charge, I_j the critical current of the jth junction, and C_j and r_j its capacitance and resistance respectively, and I_B the "bias current", while R, L, and C denote resistance, inductance, capacitance of the load circuit.

Note that the load does provide a global coupling, and when $\dot{Q} = 0$ all the junctions work independently. In such a case, assuming for simplicity $C_j \approx 0$, and $I_B > I_j$, the jth element will undergo oscillations at its natural frequency

$$\omega_j = \frac{2er_j}{\hbar}\left(I_B^2 - I_j^2\right)^{1/2}. \tag{151}$$

It was shown in (Swift *et al.*, 1992; Wiesenfeld, 1996; Wiesenfeld *et al.*, 1996, 1998), that in case of weak coupling and disorder, by a suitable averaging procedure, Eqs. (149), (150) can be mapped into the Kuramoto model. Assumptions amount to taking $\dot{Q}/I_j$ (which sizes the coupling among the junctions) sufficiently small, and the r_j's and I_j's, and thus the ω_j's are about the same. For definiteness, let ε be a parameter sizing the discrepancies among the r_j's, the I_j's, and thus among the ω_j's, as well as the size of the coupling, $\dot{Q}$. Moreover, the internal capacitances are considered negligible ($C_j \approx 0$). We first introduced the "natural" angles θ_j's, defined by

$$\theta_j = \frac{2\omega_j\hbar}{2er_j}\frac{1}{\sqrt{I_B^2 - I_j^2}}\arctan\left(\frac{I_j - I_B\tan\frac{\phi_j}{2}}{\sqrt{I_B^2 - I_j^2}}\right), \tag{152}$$

termed natural because when the coupling $\dot{Q}$ is set to zero, they describe uniform rotations, while the ϕ_j's do not. Using such transformation, Eq. (149) becomes

$$\dot{\theta}_j = \omega_j + \frac{K}{N}\sum_{k=1}^{N}\sin(\theta_k - \theta_j + \alpha), \tag{153}$$

to order $\mathcal{O}(\varepsilon)$, after averaging over the fast scale. Here K and α depend on the Josephson parameters r_j, I_j, I_B, R, L, and C. Strictly speaking the model equation (153) represents a generalization of the classical Kuramoto model, because of the presence of the parameter $\alpha \neq 0$ (see section IV.B)). This case was studied in (Sakaguchi and Kuramoto, 1986; Sakaguchi *et al.*, 1987), where it was observed that $\alpha > 0$ gives rise to a higher value of the critical coupling (for a given frequency spread), and a lower number of oscillators are involved in the synchronization.

In (Heath and Wiesenfeld, 2000; Sakaguchi and Watanabe, 2000) it was pointed out that, in general, the model equation of the Kuramoto type in Eq. (153) does not explain the operation of Josephson junction arrays described by Eq.s (149), (150) in certain regimes. In fact, both physical and numerical experiments on the latter equations show the existence of *hysteretic* phenomena (Sakaguchi and Watanabe, 2000), which were not found in the model equations (153). This puzzle was resolved by Heath and Wiesenfeld, who recognized that a more appropriate averaging procedure needed to be used. Doing that, a model formally similar to that in Eq. (153) was found, the essential difference being that now K and α depend on the dynamical state of the system.

When the capacitances are assumed to be nonzero, say $C_j = C_0 \neq 0$, in (Sakaguchi and Watanabe, 2000) hysteresis and multi-stability were found within the framework provided by equations (149), (150). Proceeding as above and considering a sufficiently small values of C_0, again a Kuramoto-type phase model like that in Eq. (153) was found, where now K and α depends also on C_0. A result is that the nonzero capacitance facilitates the mutual synchronization.

At this point, we should stress that the essential parameter distinguishing the two regimes of negligible and non negligible capacitance is given by the McCumber parameter, $\beta = 2eI_c r^2 C/\hbar$. Depending on the properties of the Josephson junction (r, I_c, and C), β can vary in the broad range 10^{-6}-10^{7} (Duzer and Turner, 1999).

In (Filatrella *et al.*, 2000) a model for a large number of Josephson junctions coupled to a cavity was considered. They were able to reproduce the experimental results such as the synchronization behavior reported in the experiments conducted in (Barbara *et al.*, 1999). Even though such experiments concerned two-dimensional arrays of Josephson junctions, they found qualitatively no differences with respect to the case of one-dimensional arrays (Filatrella *et al.*, 2001). In any case, they derived the modified KM,

$$\dot{\theta}_j = \omega_j + \frac{1}{N_a}\sum_{i=1}^{N_a}\frac{N_a}{N}K_i \sin(\theta_i - \theta_j + \alpha), \qquad (154)$$

where K_i takes two possible values, depending on whether the ith oscillator is frequency-locked or not (higher if locked), and N_a is the number of the "active oscillators". In these studies, the capacitances of the Josephson junctions are nonzero (underdamped oscillators), and the bias current is taken to be such that each junction is in the hysteretic regime. Depending on the initial conditions, the junctions may work in each of the two ensuing possible states, characterized by zero or nonzero voltage. When the junctions work in the latter case (that is when the phases are time variable (**??**)), the oscillators are called "active". The model in Eq. (154) was derived in a similar way as that in Eq. (153), that is by a suitable averaging method. These authors also predicted that some overall hysteretic behavior should be observed under certain circumstances, a feature that could not be observed in the experiments conducted in (Barbara *et al.*, 1999).

Daniels et al. (Daniels *et al.*, 2003) showed that the *RSJ* equations describing a ladder array of overdamped (zero capacitance), different (with disordered critical currents) Josephson junctions can be taken into a Kuramoto-type model. Such a model exhibits the usual sinusoidal coupling, but the coupling mechanism is of the *nearest neighbor* type. This mapping was realized by a suitable averaging method upon which the fast dynamics of the RSJ equations is integrated out, the slow scale being over which the neighboring junction synchronizes. The effect of thermal noise on the junctions has also been considered, finding a good quantitative agreement between the RSJ model and locally coupled KM, where a noisy term has been added. However, the noise term appearing now in the KM has not been obtained from the RSJ noisy model by the aforementioned transformation procedure, which fact raises doubt on the general applicability of this result. Locally coupled KM like this are analyzed in some more details in Sec. IV.A.

In closing, we mention another application that, strictly speaking, falls within the topic of the Josephson junctions arrays. A network of superconducting wires provides an additional example of exact mean-field systems (Park and Choi, 1997). Such a network consists of two sets of parallel superconducting wires, mutually coupled by Josephson junctions at each crossing point. It turns out that each wire only interacts with the half of the other, namely with those perpendicular to it, which fact realizes a *semiglobal* coupling. It was found that the model equations consists of two sets of coupled phase oscillators equations,and under special conditions, these equations reduce to the classical KM equation.

2. Laser arrays

The idea of synchronizing laser arrays of various kinds, analyzing their collective behavior, is a sensible subject of investigation, in both respects, technological and theoretical. In fact, on one hand, entrainment of many lasers results in a large output power from a high number of low power lasers. Moreover, when the lasers are phase-locked, a coherent high power can be concentrated in a single-lobe far-field pattern (Vladimirov *et al.*, 2003). On the other hand, this setting provides an additional example of a physical realization of the Kuramoto phase model. Actually, there are few other generalizations of the KM, that have been obtained in this field.

It has been observed in the literature that solid-state laser arrays and semiconductor laser arrays behave differently, due to the striking differences in their typical parameters. In fact, for solid-state lasers the linewidth enhancement factor is about zero, and the upper level fluorescence lifetime, measured in units of photon lifetime, is about 10^6, while for semiconductor lasers they are respectively about 5 and 10^3. It follows that they exhibit a quite different dynamical behavior.

Concerning the kind of coupling among lasers, both local and global coupling have been considered over the years (Li and Erneux, 1993; Silber *et al.*, 1993). As one can expect, globally coupled lasers act more efficiently when one wants to attain stationary synchronized (i.e. in-phase) states. Global coupling is usually obtained by means of an optical feedback given by an external mirror.

A widely used model, capable of describing the dynamical behavior of coupled lasers, is given by the so-called Lang-Kobayashi equations (Lang and Kobayashi, 1980; Wang and Winful, 1988; Winful and Wang, 1988), which have been obtained using the Lamb's semiclassical laser theory. They are

$$\begin{aligned}\frac{dE_j}{dt} &= i\delta_j E_j + (1+i\alpha)\frac{Z_j E_j}{\tau_p} \\ &+ i\frac{\kappa e^{-i\omega t_D}}{N}\sum_{k=1}^{N} E_k(t-t_D), \qquad (155)\\ \frac{dZ_j}{dt} &= \frac{1}{\tau_c}\left[P_j - Z_j - (1+2Z_j)|E_j|^2\right], \qquad (156)\end{aligned}$$

where E_j denotes the jth laser dimensionless electric field

envelope, Z_j the excess free carrier density (also called gain of the jth laser), $\omega = N^{-1}\sum_k \omega_k$ is the average frequency in the array, $\delta_j = \omega_j - \omega$ is the frequency mismatch, α is the linewidth enhancement factor, κ is the feedback rate. Other parameters are t_D, the external cavity roundtrip time (thus, ωt_D is the mean optical phase-shift between emitter and feedback fields), and $\tau_p \approx 10^{-12}$ s and $\tau_c \approx 10^{-9}$ s which are, respectively, the photon lifetime and the free carrier lifetime. The parameter P_j represents the excess pump above threshold (Vladimirov *et al.*, 2003). For instance, assuming that the Z_j's are given, the first equation in Eq. (156) is reminiscent of the amplitude KM (see section V.C), but with time delay.

When the coupling is realized through an external mirror located at the Talbot distance of order of 1 mm, the time delay, t_D, can be neglected. Instead, when the array and the feedback mirror is much larger, the time delay is important and should be taken into account. This was done in (Kozireff *et al.*, 2000, 2001). Here, the synchronization of a semiconductor laser array with a wide linewidth α was studied, writing out $E_j = |E_j|e^{i\Phi_j}$, and obtaining an asymptotic approximation for the Φ_j's from the *third-order* phase equation

$$\frac{d^3\Phi_j}{ds^3} + \varepsilon\frac{d^2\Phi_j}{ds^2} + (1+2\varepsilon\Omega_j)\frac{d\Phi_j}{ds} = \varepsilon\Delta_j + \varepsilon K\,\sigma(s-s_D)\,\sin[\xi(s-s_D) - \Phi_j(s)], \qquad (157)$$

where the scaled time $s = \Omega_R t$ ($s_D = \Omega_R t_D$), $\Omega_R = \sqrt{2P/\tau_c\tau_p}$,$P = N^{-1}\sum_j P_j$, has been introduced. The parameters appearing in Eq. (157) are: $\varepsilon = (2P+1)\sqrt{\tau_p/2P\tau_c}$, , $\Omega_j = (P_j/P-1)/\varepsilon$, $\Delta_j = \delta_j\tau_c/(1+2P)$, $K = \alpha\kappa\tau_c/(1+2P)$. σ and ξ are amplitude and phase of the complex-valued order parameter

$$\sigma(s)\,e^{i\xi(s)} = \frac{1}{N}\sum_{k=1}^{N} e^{i(\Phi_k(s)-\omega t_D)}. \qquad (158)$$

More details can be found in (Vladimirov *et al.*, 2003).

Note that Eq. (157) represents a generalization of the KM equation reducing to it but with delay, when the second and third order derivatives are neglected (see Section IV.C). Neglecting only the third order derivative the Kuramoto model with inertia is recovered (see Section V.D). In (Kozireff *et al.*, 2000, 2001; Vladimirov *et al.*, 2003), it was shown that the time delay induces and may be used to control phase synchronization in all dynamical regimes.

In (Oliva and Strogatz, 2001), where the interested reader can find additional references concerning this subject, large array of globally coupled solid-state lasers with randomly distributed natural frequencies, have been investigated. Based on previous work on lasers (Braiman *et al.*, 1995; Jiang and McCall, 1993; Kourtchatov *et al.*, 1995), as well as on general amplitude oscillator models, Oliva and Strogatz considered a simplified form of the Lang-Kobayashi equations, where the gain dynamics was adiabatically eliminated. The resulting model equation is

$$\frac{dE_j}{dt} = \left(\frac{1+P}{1+|E_j|^2} - 1 + i\omega_j\right)E_j + \frac{K}{N}\sum_{k=1}^{N}(E_k - E_j), \quad j = 1,\ldots,N. \qquad (159)$$

Note that this is indeed an amplitude model, similar to the Kuramoto amplitude model studied in Section V.C. Analytical results, such as stability boundaries of a number of dynamical regimes have been obtained, showing the existence of such diverse states as incoherence, phase locking, and amplitude death (when the system stops lasing).

C. Charge density waves

A model, akin to the KM, has been introduced to describe the dynamical behavior of charge-density-wave transport in quasi-one-dimensional metals and semiconductors in (Marcus *et al.*, 1989; Strogatz *et al.*, 1988, 1989). The subject of charge-density wave in such materials has been extensively studied over the years by many authors, too many to mention. Generalities on such topic are beyond the scope of this review, and the interested readers is referred to the references appearing in (Marcus *et al.*, 1989; Strogatz *et al.*, 1988, 1989). However the dynamical system of coupled oscillators,

$$\dot{\theta}_i = E + h\sin(\alpha_i - \theta_i) + \frac{K}{N}\sum_{j=1}^{N}\sin(\theta_j - \theta_i) \qquad (160)$$

has been proposed in (Strogatz *et al.*, 1988) to model charge-density wave transport in switching samples. This model generalizes the well-known Fisher's model, in that a periodic coupling among the oscillators replaces a linear coupling term. Others than the Fisher model, system (160) is capable to explain a number of phenomena that were observed in the experiments. The Fisher model, as well as the present one, describe the collective dynamics of coupled oscillators subject to random pinning impurities, α_i. In the present model, pinning transition, hysteretic behavior, switching between pinned and sliding states, as well as a delay in the onset of sliding in the vicinity of the threshold can be observed when an external field, E, acts upon the system.

The pinning term $h\sin(\alpha_i - \theta_i)$ forces the phase θ_i to stick at the random value α_i. The applied field E, as well as the coupling term, has an opposite effect. In fact, the pinning term pushes to static disorder arrangements, while the field tends to drive the θ_i's at constant angular velocities. On the other hand, the coupling mechanism tries to synchronize the entire system.

As one can expect, when E/h and K/h are small in Eq. (160), the pinning states dominate and the oscillators become static and pinned at the random phases α_i.

When E/h increases, keeping fixed K/h, such a pinned state loses stability, giving rise to a steady-state solution. This occurs, however, only at certain depinning threshold, which has been evaluated analytically in (Strogatz *et al.*, 1989). The bifurcations of system (160) have been studied as a function of the parameters E/h and K/h. One of the findings was that the pinning transition is discontinuous and moreover it is hysteretic. Both, discontinuous and hysteretic behavior have been observed experimentally in certain charge-density wave systems.

We should notice that system (160) can be cast into a KM affected by external field *and* disorder at the same time. In fact, setting $\Theta_i = \theta_i - \alpha_i$ in Eq. (160), we obtain

$$\dot{\Theta}_i = E - h\sin\Theta_i + \frac{K}{N}\sum_{j=1}^{N}\sin(\Theta_j - \Theta_i + A_{ij}), \quad (161)$$

where $A_{ij} = \alpha_j - \alpha_i$. Clearly, $h\sin\Theta_i$ plays the role of an external field (see Sec. **??**), and the A_{ij}'s represent disorder (see Sec. IV.B).

D. Chemical oscillators

The existence of oscillations in chemical reactions is well-known. The Belousov-Zhabotinsky reaction is paradigmatic and models such as the Brusselator and the Oregonator have been invented to understand its properties. These models are described in terms of a few coupled nonlinear reaction-diffusion equations, which can have time-periodic solutions and give rise to different spatio-temporal patterns for appropriate parameter values.

The relation between chemical oscillators and phase oscillator models has been matter of discussion for many years. In 1975, Marek and Stuchl (1975) coupled two Belousov-Zhabotinsky reaction systems with different parameters, and hence different periodic oscillations. Each reaction occurred in a separate stirred tank reactor, and both reactors could exchange matter through the common perforated wall. They observed phase locking if the oscillation frequencies in the two reactors were close. For large frequency differences, the coupled system had long intervals of slow variation in the phase difference separated by rapid fluctuations over very short intervals. These observations were qualitatively explained by Neu (1979). He considered two identical planar limit-cycle oscillators that were linearly and weakly coupled. In addition, one oscillator had a small imperfection of the same order as the coupling. A singular perturbation analysis showed that the phase difference between the oscillators evolved according to an equation reminiscent of the KM. Its analysis revealed phase locking and rhythm splitting (Neu, 1979). Neu (1980) extended this idea to populations of weakly coupled identical chemical oscillators. If we add small imperfections to the oscillators, the resulting model equations are

$$\dot{x}_i = F(x_i, y_i) + \frac{\epsilon}{N}\sum_j [K(d_{ij})\, x_j + \lambda_i\, f(x_i, y_i)],$$
$$\dot{y}_i = G(x_i, y_i) + \frac{\epsilon}{N}\sum_j [K(d_{ij})\, y_j + \lambda_i\, g(x_i, y_i)]. \quad (162)$$

If $\epsilon = 0$, we have N identical coupled oscillators having a stable T-periodic limit cycle given by

$$x_i = X(t + \psi_i), \quad y_i = Y(t + \psi_i), \quad i = 1, \ldots, N. \quad (163)$$

$d_{ij} = q_j - q_i$ is the spatial displacement between the oscillators and λ_i is a random imperfection parameter. Neu's analysis yields the following equation for the evolution of the phases in the slow time scale $\tau = \epsilon t$:

$$\frac{d\psi_i}{d\tau} = \frac{1}{N}\sum_j K(d_{ij})\, P(\psi_j - \psi_i) + \lambda_i\beta. \quad (164)$$

Here P is a T-periodic function determined from the basic limit cycle solution (163) that satisfies $P'(0) = 1$. β is a parameter (Neu, 1979). If $X = \cos(t + \psi)$, $Y = \sin(t+\psi)$, $P(\theta) = \sin\theta$. Then Eq. (164) is essentially the KM. Neu (1980) analyzed synchronization in the case of identical oscillators ($\lambda_i = 0$) for both mean-field and diffusive coupling in the limit of infinitely many oscillators. His method involves finding an evolution equation for the time integral of the order parameter. This equation can be solved in particular cases and it provides information on how the oscillators synchronize as time elapses (Neu, 1980).

Thus the KM describes weakly coupled chemical oscillators in a natural way, as already discussed by Bar-Eli (1985); Kuramoto (1984), and worked out by other authors later. Following previous experiments on two-coupled stirred-tank reactors, Yoshimoto *et al.* (1993) have tried to test frustration due to disorder in oscillation frequencies in a system of three coupled chemical reactors. Previous studies in systems of two coupled stirred tank reactors have shown that, depending on the coupling flow rate, different synchronization modes emerged spontaneously: in-phase mode, anti-phase mode and phase-death mode. Yoshimoto *et al.* (1993) interpreted their experiment involving three reactors by using the numerical solutions of Kuramoto-type equations for phase oscillators with asymmetric couplings. Their numerical solutions exhibit different combinations of the previous three modes, as well as new complex multistable modes whose features depend on the level of asymmetry in the interaction between oscillators. More recently, Kiss *et al.* (2002) have confirmed experimentally the existence of all these patterns and a number of other predictions of the KM by using an array of 64 nickel electrodes in sulfuric acid.

VIII. CONCLUSIONS AND FUTURE WORK

In this paper we have extensively reviewed the main features of the Kuramoto model, which has been most

successful in understanding and explaining synchronization in large populations of phase oscillators. The simplicity of the KM allows a rigorous mathematical analysis, at least for the case of mean-field coupling. Still, the long-time behavior of the KM is highly non-trivial, displaying a large variety of synchronization patterns. Furthermore, the model can be adapted so as to explain synchronization behavior in many different contexts.

Throughout the paper we have mentioned different open lines that deserve special attention. Let us summarize some of them. For the mean-field KM, the recent work by Balmforth and Sassi (2000) raises interesting questions to be tackled in the future. At zero noise strength $D = 0$, a stability analysis of the partially synchronized phase and a rigorous description of the synchronization transition are needed. The necessary work in this direction is expected to be technically hard.

Much more work is needed to understand synchronization in the KM with nearest-neighbor coupling. Recent work by Zheng *et al.* (1998) on the 1D case has shown that phase slips and bursting phenomena occur for couplings just below threshold. This is not surprising. It is well-known that spatially discrete equations with (overdamped or underdamped) dynamics are models for dislocations and other defects that can either move or be pinned. Among these models, we can cite the 1D Frenkel-Kontorova model (Braun and Kivshar, 1998; Carpio and Bonilla, 2001, 2003b) or the chain oscillator models for 2D edge dislocations (Carpio and Bonilla, 2003a). The latter is exactly the 2D KM with asymmetric nearest-neighbor coupling and zero frequency on a finite lattice. A constant external field acts on the boundary and is responsible for depinning the dislocations if it surpasses a critical value. For these models, there are analytical theories of the depinning transition, and the effects of weak disorder on the transition are also understood. Perhaps this methodology could be useful to understand synchronization or its failure in the nearest-neighbor KM. It is also interesting to analyze the entrainment properties of large populations of phase oscillators connected in a scale-free network or in a small-world network. Perhaps new clustering properties or multistability phenomena will come out in a natural way.

We have discussed extensions of the Kuramoto model to new scenarios. More work is needed to understand the stability properties of synchronized phases in models with general periodic couplings, or models with inertia and time delay.

We hope that the extensive discussion of the KM in this review can help finding new applications of the model. For the applications discussed here, Josephson junction arrays with non-zero capacitances need to be understood better given their common occurrence in real systems. More careful singular perturbation methods should yield more general, yet tractable models of the Kuramoto type. On the other hand, quantum noise in the form of spontaneous emission and shot noise is important for certain laser systems (Wieczorek and Lenstra, 2003). Examining the role of the noise in these systems suggests a new research line. Concerning biological applications, it would be interesting to investigate in depth adaptive mechanisms that go beyond the standard learning rules discussed in this review.

Finally, models of phase oscillators different from those discussed in this review must be explored. In this context, recent works on the Winfree model (Ariaratnam and Strogatz, 2001) and on circadian clocks (Daido, 2001) open paths worth pursuing.

Acknowledgments

This work was supported in part by the Spanish MCyT grants BFM2000-0626, BFM2002-04127-C02-01, by the Italian GNFM-INDAM and by the European Union under grant HPRN-CT-2002-00282.

APPENDIX A: Path integral derivation of the nonlinear Fokker-Planck equation

For the sake of completeness, we present a derivation of the NLFPE (26) satisfied by the one-oscillator probability density, together with Eq. (28) for the order parameter. Our derivation follows the ideas in (Bonilla, 1987), adapted to the case of the noisy KM. It is somewhat technical but it has one important advantage over other derivations: it shows that, in the limit as $N \to \infty$, the p-oscillator probability density factorizes in the product of p one-oscillator densities for all $t > 0$, provided all oscillators are statistically independent at time $t = 0$. This result of *propagation of molecular chaos* is usually assumed in other simpler derivations that close a hierarchy of equations for p-oscillator densities (Crawford and Davies, 1999).

To derive the NLFPE, we first write down the path integral representation of the N-oscillator probability density $\rho_N(t, \underline{\theta}, \underline{\omega})$ corresponding to the system of stochastic equations (23). ρ_N is equal to a product of $\delta(\theta_i(t) - \Theta_i(t; \underline{\xi}))$, averaged over the joint Gaussian distribution for the white noises $\xi_i(t)$ and over the initial distribution of the oscillators. $\Theta_i(t; \underline{\xi})$ are the solutions of Eqs. (23) for a given realization of the noises. We have

$$\rho_N(t, \underline{\theta}, \underline{\omega}) = \langle \prod_t \prod_{j=1}^N \delta[\theta_i(t) - \Theta_i(t; \underline{\xi})] \rangle_{\xi, \theta_0}$$

$$= \langle \prod_t \prod_{j=1}^N \delta \left(\omega_j + \xi_j(t) \mathrm{Im} \frac{K}{N} \sum_{k=1}^N e^{i(\theta_k - \theta_j)} - \dot{\theta}_j \right)$$

$$\times \det \left(\mathrm{Re} \frac{K}{N} \sum_{k=1}^N e^{i(\theta_k - \theta_j)} (\delta_{kj} - 1) - \frac{d}{dt} \right) \rangle_{\xi, \theta_0}. \quad \text{(A1)}$$

We now transform this expression by using that the delta functions are the Fourier transforms of unity, $\prod_t \delta(f_j) = \int \exp[\int_0^t i \Psi_j f_j dt] \, D\Psi_j(t)$, and the Gaussian

average $\langle \exp[\int_0^t i\Psi_j \xi_j dt]\rangle_\xi = \exp[-2D\int_0^t \Psi_j^2 dt]$. The result is:

$$\rho_N(t,\underline{\theta},\underline{\omega}) = \int\int\int_{\underline{\theta}(0)=\underline{\theta}_0}^{\underline{\theta}(t)=\underline{\theta}} \exp\left\{\int_0^t \sum_{j=1}^N \left[-2D\Psi_j^2 + i\Psi_j\left(\omega_j + \mathrm{Im}\frac{K}{N}\sum_{k=1}^N e^{i(\theta_k-\theta_j)} - \dot{\theta}_j\right) + \frac{1}{2}\mathrm{Re}\frac{K}{N}\sum_{k=1}^N e^{i(\theta_k-\theta_j)}(\delta_{jk}-1)\right] dt\right\} D\underline{\Psi}(t) D\underline{\theta}(t) \prod_{i=1}^N [\nu(\theta_{i0},\omega_i) d\theta_{i0}], \quad \text{(A2)}$$

after transforming the functional determinant as indicated in (Bausch *et al.*, 1976; Dominicis and Peliti, 1978; Phythian, 1977) and averaging over the initial conditions. In (A2), $\underline{\theta} = \theta_1,\ldots,\theta_N$ are the oscillators angles and $\underline{\Psi} = \Psi_1,\ldots,\Psi_N$ are their conjugate variables in phase space. ρ_N is 2π-periodic in each of its phase arguments θ_j. We have assumed that the initial data are independent identically distributed, $\rho_N(0,\underline{\theta},\underline{\omega}) = \prod_{j=1}^N \nu(\theta_j,\omega_j)$ (molecular chaos assumption). In addition, the normalization constant in the path integral will be omitted. If we are interested in one-time averages for systems of infinitely many oscillators, we should study the one-oscillator probability density $\rho(\theta,\omega,t)$ such that

$$\rho(\theta_1,\omega_1,t) = \lim_{N\to\infty}\int \rho_N(t,\underline{\theta},\underline{\omega}) \prod_{i=2}^N [g(\omega_i) d\omega_i d\theta_i], \quad \text{(A3)}$$

To analyze this function, we notice that the exponential in (A2) contains double sums such as:

$$\sum_{j=1}^N \tilde{\Psi}_j \cos\theta_j \sum_{k=1}^N \sin\theta_k = \frac{1}{2}\left[\left(\sum_{j=1}^N (\tilde{\Psi}_j\cos\theta_j + \sin\theta_j)\right)^2 - \left(\sum_{j=1}^N \tilde{\Psi}_j\cos\theta_j\right)^2 - \left(\sum_{j=1}^N \sin\theta_j\right)^2\right], \quad \text{(A4)}$$

and others of a similar form. Here $\tilde{\Psi}_j = i\Psi_j$. Notice that we can rid of the squares of the sums in the previous formulas by using the Gaussian path integrals:

$$\int \exp\left\{-\int_0^t \left[N\varphi^2 + i\sqrt{2K}\varphi\sum_{j=1}^N A_j\right] dt\right\} D\varphi(t) = \exp\left\{-\frac{K}{2N}\int_0^t \left(\sum_{j=1}^N A_j\right)^2 dt\right\}, \quad \text{(A5)}$$

$$\int \exp\left\{-\int_0^t \left[N\varphi^2 + \sqrt{2K}\varphi\sum_{j=1}^N A_j\right] dt\right\} D\varphi(t) = \exp\left\{\frac{K}{2N}\int_0^t \left(\sum_{j=1}^N A_j\right)^2 dt\right\}. \quad \text{(A6)}$$

Insertion of Eqs. (A2) and (A4) - (A6) in (A3) yields

$$\rho(\theta,\omega,t) = \lim_{N\to\infty}\int e^{\mathcal{A}(\theta,\omega,t;\underline{\varphi})}\left(\langle e^{\mathcal{A}}\rangle_{\theta,\omega}\right)^{N-1} D\underline{\varphi}(t), \quad \text{(A7)}$$

$$e^{\mathcal{A}} = \int\int\int_{\theta(0)=\theta_0}^{\theta(t)=\theta} \exp\left\{-\int_0^t \left[2D\Psi^2 + \tilde{\Psi}(\dot{\theta}-\omega) + \varphi_1^2 + i\sqrt{2K}\varphi_1\tilde{\Psi}\cos\theta + \varphi_2^2 + \varphi_3^2 + i\sqrt{2K}\varphi_2\sin\theta + \sqrt{2K}\varphi_3(\tilde{\Psi}\cos\theta + \sin\theta) + \ldots\right] dt\right\} D\Psi(t) D\theta(t)\nu(\theta_0,\omega) d\theta_0, \quad \text{(A8)}$$

$$\langle e^{\mathcal{A}}\rangle_{\theta,\omega} = \int\int e^{\mathcal{A}} g(\omega) d\omega d\theta. \quad \text{(A9)}$$

In Eq. (A8), we have denoted by $+\ldots$ six terms of the same type as the three specified ones. The integrals over $\underline{\varphi}(t)$ in Eq. (A7) can be approximated by the saddle point method with the results that

$$\frac{\delta}{\delta\varphi_k}\ln\langle e^{\mathcal{A}}\rangle_{\theta,\omega} = 0, \quad \text{(A10)}$$

for $k = 1,\ldots 9$. For the three terms specified in Eq. (A8), Eq. (A10) yields

$$\varphi_1 = -i\sqrt{\frac{K}{2}}\langle\tilde{\Psi}\cos\theta\rangle, \quad \varphi_2 = -i\sqrt{\frac{K}{2}}\langle\sin\theta\rangle, \quad \varphi_3 = -i(\varphi_1+\varphi_2), \quad \text{(A11)}$$

where

$$\langle A\rangle = \frac{\int A\exp(\ldots) D\Psi(t) D\theta(t)\nu(\theta_0,\omega) d\theta_0 g(\omega) d\omega d\theta}{\int \exp(\ldots) D\Psi(t) D\theta(t)\nu(\theta_0,\omega) d\theta_0 g(\omega) d\omega d\theta}, \quad \text{(A12)}$$

and the exponential is as that in the integrand in Eq. (A8). After we insert (A11) in this exponential and substitute the result in (A12), we find that the terms containing φ_k $(k = 1,2,3)$ become $-K\langle\tilde{\Psi}\sin\theta\rangle\cos\theta - K\langle\cos\theta\rangle\tilde{\Psi}\sin\theta$. The denominator in Eq. (A12) can be set to be 1 defining appropriately the path integral so that $\langle 1\rangle \equiv 1$. We have $\langle\tilde{\Psi}\sin\theta\rangle = \delta\langle 1\rangle/\delta\langle\cos\theta\rangle = 0$. The other functions φ_k can be determined similarly and we obtain

$$\rho(\theta,\omega,t) = \int\int\int_{\theta(0)=\theta_0}^{\theta(t)=\theta} \exp\mathcal{A}(\Psi,\theta;\omega,t) D\Psi(t) D\theta(t)\nu(\theta_0,\omega) d\theta_0, \quad \text{(A13)}$$

$$\mathcal{A}(\Psi,\theta;\omega,t) = -\int_0^t \left\{2D\Psi^2 + i\Psi[\dot{\theta}-\omega - Kr\sin(\psi-\theta)] + \frac{Kr}{2}\cos(\psi-\theta)\right\} dt, \quad \text{(A14)}$$

$$re^{i\psi} = \langle e^{i\theta}\rangle = \int\int e^{i\theta}\rho(\theta,\omega,t) g(\omega) d\omega d\theta. \quad \text{(A15)}$$

This is the path integral representation of the solution of the NLFPE satisfying $\rho(\theta,\omega,0)=\nu(\theta,\omega)$. Thus the one-oscillator density satisfies the NLFPE in the limit as $N\to\infty$ (Bonilla, 1987). The same method can be used to show propagation of molecular chaos: The p-oscillator probability density satisfies

$$\rho_p(\theta_1,\omega_1,\ldots,\theta_p,\omega_p,t)=\lim_{N\to\infty}\int\rho_N(t,\underline{\theta},\underline{\omega}) \times\prod_{i=p+1}^{N}[g(\omega_i)d\omega_i d\theta_i]=\prod_{j=1}^{p}\rho(\theta_j,\omega_j,t), \quad \text{(A16)}$$

provided the oscillators are independent and identically distributed initially and $(N-p)\to\infty$ (Bonilla, 1987).

APPENDIX B: Calculating bifurcations for the NLFPE by the method of multiple scales

Let us explain this method in the simple case of bifurcations to stationary synchronized phases and comment on its relation to the Chapman-Enskog method. In this case, there exist two time scales, t (fast time scale) and $\tau=\varepsilon^2 t\sim(K-K_c)t/K_2$ (slow time scale). The choice of the slowly-varying time scale is motivated as in Section III.D, and $(K-K_c)=O(\varepsilon^2)$ because the equation for ρ_3 is the first equation of the hierarchy derived below to display resonant terms. We assume

$$\rho(\theta,\omega,t;\varepsilon)\sim\frac{1}{2\pi}\left[1+\sum_{n=1}^{\infty}\varepsilon^n\rho_n(\theta,\omega,t,\tau)\right], \quad \text{(B1)}$$

and insert this asymptotic expansion in (26) - (29), thereby obtaining the hierarchy of linear equations

$$\mathcal{L}\rho_1=0,\quad \int_{-\pi}^{\pi}\rho_1 d\theta=1, \quad \text{(B2)}$$

$$\mathcal{L}\rho_2=-K_c\partial_\theta\left\{\rho_1\mathrm{Im}\ e^{-i\theta}\langle e^{-i\theta'},\rho_1\rangle\right\}+\mathrm{cc},$$
$$\int_{-\pi}^{\pi}\rho_2 d\theta=0, \quad \text{(B3)}$$

$$\mathcal{L}\rho_3=-K_c\,\partial_\theta\left\{\rho_2\mathrm{Im}\ e^{-i\theta}\langle e^{-i\theta'},\rho_1\rangle + \rho_1\mathrm{Im}\ e^{-i\theta}\langle e^{-i\theta'},\rho_2\rangle\right\} - \partial_\tau\rho_1+\mathrm{cc}-K_2\partial_\theta\mathrm{Im}\ e^{-i\theta}\langle e^{-i\theta'},\rho_1\rangle,$$
$$\int_{-\pi}^{\pi}\rho_3 d\theta=0, \quad \text{(B4)}$$

and so on. The solutions of (B1) and of (B2) are

$$\rho_1=\frac{A(\tau)\,e^{i\theta}}{D+i\omega}+\mathrm{cc}, \quad \text{(B5)}$$

$$\rho_2=\frac{A^2}{(D+i\omega)(2D+i\omega)}e^{2i\theta}+\mathrm{cc} +\frac{B(\tau)\,e^{i\theta}}{D+i\omega}+\mathrm{cc}, \quad \text{(B6)}$$

respectively. $A(\tau)$ and $B(\tau)$ are slowly-varying amplitudes to be determined later. Inserting (B5) and (B6) in (B4) and using the nonresonance condition (45), we obtain $dA/d\tau=F^{(0)}$, with $F^{(0)}$given by Eq. (48). Thus to leading order, the method of multiple scales and the Chapman-Enskog method yield the same amplitude equation. However, for a more complicated bifurcation, such as the degenerate transition described by Eq. (50), the method of multiple scales still yields $dA/d\tau=F^{(0)}$, and a linear nonhomogeneous equation for the amplitude $B(\tau)$. The reason for these unphysical results is that the method of multiple scales has the following limitation: *All terms in the reduced equations provided by the method of multiple scales are of the same order*. Eq. (50) can still be derived from these two equations by an *ad hoc* ansatz, as done by Bonilla *et al.* (1998b) in the case of the tricritical point. Note that Eq. (39) implies that $B(\tau)=0$ if we use the Chapman-Enskog method.

APPENDIX C: Calculation of the degenerate bifurcation to stationary states near $\omega_0=D/\sqrt{2}$

Here we calculate $F^{(2)}(A,\overline{A})$ needed to describe the transition from supercritical to subcritical bifurcations at the parameters $\omega_0=D/\sqrt{2}$, $K_c=3D$. The solution of Eq. (42) is

$$\rho_3=\frac{e^{i\theta}}{D+i\omega}\left[\frac{K_2A}{K_c}-\frac{F^{(0)}}{D+i\omega}-\frac{A\,|A|^2}{(D+i\omega)(2D+i\omega)}\right] +\mathrm{cc}+\frac{3A^3e^{i3\theta}}{(D+i\omega)(2D+i\omega)(3D+i\omega)}+\mathrm{cc}. \quad \text{(C1)}$$

The additional equations in the hierarchy that we need are:

$$\mathcal{L}\rho_4 = -K_c\partial_\theta\left\{\rho_3\mathrm{Im}\ e^{-i\theta}\langle e^{-i\theta'},\sigma_1\rangle\right\} - K_2\,\partial_\theta\sigma_1\mathrm{Im}\ e^{-i\theta}\langle e^{-i\theta'},\sigma_1\rangle-F^{(0)}\,\partial_A\rho_2+\mathrm{cc}, \quad \text{(C2)}$$

$$\mathcal{L}\rho_5=-K_c\partial_\theta\left\{\rho_4\mathrm{Im}\ e^{-i\theta}\langle e^{-i\theta'},\sigma_1\rangle\right\}-F^{(2)}\,\partial_A\sigma_1+\mathrm{cc} -F^{(0)}\,\partial_A\rho_3+\mathrm{cc}-K_2\,\partial_\theta\left\{\rho_2\mathrm{Im}\ e^{-i\theta}\langle e^{-i\theta'},\sigma_1\rangle\right\}. \quad \text{(C3)}$$

The solution of Eq. (C2) is

$$\rho_4=\frac{A\,e^{i2\theta}}{(D+i\omega)(2D+i\omega)}\left[\frac{3K_2A}{K_c} -2F^{(0)}\left(\frac{1}{D+i\omega}+\frac{1}{2D+i\omega}\right)-\frac{2A\,|A|^2}{2D+i\omega} \times\left(\frac{1}{D+i\omega}+\frac{3}{3D+i\omega}\right)\right]+\mathrm{cc} +\frac{12A^4e^{i4\theta}}{(D+i\omega)(2D+i\omega)(3D+i\omega)(4D+i\omega)}+\mathrm{cc}. \quad \text{(C4)}$$

The task of finding $F^{(2)}$ is simplified by noticing that, near the degenerate point, $\omega_0 = D/\sqrt{2} + \varepsilon^2\omega_2$, which yields

$$F^{(0)} = K_2 \left(1 + \frac{2\sqrt{2}\varepsilon^2\omega_2}{D}\right) A + \frac{16\sqrt{2}\varepsilon^2\omega_2}{9D^2} A\,|A|^2, \quad \text{(C5)}$$

up to $O(\varepsilon^4)$ terms. Then we only need to calculate $F^{(2)}$ at $\omega_0 = D/\sqrt{2}$ to have an amplitude equation with terms up to order $O(\varepsilon^4)$ in (38). We have to insert ρ_n, $n = 1, \ldots, 4$ in the right side of (C3) and use the nonresonance condition for the resulting equation (in which we can set $F^{(0)} = K_2 A$). We find

$$F^{(2)} = -\frac{K_2^2}{D} A - \frac{28K_2}{9D^2} A\,|A|^2 - \frac{272}{171D^3} A|A|^4. \quad \text{(C6)}$$

Up to $O(\varepsilon^4)$ terms, the amplitude equation (50) follows by inserting (C5) and (C6) in (38).

APPENDIX D: Calculation of the bifurcation at the tricritical point

Insertion of Eq. (59) in (26) and (28) leads to the modified hierarchy

$$\mathcal{L}\rho_2 = -K_c\partial_\theta \left\{\sigma_1 \mathrm{Im}\; e^{-i\theta}\langle e^{-i\theta'}, \sigma_1\rangle\right\} - \frac{A_T e^{i\theta}}{D + i\omega} + \mathrm{cc}, \quad \text{(D1)}$$

$$\mathcal{L}\rho_3 = -K_c\,\partial_\theta \left\{\rho_2 \mathrm{Im}\; e^{-i\theta}\langle e^{i\theta'}, \sigma_1\rangle\right\} - K_2\partial_\theta \mathrm{Im}\; e^{-i\theta}\langle e^{-i\theta'}, \sigma_1\rangle - \partial_T\rho_2 + \mathrm{cc}, \quad \text{(D2)}$$

$$\mathcal{L}\rho_4 = -K_c\partial_\theta \left\{\rho_3 \mathrm{Im}\; e^{-i\theta}\langle e^{-i\theta'}, \sigma_1\rangle + \omega_2\sigma_1 \mathrm{Im}\; e^{i\theta}\langle e^{i\theta'}, \sigma_1\rangle'\right\} - K_2\,\partial_\theta\sigma_1 \mathrm{Im}\; e^{-i\theta}\langle e^{-i\theta'}, \sigma_1\rangle - \partial_T\rho_3 + \mathrm{cc}. \quad \text{(D3)}$$

with $K_c = 4D$. Here we have defined

$$\langle\varphi, \psi\rangle' = \frac{1}{2\pi}\int_{-\pi}^{\pi}\int_{-\infty}^{+\infty} \overline{\varphi(\theta,\omega)}\psi(\theta,\omega)\, g_0'(\omega)\, d\omega\, d\theta,$$
$$g_0'(\omega) = \frac{1}{2}\left[\delta'(\omega + \omega_0) - \delta'(\omega - \omega_0)\right], \quad \text{(D4)}$$

We have not yet used Eq. (60). Its use will lead to a correction in (D2) and (D3). The second term in (D1) has the same form as σ_1, but it is not resonant because $\langle 1, (D + i\omega)^{-2}\rangle = 0$ at the tricritical point. The solution of (D1) is

$$\rho_2 = \left[\frac{A^2 e^{2i\theta}}{(D + i\omega)(2D + i\omega)} - \frac{A_T e^{i\theta}}{(D + i\omega)^2}\right] + \mathrm{cc}. \quad \text{(D5)}$$

We now insert this solution in Eq. (D2) and use the ansatz (60) because $\partial_T\rho_2$ contains a factor A_{TT} in a truly resonant term. (Recall that it is at this point that the routine Chapman-Enskog ansatz (38) fails to deliver a resonant term). Notice that the ansatz (60) adds the term $F^{(1)}e^{i\theta}/(D + i\omega)^2$+cc to the right side of Eq. (D3). The nonresonance condition for (D2) yields

$$F^{(0)} = \frac{D}{2}(K_2 - 4\omega_2)A + \frac{2}{5}|A|^2 A. \quad \text{(D6)}$$

The solution of Eq. (D2) is

$$\rho_3 = \left[\frac{K_2 - 4\omega_2}{4D(D + i\omega)} A + \frac{F^{(0)}}{(D + i\omega)^3} - \frac{A|A|^2}{(D + i\omega)^2(2D + i\omega)}\right] e^{i\theta} + \mathrm{cc} - \frac{AA_T\left(\frac{1}{D+i\omega} + \frac{1}{2D+i\omega}\right)}{(D + i\omega)(2D + i\omega)} e^{2i\theta} + \mathrm{cc} + \frac{A^3 e^{3i\theta}}{(D + i\omega)(2D + i\omega)(3D + i\omega)} + \mathrm{cc}. \quad \text{(D7)}$$

By applying the nonresonance condition to the right side of Eq. (D3) we obtain

$$F^{(1)} = \frac{K_2}{2} A_T - \frac{\left(|A|^2 A\right)_T}{5D} - \frac{23}{25D}|A|^2 A_T. \quad \text{(D8)}$$

Insertion of Equations (D6) and (D8) into (60) yields the sought amplitude equation (61).

APPENDIX E: Stationary solutions of the Kuramoto model are not equilibrium states

In this Appendix we show how the stationary solutions of the KM are not equilibrium states of the model defined by the Hamiltonian defined in (142). Following (Pérez-Vicente and Ritort, 1997) the equilibrium value of the moments (138) E_k^m corresponding to (142) can be easily computed,

$$E_k^m = F_k^m e^{ik\theta} = e^{ik\theta}\int_{-\pi}^{\pi} d\omega g(\omega)\omega^m \frac{J_k^\omega(\frac{Kr}{T})}{J_0^\omega(\frac{Kr}{T})} \quad \text{(E1)}$$

θ being an arbitrary phase. The functions $J_k^\omega(x)$ are of the Bessel type,

$$J_k^\omega(x) = \int_{-\pi}^{\pi} d\phi \exp(ik\phi + x\cos(\phi) + \beta\omega\phi) \quad \text{(E2)}$$

and $\beta = 1/T$. Inserting the equilibrium values of the moments E_k^m into (139) yields,

$$\left(\frac{\partial H_k^m}{\partial t}\right)_{H_k^m = E_k^m} = ikv_m \exp(ik\theta) \quad \text{(E3)}$$

with

$$v_m = T\exp(\frac{Kr}{T})\int_{-\pi}^{\pi} d\omega g(\omega)\frac{\omega^m\left(\exp(\frac{2\pi\omega}{T}) - 1\right)}{J_0^\omega(\frac{Kr}{T})} \quad \text{(E4)}$$

Stationarity of the equilibrium solution requires that v_m vanishes. In the simple case of a symmetric distribution $g(\omega) = g(-\omega)$ it can be proven that $v_{2m} = 0$, $\forall m$. However odd moments do not vanish. The temperature dependence of v_{2m-1} can be analytically computed in the high-temperature limit ($v_{2m-1} = \overline{\omega^{2m}} + \mathcal{O}(\beta^3)$) as well as in the low-temperature limit ($v_{2m-1} = \overline{\omega^{2m}} + \mathcal{O}(T)$), Interestingly, even in the zero-temperature limit (where a stability analysis reveals that the synchronized solution is neutrally stable, see section Sec. II.B) the absolute minima of $\mathcal{H}$ are not stationary configurations of the dynamics. This shows that the assumption that the stationary solutions at $T = 0$ are local minima of $\mathcal{H}$ in (142) does not hold. For a symmetric frequency distribution where $v_0 = 0$ (and therefore both $H_k^0 = h_k$ -see definition after (139)- and the synchronization parameter r are stationary) this result does not guarantee that the Boltzmann distribution $P^{\rm eq}(\{\theta_i\}) \propto \exp(-\beta\mathcal{H}(\{\theta_i\}))$ (which depends on the whole set of moments H_k^m) is stationary as well.

References

Abbott, L. F., 1990, J. Phys. A: Math. Gen. **23**, 3835.

Abeles, M., 1991, *Corticonics: Neural circuits of the cerebral cortex* (Cambridge University Press, Cambridge).

Acebrón, J. A., and L. L. Bonilla, 1998, Physica D **114**, 296.

Acebrón, J. A., L. L. Bonilla, S. D. Leo, and R. Spigler, 1998, Phys. Rev. E **57**, 5287.

Acebrón, J. A., L. L. Bonilla, and R. Spigler, 2000, Phys. Rev. E **62**, 3437.

Acebrón, J. A., A. Perales, and R. Spigler, 2001a, Phys. Rev. E **64**, 016218.

Acebrón, J. A., and R. Spigler, 1998, Phys. Rev. Lett. **81**, 2229.

Acebrón, J. A., and R. Spigler, 2000, Physica D **141**, 65.

Acebrón, J. A., R. Spigler, and M. M. Lavrentiev, 2001b, IMA J. Num. Anal **21**, 239.

Amit, D. J., 1989, *Modeling Brain Function* (Cambridge University Press, Cambridge, UK).

Aonishi, T., 1998, Phys. Rev. E **58**, 4865.

Aonishi, T., K. Kurata, and M. Okada, 2002, Phys. Rev. E **65**, 046223.

Aonishi, T., and M. Okada, 2002, Phys. Rev. Lett **88**, 024102.

Aoyagi, T., 1995, Phys. Rev. Lett. **74**, 4075.

Aoyagi, T., and K. Kitano, 1997, Phys. Rev. E **55**, 7424.

Aoyagi, T., and M. Nomura, 1999, Phys. Rev. Lett. **83**, 1062.

Arenas, A., and C. J. Pérez-Vicente, 1993, Physica **201**, 614.

Arenas, A., and C. J. Pérez-Vicente, 1994a, Phys. Rev. E **50**, 949.

Arenas, A., and C. J. Pérez-Vicente, 1994b, Europhys. Lett. **26**, 79.

Ariaratnam, J. T., and S. H. Strogatz, 2001, Phys. Rev. Lett. **86**, 4278.

Balmforth, N. J., and R. Sassi, 2000, Physica D **143**, 21.

Bar-Eli, Z., 1985, Physica D **14**, 242.

Barbara, P., A. B. Cawthorne, S. V. Shitov, and C. J. Lobb, 1999, Phys. Rev. Lett. **82**, 1963.

Bausch, R., H. J. Janssen, and H. Wagner, 1976, Z. Phys. B **24**, 113.

Bogoliubov, N. N., and Y. A. Mitropolsky, 1961, *Asymptotic methods in the theory of nonlinear oscillators* (Gordon and Breach, New York).

Bonilla, L. L., 1987, J. Stat. Phys. **659**, 47.

Bonilla, L. L., 2000, Phys. Rev. E **62**, 4862.

Bonilla, L. L., J. M. Casado, and M. Morillo, 1987, J. Stat. Phys. **571**, 48.

Bonilla, L. L., J. M. Casado, and M. Morillo, 1988, J. Stat. Phys. **50**, 849.

Bonilla, L. L., J. C. Neu, and R. Spigler, 1992, J. Stat. Phys. **67**, 313.

Bonilla, L. L., C. J. Pérez-Vicente, F. Ritort, and J. Soler, 1998a, Phys. Rev. Lett. **81**, 3643.

Bonilla, L. L., C. J. Pérez-Vicente, and J. M. Rubi, 1993, J. Stat. Phys. **70**, 921.

Bonilla, L. L., C. J. Pérez-Vicente, and R. Spigler, 1998b, Physica D **113**, 79.

Braiman, Y., T. A. B. Kennedy, K. Wiesenfeld, and A. Khibnik, 1995, Phys. Rev. A **52**, 1500.

Braun, O. M., and Y. S. Kivshar, 1998, Phys. Rep. **306**, 1.

Bulsara, A., and L. Gammaitoni, 1996, Phys. Today **49**, 39.

Carpio, A., and L. L. Bonilla, 2001, Phys. Rev. Lett. **86**, 6034.

Carpio, A., and L. L. Bonilla, 2003a, Phys. Rev. Lett. **90**, 135502.

Carpio, A., and L. L. Bonilla, 2003b, Phys. Rev. E **67**, 056621.

Chapman, S., and T. G. Cowling, 1970, *The mathematical theory of non-uniform gases, 3rd ed.* (Cambridge University Press, Cambridge, U.K.).

Choi, M. Y., H. J. Kim, D. Kim, and H. Hong, 2000, Phys. Rev. E **61**, 371.

Choi, M. Y., Y. W. Kim, and D. C. Hong, 1994, Phys. Rev. E **49**, 3825.

Coffey, W. T., Y. P. Kalmykov, and J. T. Waldron, 1996, *The Langevin equation* (World Scientific, Singapore).

Cook, J., 1989, J. Phys. A: Math. Gen. **22**, 2057.

Coolen, A. C. C., and C. J. Pérez-Vicente, 2003, J. Phys. A: Math. Gen. **36**, 4477.

Crawford, J. D., 1991, Rev. Mod. Phys. **63**, 991.

Crawford, J. D., 1994, J. Stat. Phys. **74**, 1047.

Crawford, J. D., 1995, Phys. Rev. Lett. **74**, 4341.

Crawford, J. D., and K. T. R. Davies, 1999, Physica D **125**, 1.

Crisanti, A., and F. Ritort, 2003, to appear in J. Phys. A: Math. Gen. .

Daido, H., 1987a, Prog. Theor. Phys. **77**, 622.

Daido, H., 1987b, J. Phys. A: Math. Gen. **20**, L629.

Daido, H., 1988, Phys. Rev. Lett. **61**, 231.

Daido, H., 1989, Prog. Theor. Phys. **81**, 727.

Daido, H., 1990, J. Stat. Phys **60**, 753.

Daido, H., 1992a, Prog. Theor. Phys. **88**, 1213.

Daido, H., 1992b, Phys. Rev. Lett. **68**, 1073.

Daido, H., 1993a, Prog. Theor. Phys. **89**, 929.

Daido, H., 1993b, Physica D **69**, 394.

Daido, H., 1994, Phys. Rev. Lett. **73**, 760.

Daido, H., 1995, J. Phys. A: Math. Gen. **28**, L151.

Daido, H., 1996a, Phys. Rev. Lett. **77**, 1406.

Daido, H., 1996b, Physica D **91**, 24.

Daido, H., 2000, Phys. Rev. E **61**, 2145.

Daido, H., 2001, Phys. Rev. Lett. **87**, 048101.

DaiPra, P., and F. den Hollander, 1996, J. Stat. Phys. **84**, 735.

Dangelmayr, G., and E. Knobloch, 1987, Phil. Trans. R. Soc. Lond. A **322**, 243.

Daniels, B., S. Dissanayake, and B. Trees, 2003, Phys. Rev.

E **67**, 026216.
Dawson, D. A., 1983, J. Stat. Phys. **31**, 29.
Doedel, E. J., 1997, *AUTO: software for continuation and bifurcation problems in ordinary differential equations* (California Institute of Technology).
Dominicis, C. D., and L. Peliti, 1978, Phys. Rev. B **18**, 353.
Duzer, T. V., and C. W. Turner, 1999, *Superconductive Devices and Circuits* (Prentice Hall, Upper Saddle River, NJ).
Eckhorn, R., R. Bauer, W. Jordan, M. Brosch, W. Kruse, M. Munk, and H. J. Reitboeck, 1988, Biol. Cybern. **60**, 121.
Eissfeller, H., and M. Opper, 1978, J. Stat. Phys. **19**, 1.
Enskog, D., 1917, *Inaugural Dissertation* (Uppsala).
Ermentrout, G. B., 1990, Physica D **41**, 219.
Ermentrout, G. B., 1991, J. Math. Biol. **29**, 571.
Filatrella, G., N. F. Pedersen, and K. Wiesenfeld, 2000, Phys. Rev. E **61**, 2513.
Filatrella, G., N. F. Pedersen, and K. Wiesenfeld, 2001, IEEE Trans. Appl. Supercond. **11**, 1184.
Fitzhugh, R., 1961, Biophys. J. **1**, 445.
Fornberg, B., 1996, *A practical guide to pseudospectral methods* (Cambridge Univ. Press, Cambridge).
Frank, T. D., A. Daffertshofer, C. Peper, P. J. Beek, and H. Haken, 2000, Physica D **144**, 62.
Gammaitoni, L., P. Hänggi, P. Jung, and F. Marchesoni, 1998, Rev. Mod. Phys. **70**, 223.
Gardner, E., 1988, J. Phys. A: Math. Gen. **21**, 257.
Gerl, F., K. Bauer, and U. Krey, 1992, Z. Phys. B **88**, 339.
Gerstner, W., 1996, Phys. Rev. Lett. **76**, 1755.
Golomb, D., D. Hansel, B. Shraiman, and H. Sompolinsky, 1992, Phys. Rev. E. **45**, 3516.
Grannan, E. R., D. Kleinfeld, and H. Sompolinsky, 1993, Neural computation **7**, 551.
Gray, C. M., P. Konig, A. K. Engel, and W. Singer, 1989, Nature **338**, 334.
Hansel, D., G. Mato, and C. Meunier, 1993a, Europhys. Lett. **23**, 367.
Hansel, D., G. Mato, and C. Meunier, 1993b, Phys. Rev. E **48**, 3470.
Heath, T., and K. Wiesenfeld, 2000, Ann. Phys. (Leipzig) **9**, 689.
Heath, T., K. Wiesenfeld, and R. A. York, 2000, Int. J. Bifurc. Chaos **10**, 2619.
Hebb, D. O., 1949, *The organization of behavior* (Wiley, NY).
Hemmen, J. L. V., and W. F. Wreszinski, 1993, J. Stat. Phys. **72**, 145.
Hertz, J. A., A. Krogh, and R. G. Palmer, 1991, *Introduction to the theory of neural computation* (Addison-Wesley, Wokingham, U.K.).
Higham, D. J., 2001, SIAM Rev. **43**, 525.
Hong, H., and M. Choi, 2000, Phys. Rev. E **62**, 6462.
Hong, H., M. Choi, J. Yi, and K.-S. Soh, 1999a, Phys. Rev. E **59**, 353.
Hong, H., M. Y. Choi, B. G. Yoon, K. Park, and K. S. Soh, 1999b, J. Phys. A: Math. Gen. **32**, L9.
Hong, H., G. S. Jeon, and M. Choi, 2002, Phys. Rev. E **65**, 026208.
Hong, H., T. I. Um, Y. Shim, and M. Y. Choi, 2001, J. Phys. A: Math. Gen. **34**, 5021.
Hopfield, J. J., 1982, Proc. Natl. Acad. Sci. USA **79**, 2554.
Izhikevich, E. M., 1998, Phys. Rev. E **58**, 905.
Jeong, S., T. Ko, and H. Moon, 2002, Phys. Rev. Lett. **89**, 154104.
Jiang, Z., and M. McCall, 1993, J. Opt. Soc. Am. B **10**, 155.
Jongen, G., J. Anemuller, D. Bolle, A. C. C. Coolen, and C. J. Perez-Vicente, 2001, J. Phys. A: Math. Gen. **34**, 3957.
Josephson, B. D., 1964, Rev. Mod. Phys. **36**, 216.
Kazanovich, Y. B., and R. M. Borisyuk, 1994, Biol. Cybern. **71**, 177.
Keller, J. B., and L. L. Bonilla, 1986, J. Stat. Phys. **42**, 1115.
Kim, S., S. H. Park, C. R. Doering, and C. S. Ryu, 1997a, Phys. Lett. A **224**, 147.
Kim, S., S. H. Park, and C. S. Ryu, 1996, ETRI Journal **18**, 147.
Kim, S., S. H. Park, and C. S. Ryu, 1997b, Phys. Rev. Lett. **79**, 2911.
Kim, S., S. H. Park, and C. S. Ryu, 1997c, Phys. Lett. A **236**, 409.
Kirkpatrick, S., and D. Sherrington, 1978, Phys. Rev. B **17**, 4384.
Kiss, I., Y. Zhai, and J. Hudson, 2002, Science **296**, 1676.
Kitano, K., and T. Aoyagi, 1998, Phys. Rev. E **57**, 5914.
Kloeden, P. E., and E. Platen, 1999, *The numerical solution of stochastic differential equations* (Springer-Verlag, Berlin).
Kohring, G. A., 1993, Neural networks **6**, 573.
Kori, H., and Y. Kuramoto, 2001, Phys. Rev E **63**, 046214.
Kostur, M., J. Luczka, and L. Schimansky-Geier, 2002, Phys. Rev E **65**, 051115.
Kourtchatov, S. Y., V. V. Likhanskii, A. P. Napartovich, F. T. Arecchi, and A. Lapucci, 1995, Phys. Rev. A **52**, 4089.
Kozireff, G., A. G. Vladimirov, and P. Mandel, 2000, Phys. Rev. Lett **85**, 3809.
Kozireff, G., A. G. Vladimirov, and P. Mandel, 2001, Phys. Rev. E **64**, 016613.
Kuramoto, Y., 1975, in *Int. Symp. on Mathematical problems in theoretical physics*, edited by H. Araki (Springer, New York), volume 39 of *Lect. N. Phys.*, pp. 420–422.
Kuramoto, Y., 1984, *Chemical oscillations, waves and turbulence* (Springer, New York).
Kuramoto, Y., and I. Nishikawa, 1987, J. Stat. Phys **49**, 569.
Lang, R., and K. Kobayashi, 1980, IEEE J. Quantum Eletron. **16**, 347.
Li, R., and T. Erneux, 1993, Opt. Commun. **99**, 196.
Lumer, E. D., and B. A. Huberman, 1991, Phys. Lett. A **160**, 227.
Lumer, E. D., and B. A. Huberman, 1992, Neural computation **4**, 341.
Luzyanina, T. B., 1995, Network, Computation in neural systems **6**, 43.
Marcus, C., S. Strogatz, and R. Westervelt, 1989, Phys. Rev. B **40**, 5588.
Marek, M., and I. Stuchl, 1975, Biophysical Chem. **3**, 263.
Marodi, M., F. d'Ovidio, and T. Vicsek, 2002, Phys. Rev. E **66**, 011109.
Matthews, P. C., R. E. Mirollo, and S. H. Strogatz, 1991, Physica D **52**, 293.
Matthews, P. C., and S. H. Strogatz, 1990, Phys. Rev. Lett. **65**, 1701.
Meadows, B. K., T. H. Heath, J. D. Neff, E. A. Brown, D. W. Fogliatti, M. Gabbay, V. In, P. Hasler, S. P. Deweerth, and W. L. Ditto, 2002, Proc. IEEE **90**, 882.
Mezard, M., G. Parisi, and M. Virasoro, 1987, *Spin glass theory and beyond* (World Scientific, Singapore).
Mirollo, R., and S. H. Strogatz, 1990, J. Stat. Phys. **60**, 245.
Monte, S. D., and F. D'ovidio, 2002, Europhys. Lett. **58**, 21.
Nakamura, Y., F. Tominaga, and T. Munakata, 1994, Phys. Rev. E **49**, 4849.
Neu, J., 1979, SIAP **37**, 307.

Neu, J., 1980, SIAP **38**, 305.

Niebur, E., H. G. Schuster, and D. M. Kammen, 1991a, Phys. Rev. Lett. **67**, 2753.

Niebur, E., H. G. Schuster, D. M. Kammen, and C. Koch, 1991b, Phys. Rev. A **44**, 6895.

Noest, A. J., 1988, Europhys. Lett. **6**, 469.

Okuda, K., 1993, Physica D **63**, 424.

Oliva, R. A., and S. H. Strogatz, 2001, Int. J. Bif. Chaos **11**, 2359.

Pantaleone, S., 1998, Phys. Rev. D **58**, 073002.

Park, K., and M. Y. Choi, 1995, Phys. Rev. E **52**, 2907.

Park, K., and M. Y. Choi, 1997, Phys. Rev. B **56**, 387.

Park, K., S. W. Rhee, and M. Y. Choi, 1998, Phys. Rev. E **57**, 5030.

Park, S. H., and S. Kim, 1996, Phys. Rev. E **53**, 3425.

Peretto, P., 1992, *An introduction to the modeling of neural networks* (Cambridge Univ. Press).

Pérez-Vicente, C. J., A. Arenas, and L. L. Bonilla, 1996, J. Phys. A: Math. Gen. **29**, L9.

Pérez-Vicente, C. J., and F. Ritort, 1997, J. Phys. A: Math. Gen. **30**, 8095.

Phythian, R., 1977, J. Phys. A: Math. Gen. **10**, 777.

Pikovski, A., M. Rosemblum, and J. Kurths, 2001, *Synchronization, a universal concept in nonlinear sciences* (Cambridge University Press, Cambridge).

Platen, E., 1999, Acta Numer. **8**, 197.

Press, W. M., S. A. Teukolsky, W. T. Vetterling, and B. P. Flannery, 1992, *Numerical recipes in C* (Cambridge University Press, Cambridge).

Reimann, P., C. V. den Broeck, and R. Kawai, 1999, Phys. Rev. E **60**, 6402.

Ren, L., and B. Ermentrout, 2000, Physica D **143**, 56.

Ritort, F., 1998, Phys. Rev. Lett. **80**, 6.

Rogers, J. L., and L. T. Wille, 1996, Phys. Rev. E **54**, R2193.

Sakaguchi, H., 1988, Prog. Theor. Phys. **79**, 39.

Sakaguchi, H., and Y. Kuramoto, 1986, Prog. Theor. Phys. **76**, 576.

Sakaguchi, H., S. Shinomoto, and Y. Kuramoto, 1987, Prog. Theor. Phys. **77**, 1005.

Sakaguchi, H., S. Shinomoto, and Y. Kuramoto, 1988, Prog. Theor. Phys. **79**, 1069.

Sakaguchi, H., and K. Watanabe, 2000, J. Phys. Soc. Japan **69**, 3545.

Sartoretto, F., R. Spigler, and C. J. Pérez-Vicente, 1998, M^3AS: Math. Mod. Met. Appl. Sci. **8**, 1023.

Satoh, K., 1989, J. Phys. Soc. Japan **58**, 2010.

Schuster, H. G., and P. Wagner, 1989, Prog. Theor. Phys. **81**, 939.

Schuster, H. G., and P. Wagner, 1990a, Biol. Cybern. **64**, 77.

Schuster, H. G., and P. Wagner, 1990b, Biol. Cybern. **64**, 83.

Seliger, P., S. C. Young, and L. S. Tsimring, 2002, Phys. Rev. E **65**, 041906.

Sherrington, D., and S. Kirkpatrick, 1975, Phys. Rev. Lett. **35**, 1792.

Shiino, M. ., and M. Francowicz, 1989, Phys. Lett. A **136**, 103.

Shiino, M. ., and T. Fukai, 1992, J. Phys. A: Math. Gen. **25**, L375.

Shiino, M. ., and T. Fukai, 1993, Phys. Rev. E **48**, 867.

Shinomoto, S., and Y. Kuramoto, 1986, Prog. Theor. Phys. **75**, 1105.

Silber, M., L. Fabini, and K. Wisenfeld, 1993, J. Opt. Soc. Am. B **10**, 1121.

Softky, W., and C. Koch, 1993, J. Neurosci. **13**, 334.

Sompolinsky, H., D. Golomb, and D. Kleinfeld, 1990, Proc. Natl. Acad. Sci. USA **87**, 7200.

Sompolinsky, H., D. Golomb, and D. Kleinfeld, 1991, Phys. Rev. A **43**, 6990.

Stiller, J. C., and G. Radons, 1998, Phys. Rev. E **58**, 1789.

Stiller, J. C., and G. Radons, 2000, Phys. Rev. E **61**, 2148.

Strogatz, S. H., 2000, Physica D **143**, 1.

Strogatz, S. H., 2003, *SYNC: the emerging science of spontenous order* (Hyperion, New York).

Strogatz, S. H., C. Marcus, R. Westervelt, and R. E. Mirollo, 1988, Phys. Rev. Lett. **61**, 2380.

Strogatz, S. H., C. Marcus, R. Westervelt, and R. E. Mirollo, 1989, Physica D **36**, 23.

Strogatz, S. H., and R. E. Mirollo, 1988a, J. Phys. A: Math. Gen. **21**, L699.

Strogatz, S. H., and R. E. Mirollo, 1988b, Physica D **31**, 143.

Strogatz, S. H., and R. E. Mirollo, 1991, J. Stat. Phys **63**, 613.

Strogatz, S. H., R. E. Mirollo, and P. C. Matthews, 1992, Phys. Rev. Lett. **68**, 2730.

Swift, J. W., S. H. Strogatz, and K. Wiesenfeld, 1992, Physica D **55**, 239.

Takamatsu, A., T. Fujii, and I. Endo, 2000, Phys. Rev. Lett. **85**, 2026.

Tanaka, H., A. J. Lichtenberg, and S. Oishi, 1997a, Physica D **100**, 279.

Tanaka, H., A. J. Lichtenberg, and S. Oishi, 1997b, Phys. Rev. Lett. **78**, 2104.

Tass, P., 1997, Phys. Rev. E **56**, 2043.

Thouless, D. J., P. W. Anderson, and R. G. Palmer, 1977, Philosophical Magazine **35**, 593.

Tovee, M. J., and E. T. Rolls, 1992, TINS **15**, 387.

Uchiyama, S., and H. Fujisaka, 1999, J. Phys. A: Math. Gen. **32**, 4623.

Vladimirov, A. G., G. Kozireff, and P. Mandel, 2003, Europhys. Lett. **61**, 613.

Voss, H. U., 2001, Phys. Rev. E **61**, 5115.

Wang, S. S., and H. G. Winful, 1988, Appl. Phys. Lett. **52**, 1774.

Wieczorek, S., and D. Lenstra, 2003.

Wiesenfeld, K., 1996, Physica B **222**, 315.

Wiesenfeld, K., P. Colet, and S. H. Strogatz, 1996, Phys. Rev. Lett. **76**, 404.

Wiesenfeld, K., P. Colet, and S. H. Strogatz, 1998, Phys. Rev. E **57**, 1563.

Winfree, A. T., 1967, J. Theor. Biol. **16**, 15.

Winfree, A. T., 1980, *The geometry of biological time* (Springer-Verlag, New York).

Winful, H. G., and S. S. Wang, 1988, Appl. Phys. Lett. **53**, 1894.

Yamaguchi, Y., and H. Shimizu, 1984, Physica D **11**, 212.

Yamana, M., M. Shiino, and M. Yoshioka, 1999, J. Phys. A: Math. Gen. **32**, 3525.

Yeung, M. K. S., and S. H. Strogatz, 1999, Phys. Rev. Lett. **82**, 648.

Yoshimoto, M., K. Yoshikawa, and Y. Mori, 1993, Phys. Rev. E. **47**, 864.

Yoshioka, M., and M. Shiino, 2000, Phys. Rev. E. **61**, 4732.

Zanette, D. H., 2000, Phys. Rev. E **62**, 3167.

Zheng, Z., G. Hu, and B. Hu, 1998, Phys. Rev. Lett. **81**, 5318.

APPENDIX: Figures

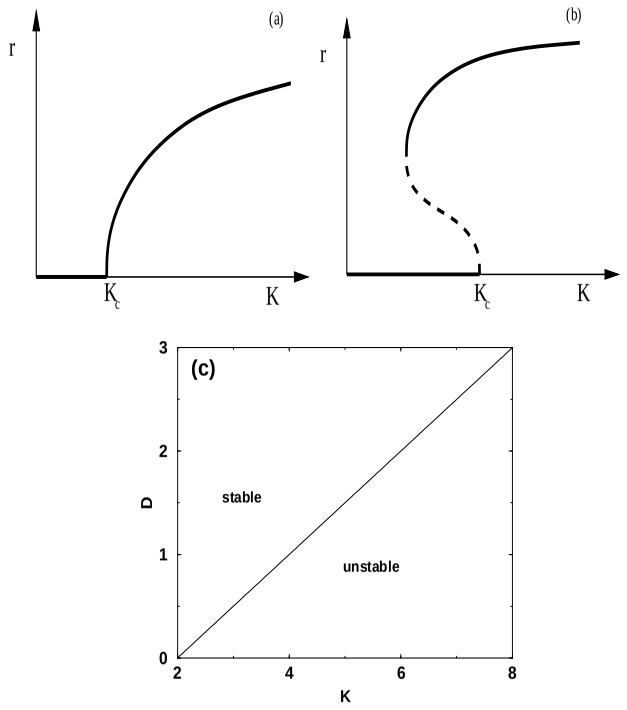

FIG. 1 (a) Supercritical bifurcation in a diagram of r vs. K. (b) Subcritical bifurcation. (c) Phase diagram of the noisy KM, D vs. K, showing the regions of linear stability for the incoherent solution $\rho_0 = 1/(2\pi)$ provided the frequency distribution is unimodal and Lorentzian with width γ. The incoherent solution is linearly stable if $0 < K < 2D + \gamma$, and unstable otherwise.

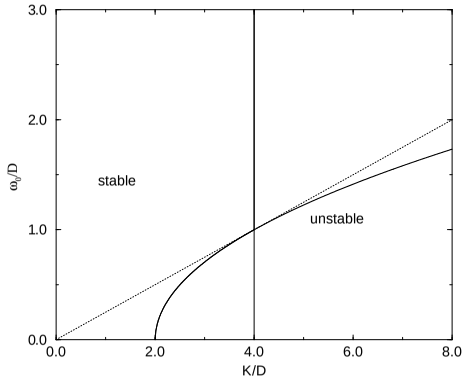

FIG. 2 Linear stability diagram for the incoherent solution $\rho_0 = 1/(2\pi)$ and the discrete bimodal frequency distribution in the parameter space $(K/D, \omega_0/D)$. ρ_0 is linearly stable to the left of the lines $K = 4D$, $\omega_0 > D$ (where Hopf bifurcations take place) and $K/(2D) = 1 + \omega_0^2/D^2$, $\omega_0 < D$ (where one solution of Eq. (34) becomes zero). To the right of these lines, the incoherent solution is unstable. At the tricritical point, $K = 4D$, $\omega_0 = D$, two solutions of Eq. (34) become simultaneously zero. The dashed line separates the region where eigenvalues are real (below the line) from that when they are complex conjugate (above the line).

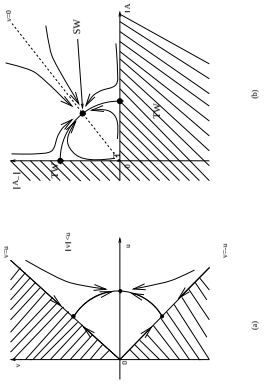

FIG. 3 Phase planes (a) (u, v) and (b) $(|A_+|, |A_-|)$ showing the critical points corresponding to travelling (TW) and standing wave (SW) solutions.

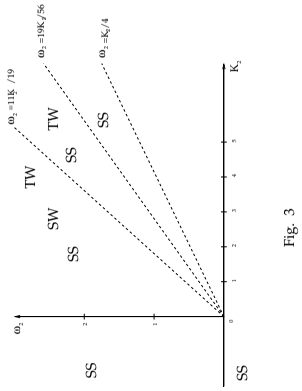

FIG. 4 Stability diagrams (K_2, ω_2) near the tricritical point.

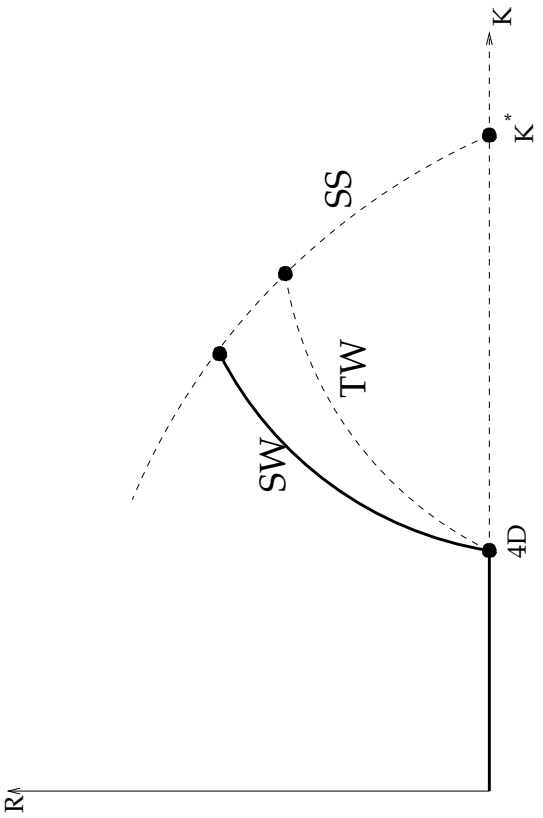

FIG. 5 Bifurcation diagram (K, R) near the tricritical point for $\omega_0 > D$ fixed. K^* is the coupling at which a subcritical branch of stationary solutions bifurcates from incoherence.

Fig. 4

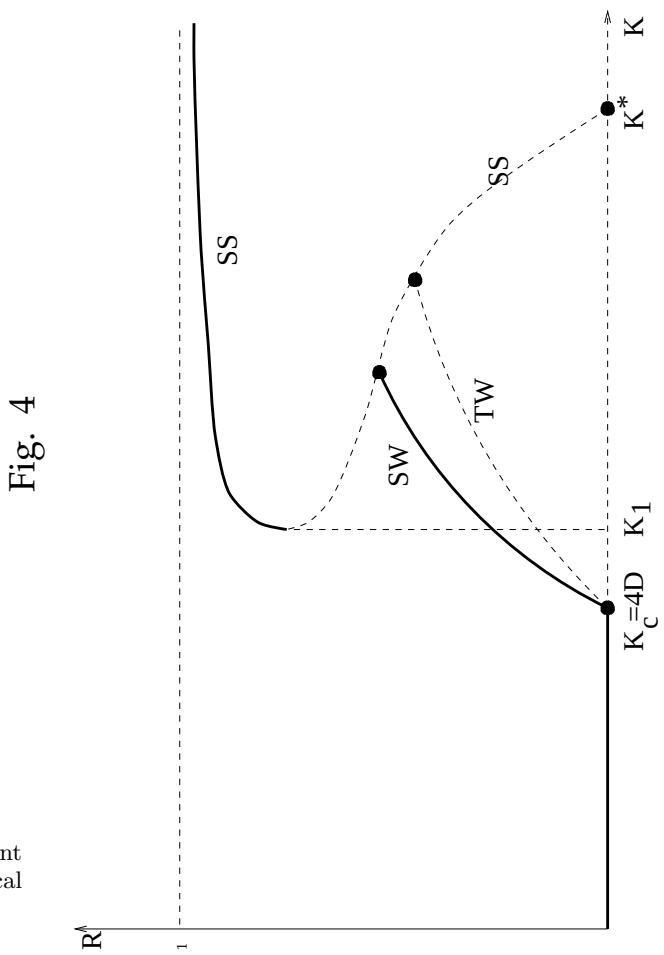

FIG. 6 Global bifurcation diagram including all stationary solution branches.

FIG. 7 A hierarchical tree with $N = 9$ two-level ($L = 2$) oscillators having branching ratio $b = 3$. The distance l_{ij} between two oscillators is given by the number of levels between them and their closest common ancestor. In this example, $l_{12} = l_{46} = l_{78} = 1$ and $l_{15} = l_{58} = 2$.

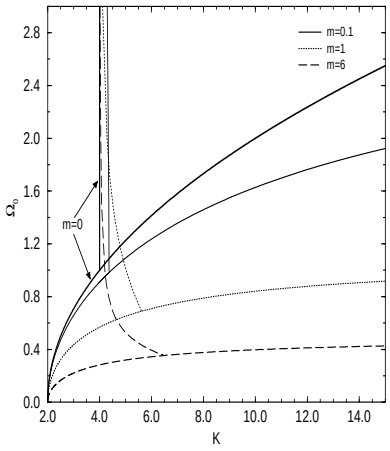

FIG. 8 Discrete bimodal frequency distribution: Stability diagram of incoherence in the parameter space (Ω_0, K) for different mass values and $D = 1$.

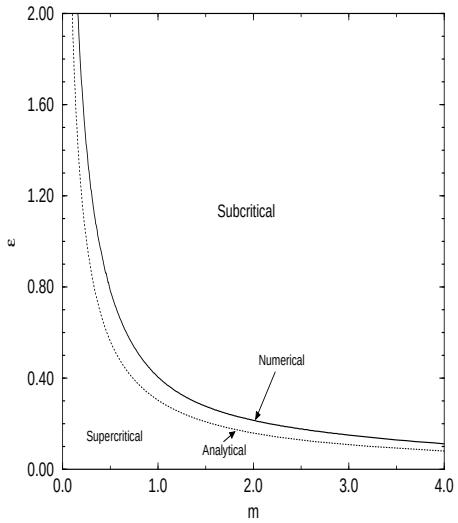

FIG. 9 Stationary solution, lorentzian frequency distribution with spread ε. The line separates the region in parameter space (m, ε) on which the transition to the synchronized state is either sub- or a super-critical. The dotted line denotes the analytical solution obtained using c_n, $n = 0, 1, 2$, while the solid line shows the solution computed numerically.

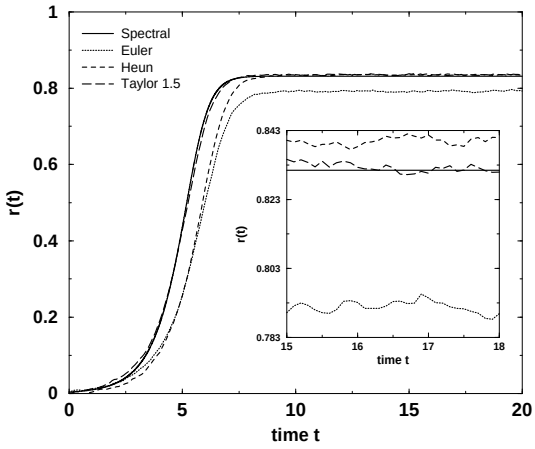

FIG. 10 Comparison between the numerical solution of the nonlinear Fokker-Planck equation using the spectral method with 40 harmonics and the numerical solution of the stochastic differential equations obtained with three different numerical schemes: Euler, Heun, and 3/2 Taylor. Here the time step is $\Delta t = 0.1$. The population comprises $N = 50000$ oscillators with the same frequency ($\omega_i = 0$); $K = 4$ and $D = 1$.

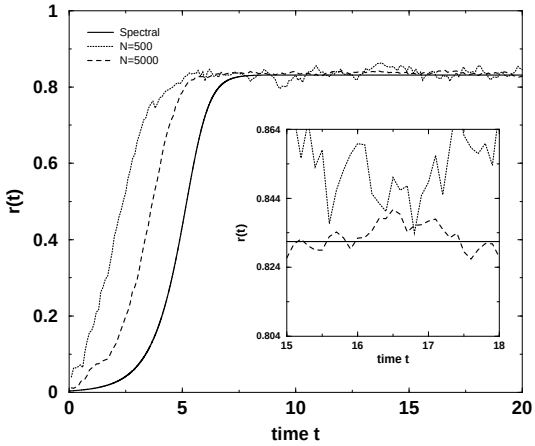

FIG. 11 Comparison between the numerical solution of the nonlinear Fokker-Planck equation using the spectral method with 40 harmonics and the numerical solution of the stochastic differential equations for $N = 500$ and $N = 5000$. Simulations haven been performed with a 3/2 Taylor scheme with a time step $\Delta t = 0.1$. Parameters are the same as in Fig. 10.

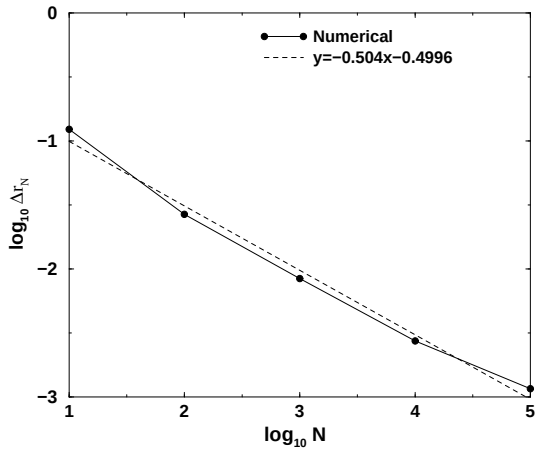

FIG. 12 Fluctuations of the order parameter as a function of the number of oscillators, N, with respect to a mean value given by $\lim_{N\to\infty} r_N$. We have used a log-log plot in which dots are the computed values of Δr_N, whereas the dashed line represents the corresponding mean square regression. The simulations have been performed using the 3/2 Taylor scheme with $\Delta t = 0.01$. Parameters are the same as in Fig. 10.

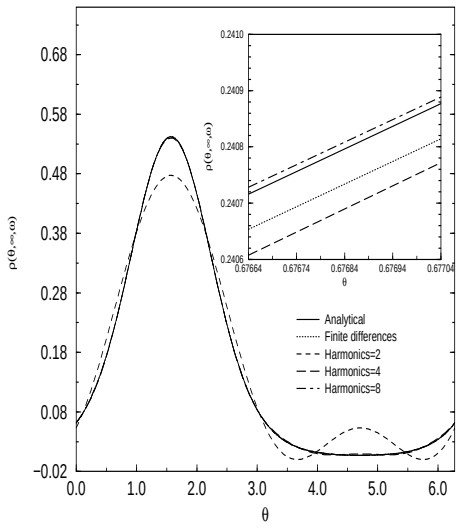

FIG. 13 Numerical simulations by finite differences (with $\Delta\theta = 0.04$, $\Delta t = 10^{-4}$), spectral method (with 2,4,8 harmonics), and the analytical stationary solution. Parameters are $K = 3$, $D = 1$, and $g(\omega) = \delta(\omega)$.

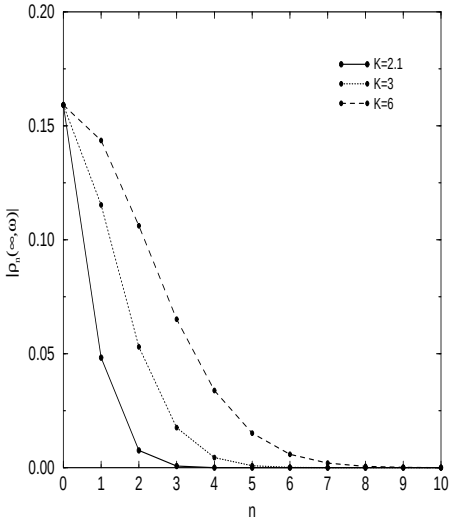

FIG. 14 The coefficients $|\rho_n(\infty,\omega)|$ corresponding to the stationary solution are shown for various coupling strength parameters, K. The frequency distribution here is $g(\omega) = \delta(\omega)$, and the diffusion constant $D = 1$.

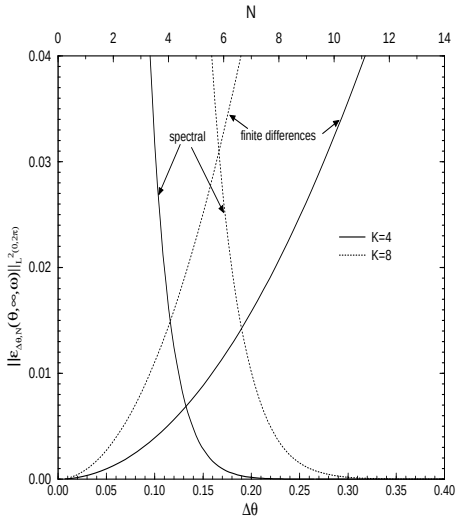

FIG. 15 Global L^2-error as function of $\Delta\theta$, or N, for $K = 4, 8$. Here $g(\omega) = \delta(\omega)$.

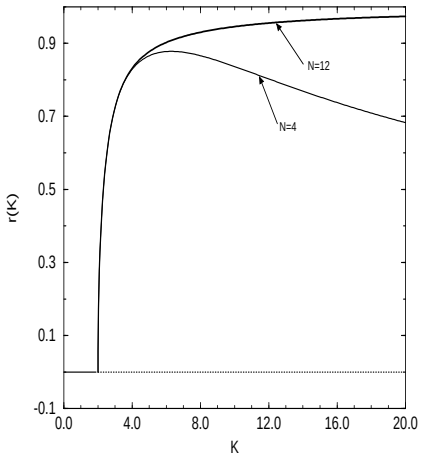

FIG. 16 Bifurcation diagram for the unimodal frequency distribution, $g(\omega) = \delta(\omega)$, calculated by using $N = 4$ and $N = 12$ harmonics in the spectral method. Dotted and solid lines correspond to unstable and stable solutions, respectively.

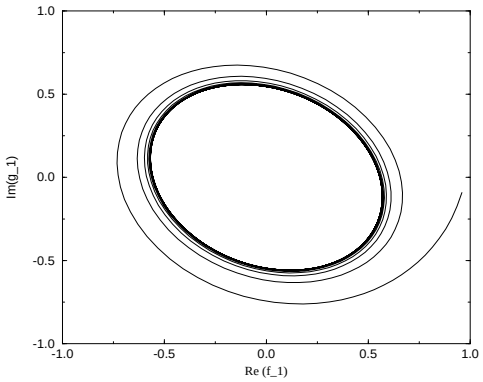

FIG. 18 Same as in Fig. 17 for $D = 0.05$ and $K = 1$. A stable oscillatory synchronized phase exists for these parameter values.

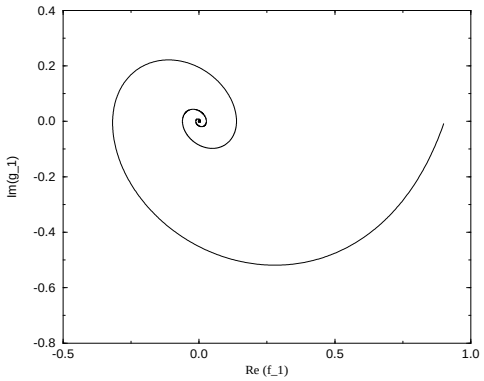

FIG. 17 Dynamical evolution of the order parameter $H_1^0 = r\exp(i\psi)$ for the KM with the discrete bimodal frequency distribution and $D = 1/2$ and $K = 1$. Incoherence is stable for these parameter values. The trajectory is represented in the complex plane $(\mathrm{Re}H_1^0, \mathrm{Im}H_1^0)$.

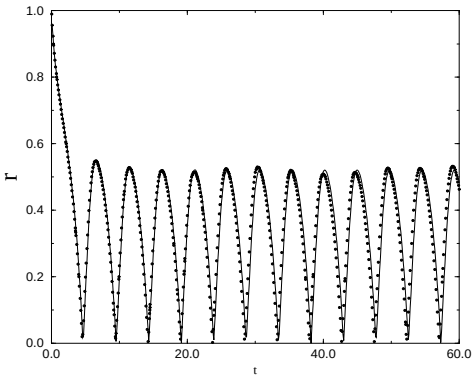

FIG. 19 Time evolution of r for the parameter values $D = 2.5$ and $K = 1/4$, for which the KM with a discrete bimodal frequency distribution has a stable oscillatory synchronized phase. The solid line has been obtained by means of the moments method described in the text, and the dots result from a single run of a Brownian simulation with $N = 50000$ oscillators.

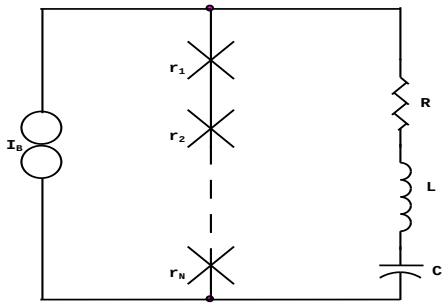

FIG. 20 Schematic circuit showing ideal Josephson junctions (each denoted by a cross) connected in series coupled through an RLC load. I_B is the bias current.